TRANSPORT OF HYDROCARBONS IN SILICONE RUBBER - POLYSTYRENE COPOLYMERS

by

Keith Munday, B.Sc., A.R.C.S.

September 1979

A thesis submitted for the degree of Doctor of Philosophy of the University of London and for the Diploma of Membership of the Imperial College

Physical Chemistry Department,
Imperial College,
London

ABSTRACT

Keith Munday, B.Sc., A.R.C.S.

Transport of Hydrocarbons in Silicone Rubber - Polystyrene Copolymers

Permeability, solubility and diffusion coefficients of methane, propane, n-butane, and iso-butane have been measured in the temperature range 20 to 50°C in polydimethylsiloxane (PDMS) and in membranes prepared from a block copolymer of PDMS and polystyrene containing 28 mole % polystyrene. The transport properties of propane and iso-butane have also been determined in a series of graft copolymers of PDMS containing up to 56.3% by weight of polystyrene. In addition, the sorption of methane and propane by polystyrene has been investigated at 30 and 50°C. DSC measurements of the copolymers indicated phase separation, and this was confirmed by transmission electron micrographs of selected samples. In all cases the polystyrene was present as a disperse phase within a PDMS continuum.

The permeabilities of PDMS and the copolymers were virtually independent of concentration, and E_p was found to be constant for each penetrant, as expected for a relatively impermeable disperse phase. Several models for the prediction of the permeability of a two-phase material have been examined, and the most successful were those of Higuchi and Bruggeman for a random dispersion of spherical domains. The sorption isotherms of polystyrene and the graft copolymers exhibit curvature typical of dual mode sorption in glassy polymers. The Langmuir component of sorption was found to be absent from the block copolymer and this has been interpreted in terms of a lowering of the glass transition temperature of polystyrene in this material. Diffusion coefficients are in agreement with a model in which the polystyrene domains of the copolymers act as impermeable absorbing filler particles to the diffusion of hydrocarbons.

ACKNOWLEDGEMENTS

I would like to thank Dr.J.A. Barrie for his interest and guidance throughout this work. I would also like to thank Dr.A.C. Sheer for the benefit of his experience at the commencement of the work, Mr.R.N. Sheppard for his advice and assistance, and Dr.M.J.L. Williams for many stimulating discussions.

Thanks are also due to the staff of the Chemistry Department workshops for their assistance in the construction and maintenance of the apparatus, and to Dr.P.G. Clay of the Nuclear Technology Department for his co-operation in the preparation of the graft copolymers. I am grateful to Dow Corning Limited for the gift of samples of PDMS and block copolymers, and to members of the staff of Queen Mary College for the electron micrographs.

I am especially indebted to Ms.Barbara Gifford for typing this thesis, and whose expertise in editing and proof-reading has proved invaluable in its preparation.

Finally, I would like to acknowledge the award of a bursary from the Science Research Council for this research.

CONTENTS

ADDENDUM: J.A. Barrie, K. Munday and M.J.L. Williams. "Sorption and Diffusion of Hydrocarbon Vapours in Glassy Polymers" Polymer Engineering and Science (in press)

TABLES

ILLUSTRATIONS

CHAPTER 1

INTRODUCTION

1.1 Permeability, Diffusivity, and Solubility

The permeability coefficient, P, of a gas or vapour in a polymer may be defined as the flux per unit area passing through a membrane of unit thickness under a unit pressure difference. The mechanism of transport within the polymer is molecular diffusion, and the permeation process can be regarded as occurring in three stages:

1. penetrant molecules in the gas phase are sorbed at the ingoing face of the membrane;
2. the sorbed molecules undergo a series of random molecular displacements and diffuse through the membrane under the influence of the concentration gradient;
3. molecules at the outgoing face of the membrane are desorbed into the gas phase.

In general the diffusion step is rate-determining, and the sorption and desorption may be considered as instantaneous processes in comparison. The diffusion coefficient, D, is defined as the amount of material passing across a plane of unit area in unit time under a unit concentration gradient, and the solubility coefficient, S, as the concentration, c, of penetrant sorbed per unit gas phase pressure. For permanent gases at moderate pressures both D and S are independent of pressure due to the low solubilities of these gases in polymers and the negligible gas-polymer and gas-gas interactions (1). When D and S are constant, or in the limit as $c \rightarrow 0$:

$$P = D.S \qquad \ldots (1.1)$$

If D is expressed in $cm^2 s^{-1}$, and S in $cm^3(STP)cm^{-3}(cm\ Hg)^{-1}$, then the units of P are $cm^3(STP)cm\ cm^{-2}(cm\ Hg)^{-1}s^{-1}$.

Diffusion is an activated process, and the temperature dependence of the diffusion coefficient can be expressed by an Arrhenius type of equation:

$$D = D_o \exp(-E_D/RT) \qquad \ldots (1.2)$$

The pre-exponential factor, D_o, is only weakly dependent upon T, and E_D, the activation energy for diffusion is essentially constant over a limited temperature range for many polymer-penetrant systems.

The solubility coefficient varies with temperature in a similar manner:

$$S = S_o \exp(-\Delta\bar{H}_S/RT) \qquad \ldots (1.3)$$

where $\Delta\bar{H}_S$ is the heat of sorption (heat of solution). When S varies with c the temperature dependence of the solubility at constant concentration gives the isosteric heat of sorption, whereas at constant pressure the isobaric heat of sorption is obtained.

Combining equations 1.1, 1.2 and 1.3 gives:

$$P = P_o \exp(-E_P/RT) \qquad \ldots (1.4)$$

E_P, the temperature coefficient of permeation is given by:

$E_P = E_D + \Delta\bar{H}_S$, and $P_o = D_o.S_o$.

A number of theories of diffusion in polymers have been proposed, and have been well reviewed (2). The free volume theory (3) postulates that a diffusion jump occurs when a "hole" in the polymer structure greater than a critical size occurs adjacent to a penetrant molecule. The activation energy for diffusion is correlated with the energy required for hole formation, and the size of a hole able to accommodate a penetrant molecule necessitates the co-operative motion of a number of polymer segments. The theory has been used to explain the concentration dependence of vapour diffusion due to plasticisation of the polymer in terms of the increased free volume of the system.

Barrer's activated zone theory (4,5) assumes that a diffusing molecule moves to successive equilibrium positions when sufficient energy has been acquired by the molecule and the surrounding medium. The activation energy is distributed through many degrees of freedom; values of the order 10 to 15 are obtained for the diffusion of simple penetrants in rubbers, and this again implies the co-operative motion of polymer chain segments.

The transition-state theory of rate processes has also been applied to molecular diffusion in polymers to give expressions for the activation energy and frequency or pre-exponential factor (6).

The equilibrium solubility of a penetrant in a polymer is dependent upon their mutual compatability, and is governed by the "like dissolves like" principle. More easily condensable vapours are more soluble in a given polymer, and a linear relationship has been found between the logarithm of the solubility and the boiling point (7,8), critical temperature (6), and Lennard-Jones force constant (9), these three factors being interdependent. The sorption process can be considered to involve two stages (10): condensation of the vapour on to the polymer, followed by solution of the condensed vapour, and thus the heat of sorption may be taken as the sum of the molar heat of condensation and the partial molar heat of mixing. For the permanent gases the hypothetical heat of condensation would be expected to be very small, and ΔH_S is small and positive. For more condensable gases and vapours the heat of condensation dominates and ΔH_S is negative.

The diffusivity is dependent upon the number of pre-existing holes in the polymer, the ease of hole formation as governed by the segmental mobility, and the ease of transit of the penetrant between holes. Polymer density is a measure of the number of holes or "looseness" of the polymer structure, and is related to the free volume content. The coefficient of thermal expansion is a measure of the ease of hole formation, and the ease of transit is determined largely by the size and shape of the penetrant molecule. Diffusion coefficients decrease with increasing molecular weight of a homologous series such as the paraffins, and branching has a much greater effect than does molecular weight (11). The molecular weight of the polymer has little effect upon D and P except in the region of very low molecular weights (12), and cross-linking is also found to have only a small effect upon these parameters except for large penetrant molecules at high degrees of cross-linking when the restricted mobility of the polymer chains may become significant (13). Polymer crystallinity decreases both D and P as the crystalline regions of a polymer are generally impermeable (14), and penetrant molecules have to follow a more tortuous path through the amorphous regions of the polymer.

The activation energy of diffusion is related to the energy required for hole formation, and can be expected to increase with increasing size and shape of the penetrant, and with increasing chain rigidity and polarity of the polymer. E_D is generally lower in the glassy state than in the rubbery state, and it has been suggested (15)

that the larger coefficient of thermal expansion of polymers above the glass transition temperature, T_g, is responsible for the increased temperature dependence of diffusion. Calculations by Meares (16) indicate that the unit path length for diffusion is much greater above T_g, involving a larger number of chain segments, and thus a correspondingly larger activation energy is required.

1.2 Diffusion Equations

The basic diffusion equation which relates the flux, J, across a plane of unit area at a position x to the concentration gradient at that position in the medium is known as Fick's first equation of diffusion (17).

$$J = -D.\frac{\partial c}{\partial x} \qquad \ldots (1.5)$$

where the negative sign indicates that the flux is in the direction of decreasing concentration.

By considering the material balance at the plane at x, Fick's second equation giving the rate of change of concentration may be derived:

$$\frac{\partial c}{\partial t} = \frac{\partial}{\partial x}\left(D.\frac{\partial c}{\partial x}\right) \qquad \ldots (1.6)$$

where D may be a function of c, x, or t. For constant D equation 1.6 reduces to:

$$\frac{\partial c}{\partial t} = D.\frac{\partial^2 c}{\partial x^2} \qquad \ldots (1.7)$$

The solutions of the diffusion equations under various boundary conditions may conveniently be divided into two types; steady state solutions in which $\frac{\partial c}{\partial t} = 0$, and transient state solutions when $\frac{\partial c}{\partial t} \neq 0$. The solutions given below are for the two most common experimental situations:

1. diffusion through a plane sheet with constant surface concentrations;
2. sorption into and desorption from a sheet with each face maintained at the same fixed concentration.

Full derivations and solutions for other sample geometries and boundary

conditions may be found in a number of standard texts (18).

The "time-lag experiment" consists of the measurement of diffusion through a plane sheet of thickness ℓ, initially free of diffusant, with a fixed concentration, c_0, at the ingoing face, $x = 0$, and negligible concentration at the outgoing face, $x = \ell$. The boundary conditions are:

$$c(x, 0) = 0 \qquad 0 < x < \ell, \quad t = 0$$
$$c(0, t) = c_0 \qquad t \geqslant 0$$
$$c(\ell, t) = 0 \qquad t \geqslant 0$$

Under steady state conditions with constant D integration of equation 1.7 gives:

$$c = c_0(1 - x/\ell) \qquad \ldots (1.8)$$

and from equation 1.5:

$$J = \frac{D.c_0}{\ell} \qquad \ldots (1.9)$$

The transient state solution under these conditions is:

$$\frac{Q_t}{\ell c_0} = \frac{D.t}{\ell^2} - \frac{1}{6} - \frac{2}{\pi^2} \sum_{n=1}^{\infty} \frac{(-1)^n}{n^2} \exp\left[\frac{-n^2.\pi^2.D.t}{\ell^2}\right] \qquad \ldots (1.10)$$

where Q_t is the amount of diffusant which has passed through the sheet at time t. At large times, as the steady state is approached, equation 1.10 tends to an asymptotic solution.
As $t \to \infty$:

$$Q_t \to \frac{D.c_0}{\ell} (t - \ell^2/6D) \qquad \ldots (1.11)$$

and hence a graph of Q_t vs. t in the steady state yields an intercept on the time axis (known as the time lag, L) given by (19, 20):

$$L = \ell^2/6D \qquad \ldots (1.12)$$

When the diffusion coefficient is concentration dependent, equation 1.9 defines an average diffusion coefficient, $\bar{D}$, such that:

$$J = \frac{\bar{D}.c_0}{\ell} = \frac{1}{\ell} \int_0^{c_0} D(c)dc \qquad \ldots (1.13)$$

where

$$\bar{D} = \frac{1}{c_o} \int_0^{c_o} D(c)dc \qquad \ldots (1.14)$$

The time lag can be obtained from (21):

$$L = \frac{\int_0^{\ell} x.c_s(x)dx}{\int_0^{c_o} D(c)dc}$$

where $c_s(x)$ is the steady state concentration profile in the sheet.

The sorption of diffusant by a plane sheet, initially free of diffusant, is defined by the following boundary conditions:

$$c(x, 0) = 0 \qquad 0 < x < \ell, \quad t = 0$$
$$c(0, t) = c_o \qquad t \geq 0$$
$$c(\ell, t) = c_o \qquad t \geq 0$$

and for constant D the solution to equation 1.7 may be written as:

$$\frac{M_t}{M_\infty} = 4\left(\frac{D.t}{\ell^2}\right)^{\frac{1}{2}}\left[\frac{1}{\pi^{\frac{1}{2}}} + 2\sum_{n=1}^{\infty}(-1)^n \text{ ierfc}\left[\frac{n\ell}{(4D.t)^{\frac{1}{2}}}\right]\right) \qquad \ldots (1.15)$$

or

$$\frac{M_t}{M_\infty} = 1 - \frac{8}{\pi^2}\sum_{n=0}^{\infty}\frac{1}{(2n+1)^2}\exp-\left[(2n+1)^2\,\pi^2\frac{D.t}{\ell^2}\right] \qquad \ldots (1.16)$$

where M_t is the amount of diffusant taken up by the sheet at time t, and M_∞ is the equilibrium uptake. Equation 1.15 is useful at early times ($M_t/M_\infty < 0.5$) when the summation term is negligible and the diffusion coefficient can be determined from:

$$\frac{M_t}{M_\infty} = 4\left(\frac{D.t}{\pi\ell^2}\right)^{\frac{1}{2}} \qquad \ldots (1.17)$$

At longer times ($M_t/M_\infty > 0.5$), only the first term in the summation in equation 1.16 is significant, and D can be determined from:

$$\ln(1 - M_t/M_\infty) = \ln(8/\pi^2) - \pi^2\frac{D.t}{\ell^2} \qquad \ldots (1.18)$$

Under the boundary conditions for the corresponding desorption:

$$c(x, 0) = c_o \qquad 0 < x < \ell, \quad t = 0$$
$$c(0, t) = 0 \qquad t \geqslant 0$$
$$c(\ell, t) = 0 \qquad t \geqslant 0$$

the above equations are still applicable if M_t is taken as the amount of diffusant lost from the sheet at time t.

When D varies with c, equation 1.17 defines some average value of D over the range 0 to c_o. The mean diffusion coefficient obtained from sorption and desorption kinetics may be defined by:

$$\overline{D} = \tfrac{1}{2}(D_s + D_d) \qquad \ldots (1.19)$$

where D_s and D_d are the values of D obtained from the initial rates of sorption and desorption respectively. $\overline{D}$ is given to a first approximation by equation 1.14 ie:

$$\overline{D} = \frac{1}{c_o} \int_0^{c_o} D(c)dc$$

Crank (18) has shown that the initial rates of sorption and desorption are controlled more closely by weighted-mean diffusion coefficients of the form:

$$D_s = p.c_o^{-p} \int_0^{c_o} c^{p-1}.D(c)dc$$

$$D_d = q.c_o^{-q} \int_0^{c_o} (c_o-c)^{q-1}.D(c)dc$$

From numerical calculations for a wide range of D, c dependences in which D increased with c, it was found that p = 1.67 and q = 1.85, and when D decreases with increasing concentration it has been shown (22) that p = 1.85 and q = 1.67.

1.3 Block and Graft Copolymers (23)

Linear block copolymers are polymers of the form AB or ABA, where A and B represent long sequences of one monomeric unit. Their preparation is generally based upon an anionic or "living" polymerisation process in which the two monomers are added sequentially, such that the living chain ends of polymer A are used to initiate polymerisation of the second monomer (24). Although this method is quite general for

AB type di-block copolymers, the preparation of ABA tri-block copolymers can present problems, since if the living polymer A is used to initiate polymerisation of monomer B, then the living chain ends of polymer B are not usually sufficiently basic to initiate polymerisation of monomer A. Difunctional initiators, such as 1,4-dilithio-1,1,4,4 tetraphenyl butane, can be used to produce living polymers having an anion at either end of the chain, both of which can then initiate polymerisation of the second monomer (25). Alternatively, a living AB di-block copolymer may be quenched with a coupling agent to join the chain ends, which produces a linear block copolymer, or a star-shaped copolymer, depending upon the functionality of the coupling agent (26).

The existence of two distinct phases in these materials is shown directly by electron microscopy and by thermal or thermomechanical analysis which show two distinct glass transitions as opposed to the single intermediate glass transition temperature of a random copolymer (27, 28). The incompatibility of the different polymer segments is due to the very small entropy gained by mixing different kinds of long chains, and in the limit of infinite molecular weight only polymer pairs with zero or negative heats of mixing form a single phase (29). A number of different morphologies have been observed for block copolymers depending upon the molecular weight of the blocks, the volume fraction of each component, and the method of sample preparation. At low volume fractions of polymer A spheres of A are formed dispersed in a matrix of B, and a morphology consisting of rods of A is observed at higher volume fractions. As the volume fraction of A approaches 0.5, alternating lamellae of A and B are formed, and the morphologies are reversed when the volume fraction of A exceeds that of B.

Commercially available block copolymers are the tri-block SIS (styrene-isoprene-styrene) and SBS (styrene-butadiene-styrene) thermoplastic elastomers. At normal temperatures these are tough, highly elastic materials, while at higher temperatures the flow behaviour of linear polymers is approached. The molecular weight of the polystyrene end blocks is typically 5,000 to 10,000, and that of the central rubbery block 50,000 to 100,000, giving a composition of approximately 20% polystyrene. The morphology of these materials is generally spheres of the glassy polymer in a rubber matrix; the glassy domains anchor the polystyrene chain ends to behave as multifunctional cross-links in the rubber, and also act as reinforcing filler particles.

Thus the material is a tough elastomer, although some permanent deformation occurs at high strains when the glassy domains may become elongated. At temperatures above the T_g of the glassy polymer the material is able to flow, but viscosities remain appreciably higher than for a linear polymer of corresponding molecular weight (30).

Graft copolymers consist of pendant chains of polymer B chemically linked to a backbone of polymer A. A number of methods have been used to prepare graft copolymers (31) the most important of which is radiation grafting using either ^{60}Co gamma radiation or Van de Graff type electron accelerators. There are four major types of radiation grafting (32):

1. the direct irradiation of polymer A containing a second monomer B;
2. grafting on to radiation-peroxidized polymers;
3. grafting initiated by trapped radicals;
4. the intercrosslinking of two different polymers;

and of these the first is the most widely used.

Other methods of preparation include chemical syntheses in which the initiation of the polymerisation of B is by the removal of a labile atom or group from polymer A, or in which chain transfer from the growing polymer chain to the backbone polymer occurs, and mechanical syntheses where a mixture of two or more polymers are subjected to mechanical degradation. Although the latter method often forms block copolymers, graft copolymers are obtained if the polymers undergo disproportionation reactions.

The morphology of grafted copolymers has not been studied as extensively as that of block copolymers, although the two-phase nature of these systems is well established (33).

1.4 The Present Investigation

The aim of the work presented here is the investigation of the transport properties of hydrocarbon gases in block and graft copolymers and the correlation of these properties with the sample morphology. The graft copolymers were prepared by the radiation grafting of styrene on to poly({c.l.}-dimethylsiloxane) (PDMS). In addition, PDMS and

three membranes prepared from a block copolymer of PDMS and polystyrene were studied. The compositon of the graft copolymers varied from 0 to 56% by weight of polystyrene and in each case the PDMS formed a continuous rubbery matrix and the polystyrene was present as a dispersed glassy phase. This was confirmed by transmission electron microscopy of selected samples. The transport properties of methane and propane in polystyrene were also studied and the results analysed in terms of the dual mode sorption theory for glassy polymers.

The measurement of P, D, and S for the series of graft copolymers, which had been prepared and studied in the same manner, allows comparisons to be made between the results obtained for each membrane and constitutes a reliable test for the models of transport in heterogeneous media. The three membranes which had been prepared by different methods from the same block copolymer illustrate the effect that the method of preparation can have upon the morphology of the copolymer and also show significant differences from a graft copolymer of a similar composition. Diffusion coefficients were measured by steady state, time lag, and sorption rate methods for PDMS and the copolymers and by the sorption rate method only for polystyrene. The low permeabilities of hydrocarbons in polystyrene relative to PDMS mean that the glassy domains of the copolymers are effectively impermeable although they have a significant solubility. These materials thus provide examples of diffusion with immobilisation and the diffusion coefficients are interpreted in this way.

CHAPTER 2

LITERATURE REVIEW

2.1 Transport in Heterogeneous Media: Models

A large number of materials in common usage are heterogeneous in nature and estimation of the properties of such materials from the properties of the individual phases making up the composite is an important area of study. Heterogeneous polymer systems include block and graft copolymers, polymer blends, and partially crystalline polymers in addition to filled polymers and fibre reinforced plastics. The models for transport in heterogeneous media have largely been derived for analogous properties, chiefly electrical permittivity, electrical conductance, and thermal conductivity, which are also described by Laplace's equation. Only binary phase systems have been studied in any detail, and, with one or two exceptions, only the steady-state solutions have been obtained. The literature has been reviewed many times, (34, 35, 36) and in some detail by Barrer (37). In the following section all equations are given in terms of permeabilities irrespective of the original derivation; P_M is used to denote the permeability of the material and P_C and P_D the permeabilities of the component phases, present in volume fractions V_C and V_D, where the subscripts C and D are used to denote the continuous and disperse phases where applicable.

The simplest equations, representing the upper and lower limits for the permeability of the composite, are the parallel (two phases parallel to the direction of flow) and series (laminate structure) models.

$$\text{Parallel:} \quad P_M = P_C.V_C + P_D.V_D \qquad \ldots (2.1)$$

$$\text{Series:} \quad 1/P_M = V_C/P_C + V_D/P_D \qquad \ldots (2.2)$$

A simple empirical expression applicable to a heterogeneous mixture was given by Lichtenecker (38) and an attempt to justify this expression was made by Lichtenecker and Rother (39).

$$\log P_M = V_C.\log P_C + V_D.\log P_D \qquad \ldots (2.3)$$

Although it has been pointed out several times in the literature that

the Lichtenecker model is fundamentally incorrect (40), its simplicity and success in describing experimental results (particularly when P_D is not very different from P_C) has led to fairly wide usage as a working approximation. Reynolds and Hough (34) have pointed out that the assumption of repeated mixing, namely that P_M is independent of the method of preparation of the mixture, is unjustified for a two-phase mixture. The assumption is valid for a miscible system, and it is of interest to note that the Lichtenecker equation has been used for the permeability of homogeneous polymer systems, and also that it is virtually equivalent to the method of "permachors" developed by Salame (41) for the permeability of homogeneous random copolymers.

An exact expression for the permittivity of a single sphere in a continuum was presented by Maxwell (42) and has been applied successfully to dilute suspensions of spheres.

$$\frac{P_M}{P_C} = \frac{P_D + 2P_C - 2V_D(P_C - P_D)}{P_D + 2P_C + V_D(P_C - P_D)} \qquad \ldots (2.4)$$

This expression has been further developed by Fricke (43) and by Burger (44) to cover the cases of spheroidal and ellipsoidal particles respectively. Lord Rayleigh (45) considered a cubic array of spheres and analysed the effect on the potential in the neighbourhood of a sphere due to 248 of its closest neighbours lying within the first 15 surrounding shells, and derived the expression:

$$\frac{P_M}{P_C} = \frac{(2P_C + P_D)/(P_C - P_D) - 2V_D - K[(3P_C - 3P_D)/(4P_C + 3P_D)]V_D^{10/3}}{(2P_C + P_D)/(P_C - P_D) + V_D - K[(3P_C - 3P_D)/(4P_C + 3P_D)]V_D^{10/3}} \qquad \ldots (2.5)$$

Rayleigh's original value of K (1.65) was corrected for a missing factor of $1/\pi$ by Runge (46), who gave the value of K as 0.525. De Vries (47) calculated values of K for the simple lattices: simple cubic (1.31), body centred cubic (0.129), and face centred cubic (0.0752). A re-examination of Rayleigh's original solution by Meredith and Tobias (48) gave an expression similar to equation 2.5 but involving terms in $V_D^{7/3}$, which leads to significant deviations from the Rayleigh-Runge equation as the limit for close packing of spheres ($V_D = 0.5236$) is approached. Their equation gave the coefficient of the $V_D^{10/3}$ term as 1.315, in good agreement with the K value of de Vries, and gave

better agreement with experimental results obtained for a model system.

Several approximations have been proposed for a random dispersion of particles in a continuum, and one of the most widely used is that of Bruggeman (49), who calculated the permittivity of a dispersion of ellipsoids by an integration method. In effect he used the first two terms of the Taylor's expansion of equation 2.4 to determine the change in permittivity caused by a small addition to the disperse phase, and integration between limits gave the following expression for a random dispersion of spheres:

$$V_C = \frac{(P_D - P_M)}{(P_D - P_C)}\left(\frac{P_C}{P_M}\right)^{1/3} \qquad \ldots (2.6)$$

Meredith and Tobias (50) pointed out that the integration method of Bruggeman is only strictly applicable for a large range of particle sizes such that, at any point during the integration, the dispersion may be considered as a continuum with respect to the particles of disperse phase added. By use of a similar technique but using only two particle sizes, present in equal volume fractions, these authors obtained an expression which gave better agreement with experimental results for a small range of particle sizes, but attribute their success, in part, to compensating errors.

The expression due to Böttcher (51), and also Polder and Van Santen (52), was derived by assuming that the permittivity and electric field in the continuum surrounding each particle was equal to that of the composite. They obtained, for a random dispersion of spheres:

$$P_M = \frac{1}{2}\left\{3(V_C.P_C + V_D.P_D) - (P_D + P_C) + \frac{P_C.P_D}{P_M}\right\} \qquad \ldots (2.7)$$

where the original expression has been rearranged to show that the continuous and disperse phases are interchangeable. Equations 2.3 and 2.7 produce single continuous curves over the range of volume fraction, whereas all other approximations give two curves depending upon the choice of continuous phase.

Higuchi (53, 54) used an approximation for the perturbation of the electric field in the neighbourhood of a particle due to the influence of neighbouring particles to derive the following expression:

$$\frac{P_M}{P_C} = \frac{2P_C.V_C + P_D(1 + 2V_D) - K[(P_D - P_C)/(2P_C + P_D)]^2(2P_C + P_D)V_C}{P_C(2 + V_D) + P_D.V_C - K[(P_D - P_C)/(2P_C + P_D)]^2(2P_C + P_D)V_C} \quad ...(2.8)$$

The parameter K in equation 2.8 is a function of volume fraction involving the radial distribution function for random spheres. Higuchi found the expression to be relatively insensitive to K, and a value of K=0.78 gave a good fit to a wide range of experimental data. Due to this "neglected" function of volume fraction, equation 2.8, unlike equations 2.5 to 2.7, does not reduce to the Maxwell expression at low V_D, except for the case of K=0.

Several authors have considered the case of a membrane containing rectangular heterogeneities arranged in a simple lattice. Barrer and Petropoulos(55) considered regular lattices of rectangular parallelepipeds and derived a general expression containing several undetermined parameters. More useful expressions were obtained for a number of special cases such as impermeable filler particles, laminated materials, and materials having a high volume fraction of disperse phase. A similar model was employed by Kubin and Spacek (56) who, by the use of simplifying assumptions, derived explicit expressions for the permeability and diffusion coefficients. Bell and Crank (57) obtained numerical solutions for the problem in two dimensions and, on the basis of these results, suggested a weighted average of the series and parallel equations to obtain effective diffusion coefficients for long particles of a disperse phase arranged in a regular lattice. These authors also reviewed several previous approximations based on the series-parallel formulation and found that their expression gave better agreement with more accurate treatments. A simplified model of a filled polymer was used by Nielsen (58) to obtain the following expression:

$$P_M = P_C.V_D/[1 + (L/2W)V_D] \quad ... (2.9)$$

where L is the length of the face and W the width of a filler particle, and the disperse phase (filler) is impermeable. Equation 2.9 was derived from a simple approximation to the tortuosity, or increased path length of a permeating molecule, due to the presence of idealised rectangular filler particles. Nielsen also considered the case of liquid permeants in which the flux at the surface of the filler is

significant, and derived expressions for the permeability under these circumstances.

A novel approach adopted by Brown (59), and later by Prager (60), was the calculation of permeability by the statistical averaging of the permeabilities at all points within a composite. Brown developed a solution in the form of a power series containing an undetermined parameter λ which, by suitable choice of λ, could be made equivalent to the expressions of Maxwell, Bruggeman, or Böttcher, to the third order of small quantities. Prager employed a different averaging technique and obtained expressions for the diffusion coefficient in the limiting cases of zero and infinite diffusivity of the disperse phase, corresponding to porous materials and solidified foams respectively. In principle Prager's expression for the diffusion coefficient of porous media should also be applicable to a filled polymer system with impermeable filler. It is readily shown that for an impermeable, non-sorbing filler $P_M/P_C = D_M.V_C/D_C$ where D_M and D_C are the diffusion coefficients of the composite and continuous phases respectively. It is suggested here, however, that the expression given by Prager contains an additional factor of V_C and hence is applicable to the permeability rather than the diffusion coefficient which then gives:

$$P_M = \frac{P_C.V_C(V_D + V_C.\ln V_C)}{2(V_D + V_C.\ln V_C) - \frac{1}{2}V_C(\ln V_C)^2} \qquad \ldots (2.10)$$

Prager's method essentially consists of taking the diffusion coefficient and the concentration gradient at each point within the medium and averaging over all points to obtain the mean flux. For this procedure the correct concentration should be referred to a unit volume of the particular phase at the point, rather than a unit volume of the composite, and use of the latter leads to an expression for D_M containing and additional factor of V_C. As given above equation 2.10 is in good agreement with the expressions of Maxwell and others over a large range of volume fraction.

Several authors of review articles have proposed their own empirical relationships for the permeability of heterogeneous media. In particular Pearce (35) proposed the following equation:

$$\frac{P_M - P_C}{P_D - P_C} = \frac{(1 - \nu)V_D}{1 - \nu.V_D} \quad \ldots (2.11)$$

where the parameter ν is constant for given conditions, and showed the validity of his expression for a wide range of experimental data. The usefulness of equation 2.11 is severely limited by the use of the adjustable parameter ν. Mitoff (40) points out that in many cases the models are more exact than the morphology of the composite or the experimental data. Simple equations are offered, which it is claimed, are just as likely to give good approximations as more sophisticated treatments when the above factors are not accurately known.

It is apparent from comparisons of the models (36) that, despite the wide variety of mathematical forms, the differences remain small under most circumstances, and the equation of Maxwell is a good approximation at low volume fractions of the disperse phase. The spatial arrangement of the disperse phase is found to have little effect upon the overall permeability whereas the effect of particle shape is much more pronounced. An impermeable lamellar filler, for example, will give a much larger reduction in permeability than an equal volume fraction of spherical or spheroidal particles.

2.2 Transport in Heterogeneous Polymer Systems

There is a large volume of literature concerning transport in heterogeneous polymer systems although little reference has been made to the models reviewed in the previous section. Polymers containing an impermeable filler are in principle the simplest of heterogeneous systems and an early study by Van Amerongen (61) showed most of the general effects exhibited by filled polymers. For rubber filled with inorganic fillers the effect of the filler upon gas permeability was independent of the nature of the filler and depended only upon its volume fraction. E_p values were found to be constant for all these systems. Lamellar fillers such as mica showed a much greater effect and carbon black, an adsorbing filler, was found to influence both solubility and diffusion coefficients to a much greater extent than permeabilities. Natural rubber membranes containing up to 40% by volume of zinc oxide filler were studied by Barrer et al (62).

Although the membranes were thought to contain non-uniform dispersions with particle conglomerates, particularly at high volume fractions of filler, satisfactory agreement was obtained with permeability values based on a randomly oriented array of cylinders. Kwei (63) investigated the sorption of water vapour by filled and unfilled epoxy polymers and discussed the derived thermodynamic quantities in terms of the reduced mobility of the polymer in the region of a filler particle. Kwei and Arnheim (64) measured diffusion coefficients of gases in filled polyvinyl acetate and compared the activation energies for diffusion with those obtained by Meares for the unfilled polymer (65). The ratio of the diffusion coefficients quoted in this work is significantly lower than that calculated from any of the models, and this may be due to adsorption by the filler as discussed later in this section. The transport of water vapour in filled and unfilled silicone rubbers has been studied by Barrie and Machin (66, 67). One series of samples contained small amounts (less than 5% by weight) of sodium chloride, and the permeabilities of these samples were little changed from that of the unfilled polymer. A second series of samples containing from 20 to 40% by weight of silica filler showed reduced permeabilities although it was thought that appreciable transport may have occurred through the filler or through air gaps between filler particles. This is consistent with the reported permeabilities which are 5 to 8% higher than permeabilities predicted by the models.

Finger et al (68) investigated the influence of adsorptive fillers upon permeation with particular regard to the effect upon the diffusion time lag. Expressions for the time lag are given for two distinct cases; case 1 for a filler exhibiting Henry's law sorption, and case 2 for a filler which saturates at low penetrant activity. Cooper (69) pointed out that the expressions of Finger et al are erroneous and gave a more rigorous derivation of the time lag equation for a membrane containing an adsorbing filler. The limiting expressions corresponding to both cases are correctly given although the conditions implied for the case 2 approximation of Finger are such that, for this particular case, the correction is of little significance. The diffusion of ethyl p-aminobenzoate in silicone rubber membranes containing up to 25% by weight of silica filler was studied by Most (70). Diffusion coefficients obtained by the simple time lag expression (equation 1.12) were decreased by a factor of 15 for the 25% filled membrane due to

adsorption by the filler, whereas steady state permeabilities were decreased by only 21%. It has been found by the author that the permeability values are in excellent agreement with the models of Maxwell and others, which are not widely different for the low volume fractions of filler employed. Flynn and Roseman (71) analysed the data of Most in addition to their own data obtained using a membrane of commercial silicone rubber of unknown filler content. These authors pointed out that the case 1 expression of Finger et al does not reduce to the correct value for zero filler content, and correctly stated that the time lag is influenced by the amount of penetrant lost to the adsorbing filler relative to that diffusing in the continuum. However they then derived their own expression based upon the ratio of concentration gradients in filled and unfilled membranes instead of adsorbing and non-adsorbing filled membranes. Their expression is incorrect, but does reduce to the correct limit at zero filler content. Their paper also contains a number of errors which imply an incomplete understanding of the transport process. A silicone rubber membrane containing a dispersion of a highly adsorptive molecular sieve was used by Paul and Kemp (72) as a model for dual mode sorption. They were able to verify the variation in the time lag with ingoing pressure predicted earlier by Paul (73) for this type of system and obtained good agreement with the Higuchi model for experimentally determined permeabilities. In a later paper (74) the kinetics of sorption in these membranes is reported.

The dependence of the transport properties of gases upon the degree of crystallinity of a polymer has been studied by several workers. Michaels and Parker (14) used samples of polyethylene and ascribed the reduction in diffusion coefficient with increasing degree of crystallinity to two distinct factors; the tortuosity due to the presence of impermeable crystallites, and a chain immobilisation effect in the amorphous region immediately surrounding the crystallites. The latter factor was deduced from the dependence of the reduction in diffusion coefficient upon the molecular size of the penetrant since this reduction would be a constant factor if it were due only to the geometrical impedance of the crystalline regions. (This analysis is analogous in many respects to that of Klute (75) whose "transmission function" is the product of two factors, one the "detour ratio" which is the reciprocal of the tortuosity.) The tortuosities determined

were found to be significantly higher than those predicted by the expression of Maxwell or by that of Fricke for oblate spheroids with a 4 : 1 axial ratio. Later work by Michaels and Bixler (76) led to estimates of between 20 and 50 for the axial ratio of polyethylene crystallites and was interpreted by these authors as evidence for the ribbon-like lamellar nature of the crystallites. The additional lowering of the diffusion coefficients due to the reduced chain mobility has been noted by several authors (77 - 79) and an alternative explanation that small molecules are able to diffuse through imperfections in the crystallites has been proposed (80). This has meant that useful comparisons with the predictions of the models have not been possible unless some estimate of the chain immobilisation factor is made and, in general, this has not been attempted.

Gas and vapour transport in graft copolymers have been reported extensively in the literature. Much of the early work in this field was concerned with the modification of the water sorption properties of polyethylene, cellulose, and natural fibres, and has been reviewed by Sheer (81). The morphology of these copolymers is generally uncertain and may be dependent upon the method of preparation. In a series of papers by Huang and co-workers (82 - 84) describing transport in polyethylene grafted with styrene, the results are analysed in terms of the decreased free volume of the polymer using expressions for the free volume applicable to a homogeneous random copolymer. No justification is given for this procedure and no evidence for the single phase nature of the copolymer is available. The results are further complicated by decreases in the crystallinity of polyethylene upon grafting and, in the case of styrene grafting, a minimum permeability was observed at 20 to 30% of styrene. At this point further decreases in permeability due to increasing styrene content are offset by the increase in the amorphous volume fraction of the substrate. Similar work was reported by Toi et al (85) who stated that short polystyrene chains exhibiting the nature of a random copolymer are to be expected at low levels of grafting, although this statement remains unsupported.

The grafting of acrylonitrile on to polyethylene has also been studied, (83, 86) and in this case the grafted polymer was presumed to act as an impermeable filler to the permeation of gases. The constant values of E_p reported for this copolymer are indicative of a two-phase material in which the permeability is controlled solely by the

continuous phase, (see section 4.4) but the changes in degree of crystallinity on grafting make this system unsuitable for comparisons with the predictions of the models. The permeability of gases and water vapour in cellulose acetate-styrene graft copolymers was investigated by Wellons et al (87) and it was suggested that the grafted polymer films contained domains of each polymer type. Reported viscosity average molecular weights of the component polymers are greater than 30,000 for all the samples studied and phase separation is therefore to be expected. The data, however, are highly inconsistent; reported permeability values for the graft copolymers are both larger and smaller than the limiting values of the homopolymers. Later work from the same laboratory concerned polyoxymethylene grafted with butadiene and with acrylonitrile (89). Increased permeabilities were observed for the butadiene copolymers whereas grafting with the relatively impermeable acrylonitrile led to decreases in the overall permeability. The morphology of the copolymers is not clear and, as is the case for the majority of studies on transport in graft copolymers, the results were interpreted in terms of the change in free volume of the polymer. Grafting with butadiene was presumed to cause swelling and disruption of the polymer structure leading to an increased free volume, whereas the relatively insoluble acrylonitrile was thought to fill the available free volume with grafted polymer. No supporting evidence for this rather simple explanation is available in the literature.

The gas permeabilities of polyisoprene membranes grafted with methyl methacrylate were studied by Rogers et al (88). Preferential solvents for the rubber or for the graft polymer were present during the polymerisation process, and samples were also prepared both with and without the use of a chain transfer agent. Although qualitative agreement was obtained between the permeabilities and the proposed changes in domain structure caused by the different polymerisation conditions, the reported permeabilities are significantly lower than values predicted by the models for the proposed two-phase morphology. Sheer (81) has studied the transport of water vapour in a series of copolymers of PDMS grafted with up to 44% by volume of vinyl acetate. Glass transition temperatures, density, and solubility measurements indicated complete phase separation, and electron microscopy showed the polyvinyl acetate to be dispersed as discrete spherical domains.

Excellent agreement with the Higuchi model was obtained for both P and E_p in this well characterised system.

There have been relatively few reports of transport in block copolymers and this undoubtedly reflects the more recent development of these polymers. Chen and Ferry (90) used radioactively tagged hydrocarbons in a study of diffusion through rubbery polymers including both block and random copolymers of butadiene and styrene. Diffusion in the block copolymers was interpreted in terms of relatively impermeable polystyrene domains in the polymer and it was suggested that the lower diffusion coefficients in the SBR random copolymers are due to their lower free volume compared with homopolybutadiene. No attempt was made to interpret the results quantitatively. Modulus and gas permeability data have been determined by Robeson et al (91) for a range of polysulphone-PDMS block copolymers of the $(AB)_n$ type. The molecular weights of the blocks were typically 5,000 or greater and all results were interpreted in terms of a two-phase system. These authors considered that at the extremes of the composition range the permeabilities can be represented by the expression of Maxwell with either PDMS or polysulphone as the continuous phase, and at intermediate compositions a weighted mean of these two cases was proposed. (A similar analysis using an equation due to Kerner (92) was proposed for the modulus of the copolymers.) Phase inversion was considered to occur at the composition at which the fractional contribution of the two expressions is equal, and values of 0.53 and 0.51 volume fraction of polysulphone were obtained from the permeability and modulus data respectively. It was recognised that the morphology of the copolymer at intermediate compositions is expected to be quite different from the spherical particles upon which both Maxwell's and Kerner's models are based but it was suggested that the consistency of the two sets of results offers a strong argument for the validity of the proposed model. Further work contrasted the gas permeability characteristics of block and random copolymers of styrene and methacrylonitrile (93). Plots of log P against composition for the block copolymers were sigmoidal in shape, as expected from the earlier work, whereas similar plots for the random copolymers were in reasonable agreement with the Lichtenecker rule (equation 2.3).

Ziegel (94) has studied the transport of gases in four segmented polyurethanes and used a model in which the rigid phase is dispersed

as uniform spheres within the soft phase elastomer. For the larger penetrants studied, namely argon, nitrogen, and oxygen, the permeation appeared to be the sum of two individual gas flow patterns which was interpreted as being due to the relatively slow diffusion into the rigid phase. This behaviour is unique within the literature and has not been substantiated by any later work. Higuchi (54) gives the condition for Fickian behaviour of a heterogeneous membrane in terms of the transport properties of the two phases and the characteristic dimension of the disperse phase. Applying this condition to the data of Ziegel leads to a radius of approximately 20 μm for the disperse phase for equilibriation on a one second time scale, whereas domain sizes reported for block copolymers are typically two or three orders of magnitude smaller. In addition, the experimental time scale is several minutes and much larger domains would consequently be required in order to produce the observed effects. The interpretation offered by Ziegel is clearly questionable and further elucidation is not assisted by the novel gas flow technique employed (95).

Permeation, diffusion, and solubilities of inert gases in styrene-butadiene-styrene block copolymers have been investigated by Odani et al (96, 97). Apparent permeabilities for the polybutadiene matrix were evaluated from the parallel model (equation 2.1) and comparison with the permeability of the homopolymer was then used to obtain the product of the tortuosity and chain immobilisation factor, as defined by Michaels and Parker (14). This amounts to the use of tortuosities to overcome the inadequacies of the parallel model, a procedure which would give correct permeabilities only for the case of an impermeable disperse phase. The failure of this approach is evident from the calculated tortuosities (which are less than 1 for a membrane with rod-like domains of polystyrene), and may be due to the finite permeability of polystyrene to the gases used. Propane transport in a series of PDMS-polycarbonate block copolymers has been studied by Williams (98). The polymers were of the $(AB)_n$ type in which the block lengths were relatively short, the average length of the PDMS blocks being between 20 and 80 monomer units. Permeabilities were much lower than those predicted by the models, due to incomplete phase separation in these systems, and the results were interpreted in terms of a disperse phase of polycarbonate within a continuum containing both polymers. By use of the Lichtenecker rule for the permeability of the continuum, an

analysis was developed to determine the composition of the continuous phase and the volume fraction of disperse phase for each membrane studied.

The transport properties of polymer blends have recently been well reviewed by Hopfenberg and Paul (99) and much of the literature on other heterogeneous polymer systems is also included. Early studies of gas permeabilities of natural rubber blended with a variety of synthetic elastomers by Barbier (100) led to the formulation of an empirical equation for the prediction of blend permeabilities. The data have been found to give good agreement with the Maxwell model with natural rubber as the disperse phase (99). Permeability and solubility coefficients of polyethylene blends have been determined by Ito (101). A maximum permeability was observed for blends with polypropylene and polyisobutylene which is presumably due to a lowering in the crystalline content of the polymer. Blends of high and low density polyethylene (HDPE/LDPE) showed a continuous decrease in permeability with increasing volume fraction of HDPE. Pieski (102) has also reported on the water permeability of HDPE/LDPE blends and the linear relationship obtained when his data are plotted as log P against composition may be indicative of a homogeneous blend (99). A series of papers by Shur and Ranby (103 - 107) concerning gas permeability in polyvinyl chloride blends adds further evidence to the view that the Lichtenecker rule (equation 2.3) is a valid approximation for a homogeneous system. Increased polarity of the second polymer was shown by dynamic mechanical loss measurements to result in increased compatibility of the polymers, and semi-log plots of permeability against composition exhibited increasing linearity. The partial miscibility of these systems renders them unsuitable for analysis using the models for transport in heterogeneous media. Stallings et al (108) have studied the transport of fixed gases in glassy blends of polystyrene and polyphenylene oxide, a blend system which shows complete compatability over the whole composition range. Anomolous behaviour was observed for the transport of neon and this was attributed to changes in the dual mode sorption characteristics of the blends.

Oxygen permeability data in heterogeneous films prepared from mixtures of polymer latices were obtained by Peterson (109) and good agreement with the predictions of Higuchi for both steady state and transient state permeation is reported. In fact, Peterson used a

simplification of the Higuchi equation by taking the K of equation 2.8 equal to zero, and under these circumstances the equation reduces to that of Maxwell.

It is evident that the transport properties of a wide variety of heterogeneous polymer systems have been studied although in the majority of cases useful comparisons with the theoretical models are not possible. This is due to the unknown morphology of the polymers, often due to changes in crystallinity or partial miscibility of the components. The equations of Maxwell and Higuchi have been used almost exclusively in the few comparisons reported, and have proved to be adequate for much of the data. It is also apparent that there is a growing volume of evidence to support the use of the Lichtenecker rule for homogeneous systems although, as yet, this has no theoretical justification.

2.3 Dual Mode Sorption

The concept that two concurrent modes of sorption are operative in glassy polymers has recieved considerable attention in recent years and has become known as the dual mode sorption or, more simply, dual sorption theory. The early development of the theory has been well reviewed by Vieth (110) and only a brief outline and the more recent developments will be given here.

The equilibrium sorption part of the theory is simply expressed by the following equation:

$$c = c_D + c_H$$

$$= k_D.p + c'_H.\frac{b.p}{1 + b.p} \qquad \ldots (2.12)$$

Here c is the overall concentration of penetrant at pressure p which may be divided into the two modes of sorption: c_D, the concentration of penetrant sorbed by the normal dissolution process, and c_H, the concentration of penetrant sorbed into pre-existing "holes" or micro-voids within the glassy polymer. Normal dissolution is envisaged as essentially the same process as occurs in rubbery polymers and c_D obeys Henry's law with a dissolution constant k_D. Hole filling represents localised sorption and the concentration c_H is given by a Langmuir isotherm. In equation 2.12 c'_H is the hole saturation constant

and b the hole affinity constant.

In much of the early work in this field the dual mode sorption parameters, k_D, c'_H, and b, were obtained by graphical analysis of the isotherm. At low pressures, such that $b.p << 1$, equation 2.12 reduces to the linear form:

$$c = (k_D + c'_H.b).p \qquad \ldots (2.13)$$

and at high pressures ($b.p >> 1$) a linear asymptote is approached given by:

$$c = k_D.p + c'_H \qquad \ldots (2.14)$$

The method of analysis employed by Vieth (110) was to determine k_D from the limiting high pressure slope of the isotherm (equation 2.14) and, by subtraction of the dissolved gas concentration, c_H was obtained as a function of pressure. This was then plotted according to the following linearisation of the Langmuir isotherm:

$$\frac{p}{c_H} = \frac{1}{c'_H.b} + \frac{p}{c'_H} \qquad \ldots (2.15)$$

and the parameters c'_H and b determined from the slope and intercept. Koros et al (111) have demonstrated the inadequacies of the graphical method of analysis, and use of a computerised least squares regression analysis was shown to give a more accurate determination of the dual sorption parameters. These authors also tested the Langmuir component of the sorption by the alternative linearisation:

$$\frac{1}{c_H} = \frac{1}{c'_H} + \frac{1}{c'_H.b.p} \qquad \ldots (2.16)$$

which is a more stringent test, since it does not involve pressure in both ordinate and abscissa.

Heats of sorption in glassy polymers provided the origins of dual mode sorption theory as attempts were made to explain the more exothermic heats of sorption of gases in polymers below their glass transition temperature (T_g). Meares (65) suggested that in the rubbery state the heat of sorption contains an endothermic contribution arising from the need of dissolving molecules to create their own space by separating interchain polymer contacts. In a glassy polymer dissolving molecules would be accomodated in pre-existing holes in the bulk polymer structure and the endothermic term would then be absent.

Evaluation of the dual mode sorption parameters has led to two distinct heats of sorption: ΔH_D, the heat of dissolution, and ΔH_H, the heat of the hole filling process. These have been determined from van't Hoff plots of k_D and b respectively.

The temperature dependence of the hole saturation constant, c'_H, has also received some attention, and it has been shown several times, (112, 113) that the Langmuir component of the sorption is absent above T_g. Further, c'_H has been shown to go to zero in the region of the glass transition and Koros and Paul (112) have suggested a tentative quantitative relationship between c'_H and the frozen-in free volume given by the difference between the polymer specific volume and the specific volume obtained by extrapolation from the liquid state.

As originally formulated the dual mode sorption diffusion model for glassy polymers was based upon a set of postulates which may be summarised as follows:

1. gas sorbed according to the Langmuir isotherm is immobilised in frozen-in microvoids;
2. rapid equilibriation occurs between the immobilised gas and mobile gas sorbed according to Henry's law;
3. the diffusion coefficient of the mobile gas is a constant, independent of concentration.

This simple model has proved adequate for much of the data although more recently a small mobility has been ascribed to the Langmuir component of sorption (114, 115). The dependence of the time lag upon ingoing pressure for the case of complete immobilisation has been given by Paul (73), who has also verified the result experimentally for a model system (72). Tshudy and von Frankenberg (116) have examined the effects on the model of a finite rate of equilibriation between the two modes of sorption. No evidence has been reported to suggest that equilibriation is not rapid, and an NMR study of dissolved gas by Assink (117) supports the rapid equilibriation assumption and also suggests the possibility of some small mobility for the Langmuir component.

CHAPTER 3

EXPERIMENTAL

3.1 Materials

Sheets of poly({c.l.}-dimethylsiloxane), PDMS, supplied by Dow Corning Ltd., were prepared by curing a PDMS gum containing 0.143 methylvinylsiloxane units per 100 dimethylsiloxane units with 1% by weight of 2,4 dichlorobenzoyl peroxide. The curing conditions were 5 hours at 115°C followed by a post cure at 200°C for 4 hours. Traces of low molecular weight material were removed by soxhlet extraction with ethyl acetate and samples were then outgassed under high vacuum for 24 hours before use.

Polystyrene of molecular weight approximately 150,000 was obtained from BDH Chemicals Ltd. and polystyrene sheets were prepared by casting solutions in methylene chloride on to a clean mercury surface in a rectangular glass tank. Solutions of less than 5% w/v were used, the concentration being determined by the weight of polystyrene needed to give a film of the required thickness, and the minimum volume of solution necessary to cover the mercury surface. The solutions were filtered using a "Millipore" filter (Mitex, 5μm pore diameter) and the tank covered to exclude dust and to slow the rate of evaporation. Films were formed over a period of 2 to 3 days and samples cut from the centre of the films were outgassed in a vacuum oven at 70°C for several days before use. No attempt was made to anneal the samples. The average film thickness was determined from the weight of a known area of film and the density of polystyrene given in the literature (118).

Two sheets of a polydimethylsiloxane-polystyrene block copolymer of overall molecular weight by GPC of 200,000 and containing 28 mole % polystyrene were supplied by Dow Corning Ltd. The copolymer was prepared by coupling a PDMS-PS diblock copolymer using a coupling agent with a functionality of four, giving a star-shaped molecule with polystyrene end blocks. M_w/M_n by GPC was 1.3 for the polystyrene segments, and less than 1.2 for the PDMS segments. One sheet, CM, was prepared by compression moulding; first pre-heating for 15 mins at 150°C, then moulding at 150°C for 60 mins with a pressure of 2500 psi.

Sheet CC was cast from a 10% by weight solution in cyclohexane and dried under vacuum at room temperature. A further sheet, SC, was cast from a solution of the supplied copolymer in styrene. In order to obtain a sheet of uniform thickness the solvent was evaporated rapidly under reduced pressure.

Poly({c.l.}-dimethylsiloxane-g-styrene) sheets were prepared by mutual irradiation of PDMS swollen with styrene monomer in the ^{60}Co γ-radiation unit of the Nuclear Technology Department. Styrene monomer was first washed with a 10% aqueous sodium hydroxide solution to remove inhibitor, then further washed several times with distilled water and dried over anhydrous calcium sulphate. The monomer was outgassed by freezing in a pear-shaped flask with liquid nitrogen and pumping away the surrounding atmosphere. The sample was then allowed to thaw to release entrapped and dissolved gas before repeating the procedure. After several freeze-pump-thaw cycles the monomer was distilled into an evacuated vessel containing a previously extracted and outgassed sample of PDMS sheet. The vessel was sealed under vacuum and left for several hours to attain sorption equilibrium before overnight irradiation (approximately 18 hrs) with a dose rate of 0.8 Mrad hr^{-1}.

TABLE 3.1 (T_g measured at 10°C/min)

Polymer	Vol. fract. PS	Density (gm cm^{-3})	T_g (°C)
PDMS	0	0.975	-124
PDMS-g-4.9% PS	0.046	0.988	-124, 100
PDMS-g-15.5% PS	0.146	0.990	-124, 101
PDMS-g-26.2% PS	0.248	0.992	-124, 98
PDMS-g-38.2% PS	0.365	1.007	-123, 98
PDMS-g-56.3% PS	0.545	1.015	-124, 99
CM	0.337	1.000	-123, 69
CC	0.337	0.999	-124, 73
SC	0.337	1.002	-123, 72
Polystyrene	1.00	1.047(118)	101

The irradiated polymer was extracted with ethyl acetate in a soxhlet apparatus for 48 hrs to remove all loosely bound homopolymer, and then outgassed under high vacuum for 24 hr. In order to prepare samples with a high polystyrene content (>30%), a second grafting, following the same procedure, was required. The polystyrene content of the material was determined from the weight increase of the sample. Although it is possible that some high molecular weight homopolymer remains after extraction, it is believed that this does not affect the transport properties of the gases investigated and no distinction has been attempted between grafted polystyrene and high molecular weight polystyrene held by entanglements.

Densities of the PDMS polymers were measured by the water displacement method, and glass transition temperatures of all samples were obtained by DSC using a Du Pont 990 Thermal Analyser. The physical properties of the polymers are listed in table 3.1 and transmission electron micrographs of selected copolymer samples are included in appendix C.

The gases used in this investigation, methane, propane, n-butane, and iso-butane, were obtained from the National Physical Laboratory and were all of purity 99.9 mole % or greater.

3.2 Permeation

The permeation apparatus illustrated in figure 3.1 consisted essentially of two distinct sections; the high pressure or upstream side of the membrane consisting of a gas reservoir, G, buffer volume, V_1, and pressure transducer, T, connected via the diffusion cell, C, to the downstream section consisting of a calibrated buffer volume, V_2, and a Baratron capacitance manometer, B. The two sections were connected via taps T_8 and T_5 to the high vacuum or "hivac" line which contained a Pirani gauge, P, (Edwards Vacuum Components) to monitor the vacuum attained and to assist with leak detection. The hivac line was connected via tap T_{11} to the pumping system which consisted of a liquid nitrogen cold trap and a three-stage mercury diffusion pump backed by an Edwards two-stage rotary oil pump.

The gas under investigation was contained in the gas reservoir, G, fitted with a side arm to allow the gas to be frozen back into the

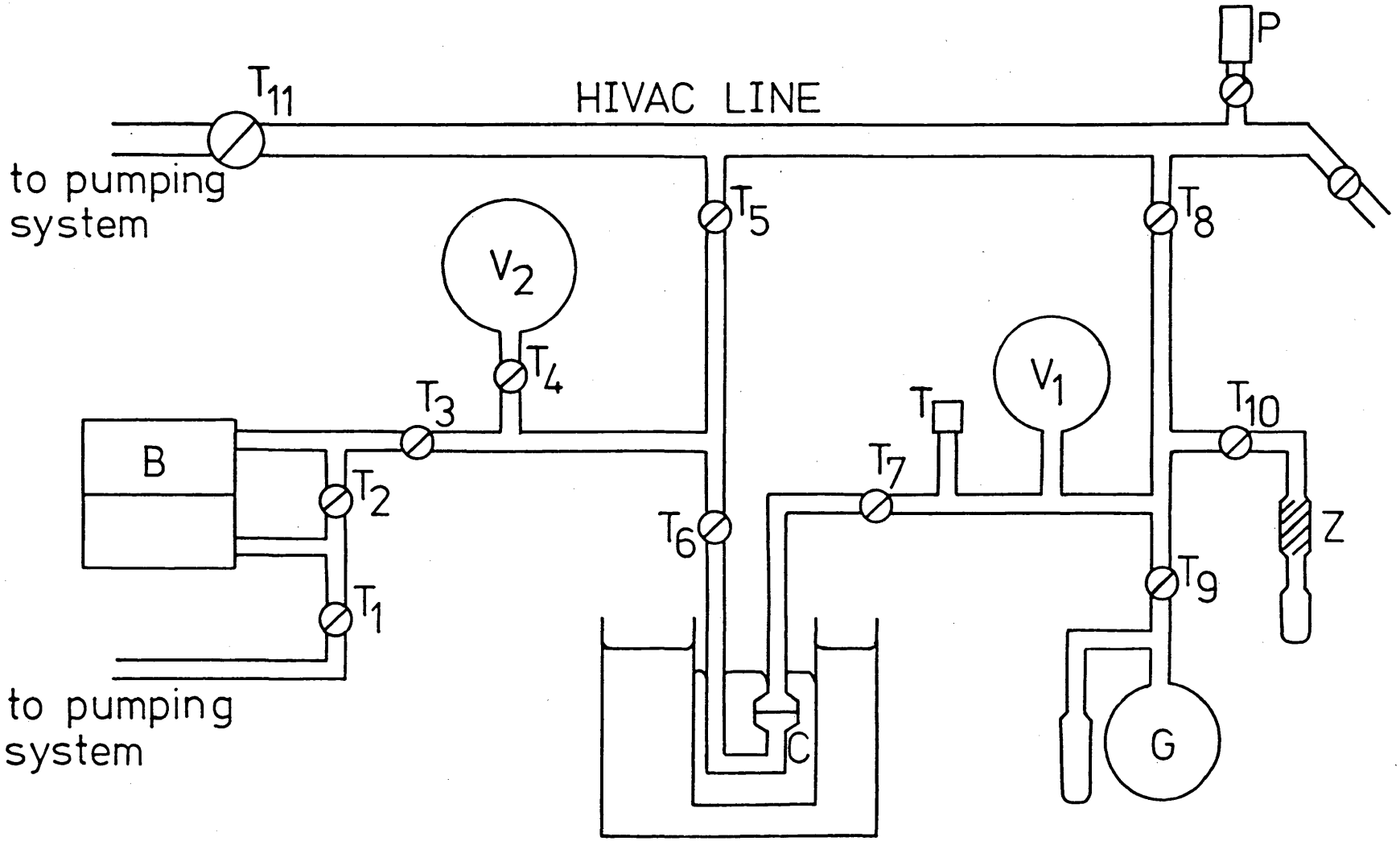

Figure 3.1 : Permeation Apparatus

reservoir after each run. The tube Z, attached to the upstream section of the apparatus via tap T_{10}, contained a zeolite, molecular sieve 4A (BDH Chemicals Ltd.) and was used to remove condensable contaminants, such as carbon dioxide and water, which might otherwise affect the purity of the gas over long periods. A one litre buffer volume V_1 was used to maintain the upstream gas pressure essentially constant during the course of each run, and this pressure was monitored by use of the strain-gauge pressure transducer T (Bell and Howell Ltd., 0 - 10 psi). The transducer was connected to a stable 10 volts DC power supply, and the output measured with a sensitive potentiometer (Pye Portable). The output was found to be directly proportional to the applied pressure and was calibrated against a mercury manometer connected to the hivac line.

The buffer volume on the downstream section of the apparatus, V_2, was calibrated before connection to the apparatus. This was then used to determine the volume of the downstream section by the gas expansion technique. Pressure measurements in the downstream section were made by a Baratron capacitance manometer B (MKS Instruments Ltd. type 90H-3E) connected to a digital pressure indicator, type 100-A. The pressure sensor, which was maintained at $50^{o}C$ by a proportional temperature controller type 1090-1, consists of a thin metal diaphragm held under tension between two fixed electrodes. Small deflections of the diaphragm due to pressure differences between the measuring side and reference side of the instrument are detected as changes in the capacitance of the sensor, and the indicator is essentially an automatically balancing capacitance bridge calibrated in mm Hg. The reference side of the Baratron was connected directly to the pumping system and thus effectively maintained at zero pressure. The range of the instrument was 0 to 3 mm Hg, and a resolution of 10^{-4} mm Hg was possible for all readings.

The diffusion cell, C, was immersed in mercury contained in a specially constructed tall beaker. The beaker was surrounded by a water bath containing two 300 watt "red-rod" immersion heaters controlled by a contact thermometer and mercury relay which controlled the cell temperature to $\pm 0.01^{o}C$. A mercury thermometer immersed in the mercury surrounding the diffusion cell was used to determine the temperature of the membrane. Cotton wool was placed above the mercury as thermal insulation and the top of the beaker was covered with aluminium

foil to minimise escape of mercury vapour into the atmosphere.

The glass diffusion cell is illustrated in figure 3.2 which shows the membrane sealed between two pieces of thick-walled glass tubing. This construction was designed to minimise the clamped area of the membrane which may give rise to significant errors for the relatively thick (>1 mm) membranes employed. The glass tubing of approximately 3 cm o.d. had the edges ground flat to enable a reliable seal to be made to the membrane. A piece of copper gauze, shaped to give a flat surface flush with the rim of the lower piece of tubing, was fixed in place with "Araldite" epoxy resin, and a disc of coarse filter paper (Whatman 540) was placed over the gauze. The membrane was cut to the outside diameter of the tubing and then sealed to the ground glass surfaces with silicone adhesive (Silastic 732-RTV, Dow Corning Ltd.). The assembled cell was clamped under slight pressure for the curing time of the adhesive. After releasing the pressure, the outside of the cell was coated with "Araldite" epoxy resin to prevent strain on the membrane seal during glass-blowing on to the permeation apparatus.

Before taking any measurements, the Baratron was evacuated to 10^{-5} mm Hg and baked out overnight at 140°C with taps T_1 and T_2 (figure 3.1) open to connect both sides of the instrument directly to the pumping system. After cooling to the operating temperature of 50°C, tap T_2 was closed and the measuring side of the Baratron connected to the rest of the apparatus via tap T_3. The diffusion cell was outgassed at 50°C until the build-up of pressure with tap T_5 closed was very small, generally of the order of 10^{-4} mm Hg per hour, and negligible compared with the subsequent permeation rate. This leak rate was also checked prior to each run and, by closing off the buffer volume V_2, this could be achieved in a much smaller time.

The membrane temperature for each run was set on the contact thermometer, and the water bath and diffusion cell left for several hours (usually overnight) to attain thermal equilibrium. Taps T_5, T_7, and T_8 were then closed and gas was admitted to the upstream section of the apparatus via tap T_9. In this way the ingoing pressure could be checked and, if necessary, adjusted before admitting gas to the membrane via tap T_7. The increase in pressure in the downstream section of the apparatus was then monitored as a function of time, and the ingoing pressure and room temperature were checked periodically throughout the run. Pressure readings were recorded once the steady state was

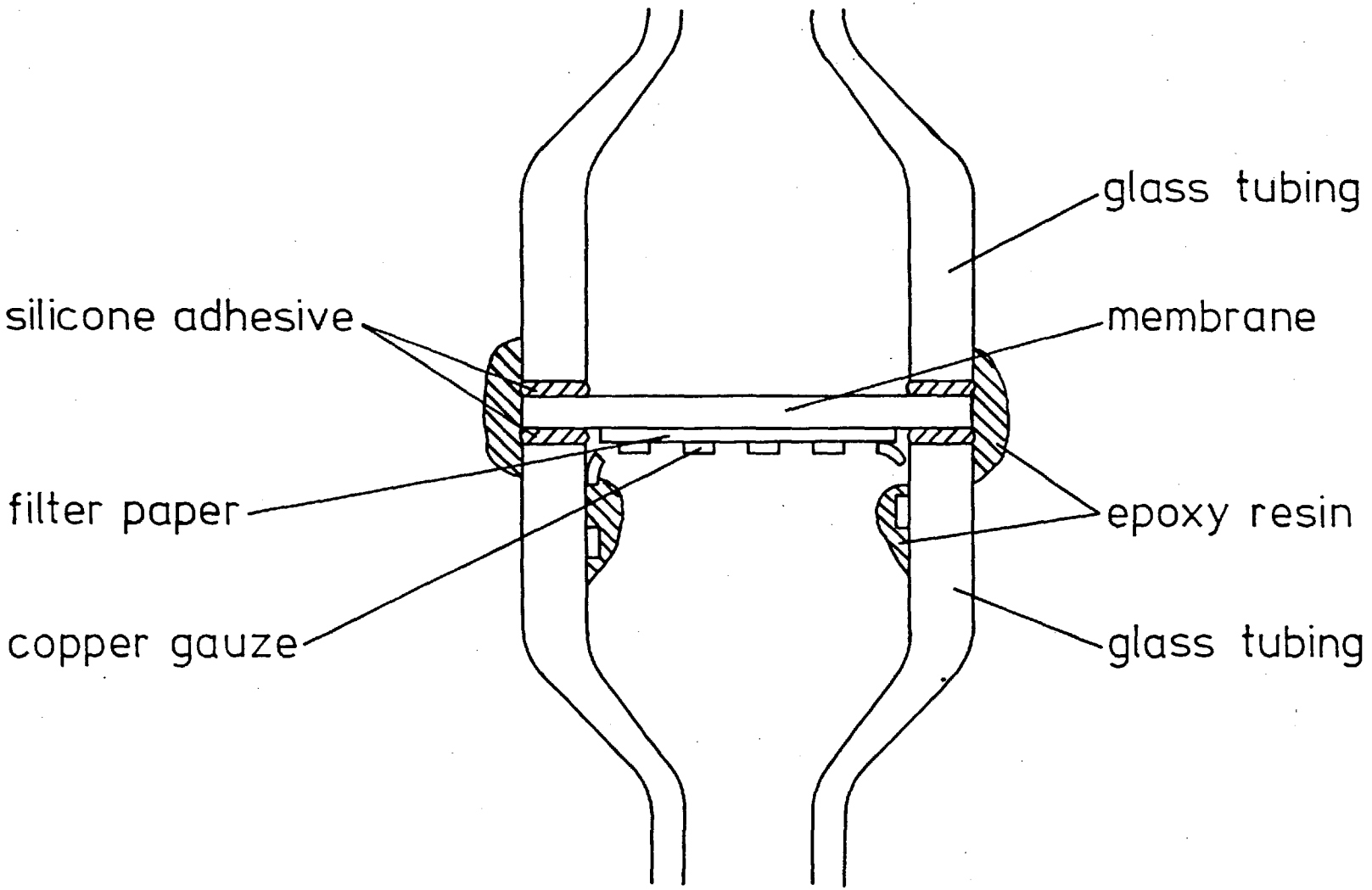

Figure 3.2: Diffusion Cell

attained (after three time lags) and continued for at least a further two time lags to allow an accurate extrapolation back to zero pressure, although the downstream pressure was never allowed to exceed 0.5% of the ingoing pressure.

At the end of each run the gas was condensed back into the gas reservoir G by surrounding the side arm with liquid nitrogen. The hivac line was then isolated from the pumping system and taps T_5 and T_8 were opened. By following this procedure the gas pressure could be monitored using the Baratron and, after isolating the diffusion cell, the residual pressure was generally less than 10^{-3} mm Hg, showing that no significant leaks of air into the apparatus had occurred during the run. The hivac line was then opened to the pumping system to pump away the remaining gas before closing off the gas reservoir so as to maintain the purity of the gas. As a further precaution against the gradual build up of condensable vapours the gas was periodically passed over the zeolite molecular sieve Z. (The above procedures were not applicable to methane which has a significant vapour pressure at liquid nitrogen temperatures and is also adsorbed by the molecular sieve.)

The membrane area for diffusion was calculated from measurements of the internal diameter of the diffusion cell, made using vernier calipers, and the membrane thickness was measured with a micrometer screw gauge before assembly of the cell. Permeability coefficients were calculated from the slope of the best fit straight line to the steady state readings, as determined by the method of least squares, and time lags were determined analytically from the best fit parameters. Sample calculations and estimates of error are given in appendix A.

3.3 Sorption

Gas sorption measurements were made using a Sartorius electronic microbalance (model 4102) which operates on the principle of automatic torque compensation. Figure 3.3a shows the beam B, a quartz tube, and rotating coil C held in position by the suspension wire W. A permanent magnet (not shown) is fixed inside C, and opposing high frequency (500 kHz) currents are passed through the stationary oscillator coils O. When the beam is deflected from the horizontal an AC voltage is induced

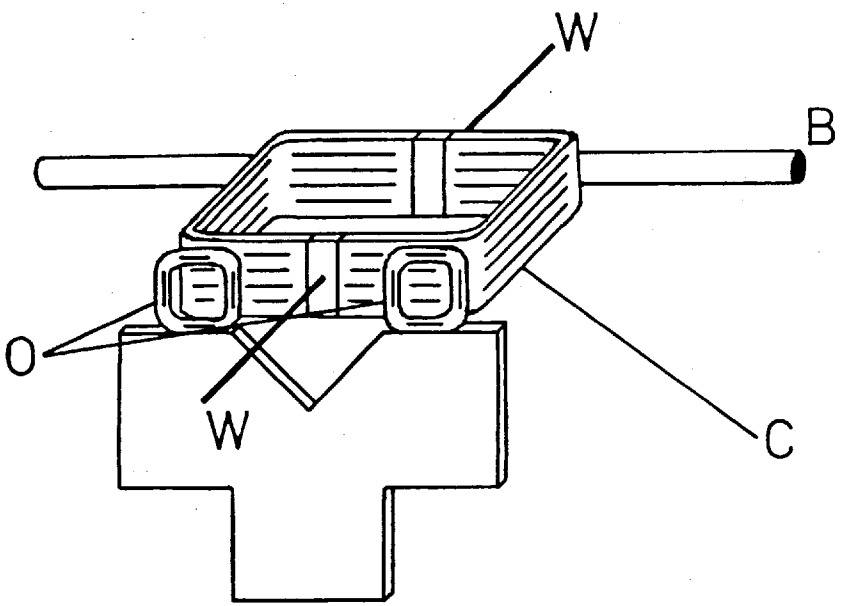

Figure 3.3a

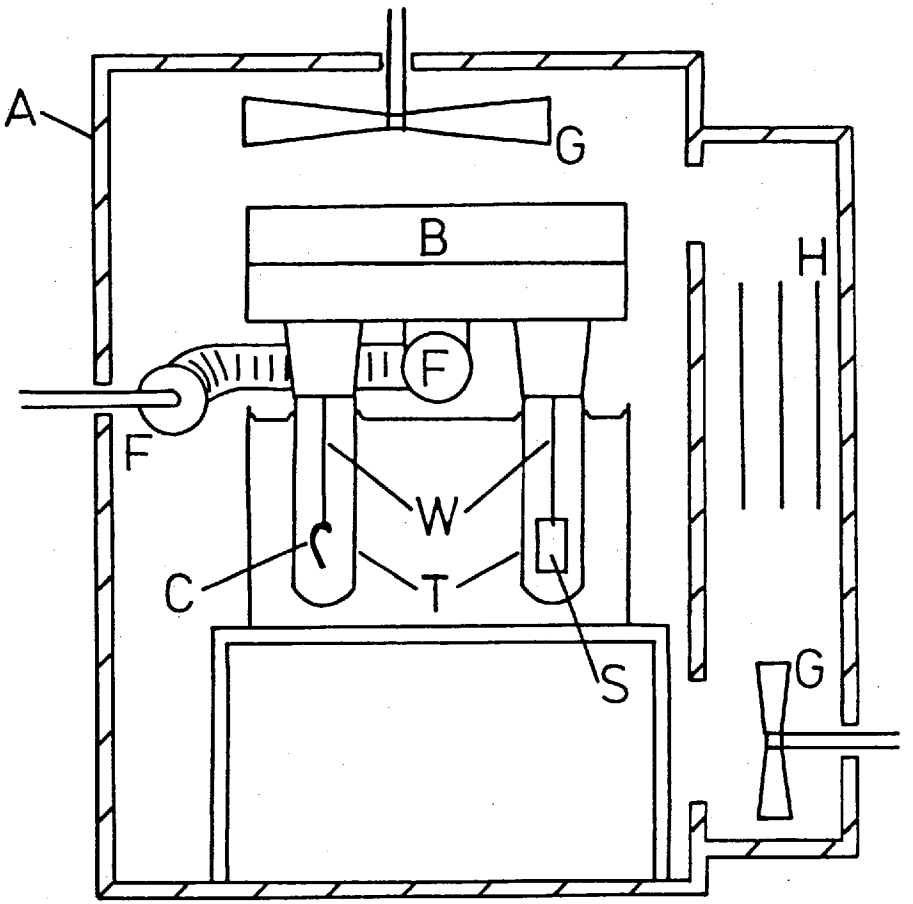

Figure 3.3b

in C whose amplitude and phase are governed by the extent and direction of the deflection. The induced voltage controls a regulating network with DC output which is returned to C to provide the counter torque necessary to return the balance to the null position, and is also used to measure the weight difference causing the deflection.

The sample S (figure 3.3b) and counterweight C were hung from the beam by aluminium stirrups and platinum suspension wires W. Both the sample and counterweight were contained in glass tubes T, connected to the stainless steel balance case by cone and socket joints. The tubes were sprayed with metal salts and earthed to eliminate static electrical charges. A flexible metal tube with flange fittings F connected the balance to the vacuum line which consisted of a calibrated pressure transducer (Bell and Howell Ltd. 0 - 10 psi), gas reservoir, and Pirani gauge. The pumping system for the vacuum line was as described previously for the permeation apparatus. The tubes T were immersed in a water bath controlled by an external thermo-circulator (Churchill Instrument Co.) which controlled the temperature of the sample to within $0.1^{o}C$. The balance was attached to a wall by a steel bracket, and enclosed in an air thermostat A. Air was circulated by fans G and heated in a circulating channel by three 500 W heaters H. The heaters were controlled by a contact thermometer and mercury relay which controlled the air temperature to within $0.5^{o}C$. It was found that careful matching of the air and water temperatures was required to eliminate zero drift of the balance. The outputs of the pressure transducer and the balance were recorded on a Honeywell "Electronik" two-pen chart recorder.

PDMS and copolymer samples for the sorption balance were weighed, their thicknesses measured with a micrometer screw gauge, and densities determined by the water displacement method. The counterweight, cut from a length of copper wire, was also weighed in order to calculate the required buoyancy correction. Samples of polystyrene film were wound into a spiral using lengths of thin copper wire as spacers to ensure separation of adjacent turns, and in this way adequate amounts of thin film could be suspended inside the microbalance tubes. The sample and counterweight were placed on the balance and the air and water thermostats set to the required temperature and left for several hours to attain thermal equilibrium. For the polystyrene samples, which required up to 2 days to reach sorption equilibrium, the water

thermostat was removed thus effectively eliminating zero drift of the balance although at the expense of temperature control. The balance was outgassed under high vacuum for 24 hours or longer, so that the build up in pressure when isolated from the pumping system was small, generally less than 10^{-2} mm Hg over several hours.

At the start of each run the balance was isolated from the pumping system and a charge of gas admitted from the gas reservoir. The weight change and pressure were recorded continuously on the chart recorder, and sorption equilibrium was indicated by constant weight. The volume of the apparatus was sufficiently large for the decrease in pressure due to sorption by the sample to be negligible, and the results were consequently analysed in terms of sorption at constant pressure. Desorption was achieved by surrounding the side arm of the gas reservoir with liquid nitrogen and, after allowing sufficient time for the condensation of the remaining gas, the reservoir was opened to the balance. The weight and pressure changes were again recorded. When using methane as penetrant, it was found that sorption was too rapid for an accurate determination of the diffusion coefficient (except in the case of the polystyrene sample), and desorption to zero pressure was not possible due to the finite vapour pressure of methane at liquid nitrogen temperatures.

Equilibrium concentrations were determined from the final weight increase and the calculated buoyancy correction, and diffusion coefficients were calculated from plots of fractional weight change against square root time. Sample calculations are given in appendix A.

CHAPTER 4

RESULTS AND DISCUSSION

4.1 Polydimethylsiloxane

PDMS is an elastomer and is well above its glass transition temperature at normal temperatures. The transport characteristics of PDMS are therefore expected to be independent of concentration at low penetrant activities, as has been found by previous workers (119, 120).

The sorption isotherms of the hydrocarbons methane, propane, n-butane, and iso-butane were all linear over the pressure range studied as illustrated in figure 4.1 which shows sample isotherms at approximately 30°C. (Full experimental data are given in appendix C.) The solubilities increase with increasing molecular weight of the penetrant and correlate well with the boiling points, critical temperatures, and Lennard-Jones force constants of the gases. The slope of the least squares regression line to the plot of the logarithm of the solubility at 25°C against the Lennard-Jones force constant (ε/k), illustrated in figure 4.2, is 0.030, which is in good agreement with the theoretical value of 0.026 given by Michaels and Bixler (9). The solubilities used in this figure were interpolated from the van't Hoff plots of log S against reciprocal absolute temperature shown in figure 4.3. Good linear plots were obtained for all the gases which allowed an accurate determination of the heat of sorption from equation 1.3. Table 4.1 lists the interpolated values of the solubility at 30°C, heats of sorption ($\Delta\bar{H}_S$), and literature values of the heats of

Table 4.1 PDMS Solubilities (30°C)

	S / $cm^3(STP)cm^{-3}(cm\ Hg)^{-1}$	$\Delta\bar{H}_S$ / $kJ\ mol^{-1}$	ΔH_C / $kJ\ mol^{-1}$
methane	6.44×10^{-3}	-6.4	(-8.9)
propane	1.04×10^{-1}	-17.0	-20.1
n-butane	3.21×10^{-1}	-21.9	-24.3
iso-butane	2.2×10^{-1}	-20.3	-22.7

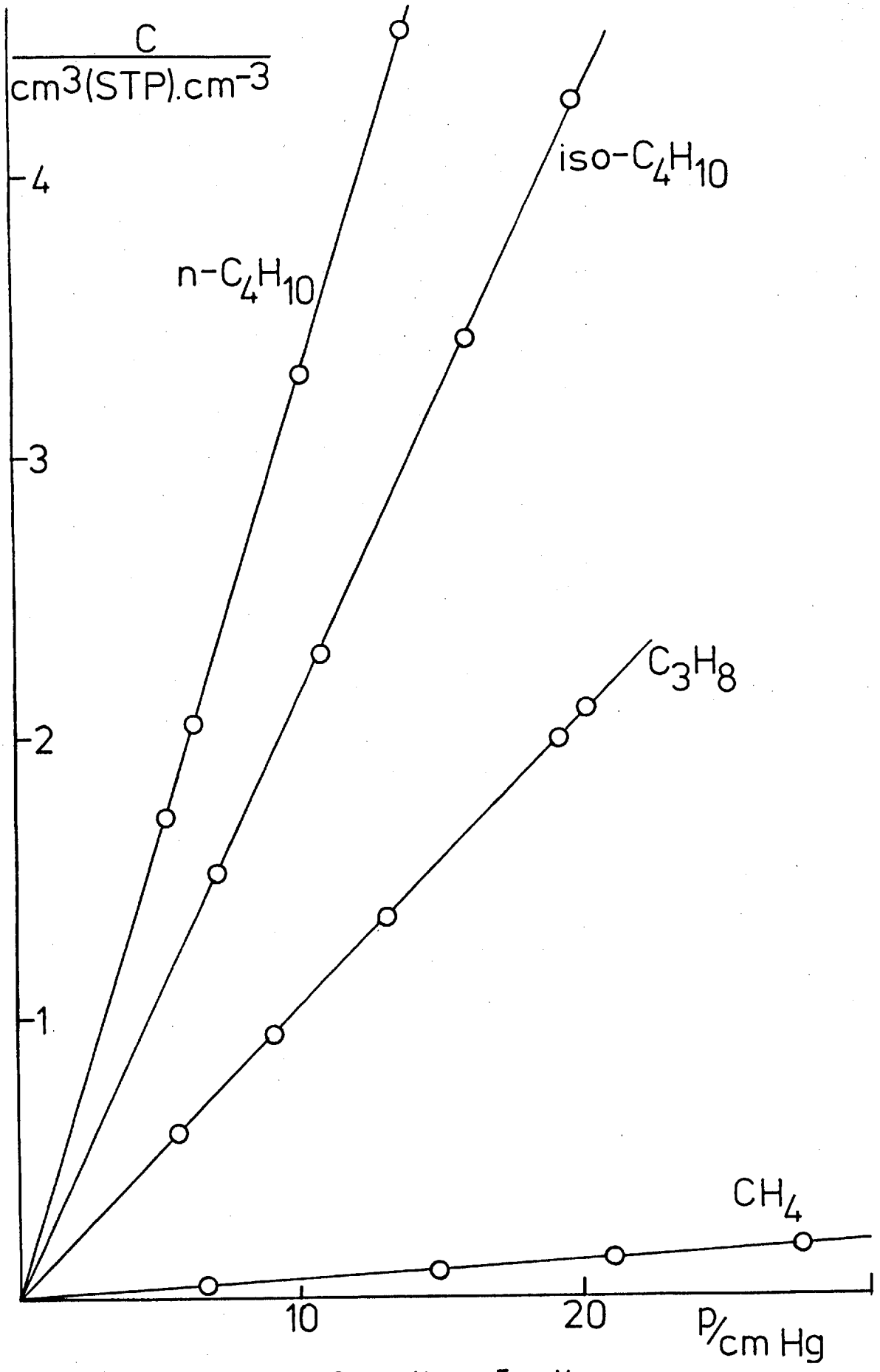

Figure 4.1: PDMS Sorption Isotherms

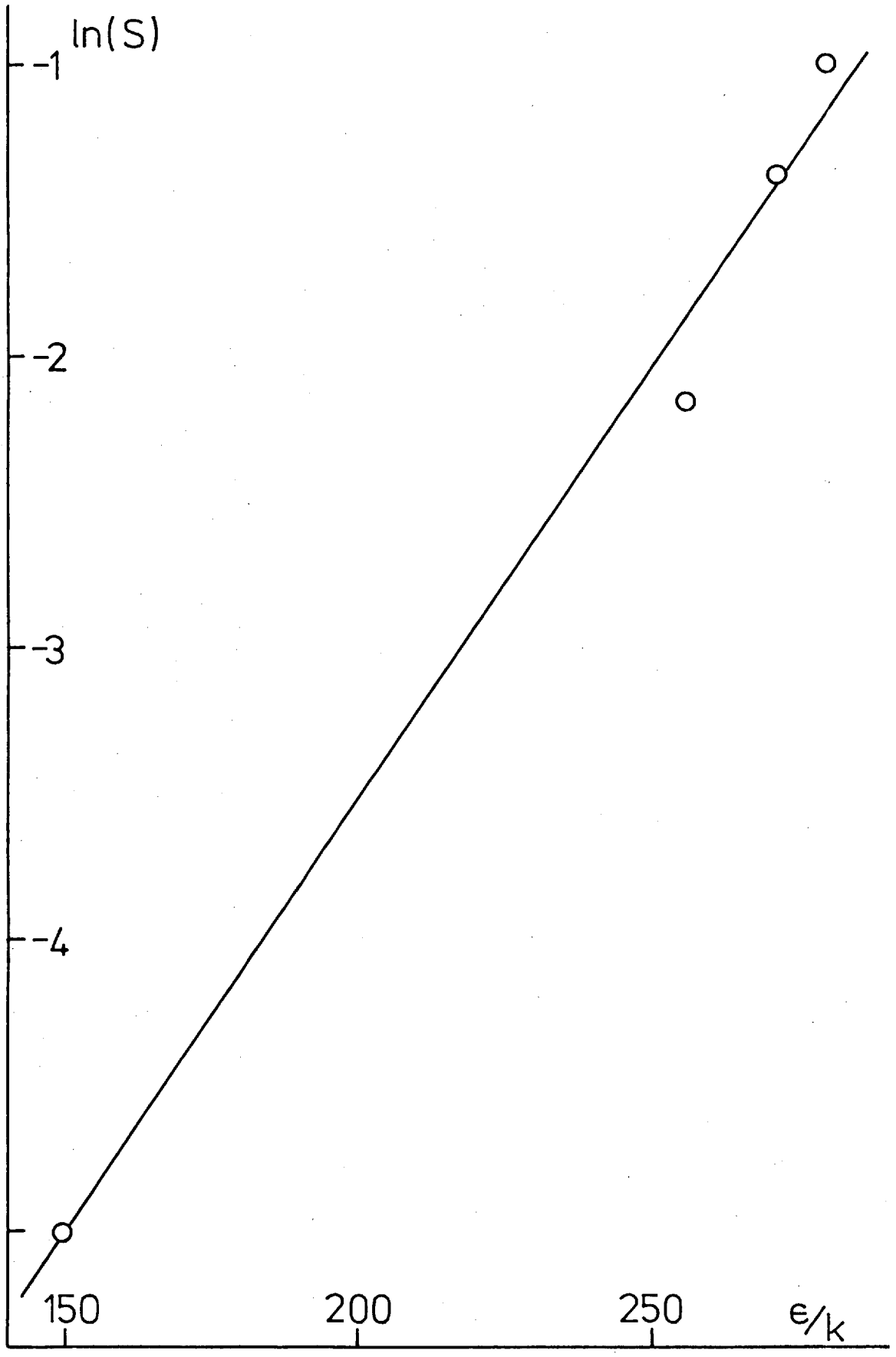

Figure 4.2: Solubility Correlation

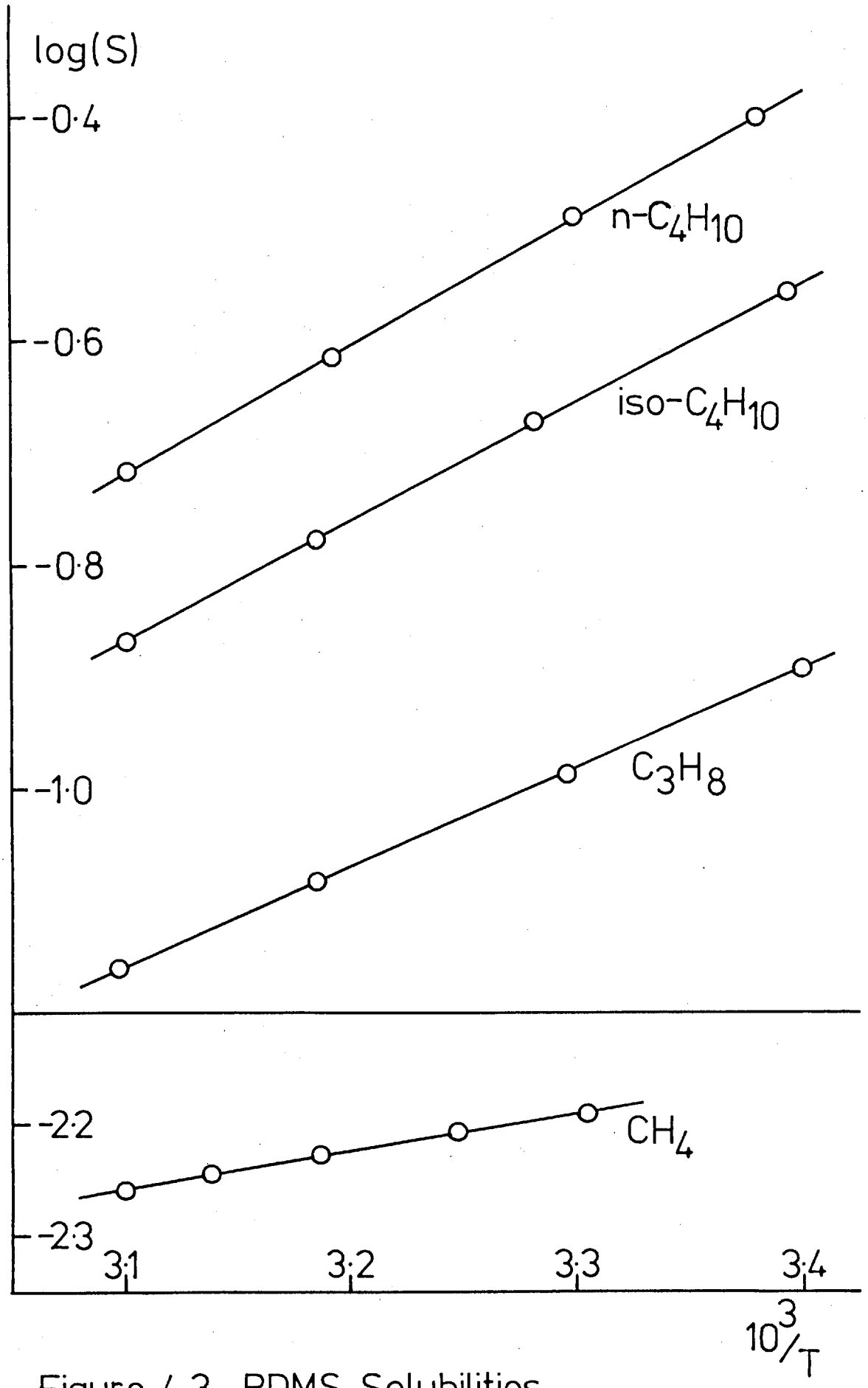

Figure 4.3: PDMS Solubilities

condensation (ΔH_c) of the four gases studied. The close correspondence of these two heats and the Henry's law solubility behaviour are indicative of the absence of any strong gas-gas or gas-polymer interactions at the low penetrant activities employed. (The SVP of n-butane, the most easily condensable of the gases, is 2.7 atm at 30°C, and the corresponding vapour activity ~0.2 at the highest pressures used in this study.)

The permeability coefficients of the four penetrants were measured in the temperature range 25 to 50°C and the results are shown in the form of an Arrhenius plot in figure 4.4. The permeabilities were found to be independent of ingoing pressure except for the more soluble gases when a slight trend towards increasing P with increasing pressure was noted. Although statistically significant the increase is too small to be amenable to analysis, and is approximately equal to the uncertainty in the determination of P. For this reason the trend has been ignored, and average values of P used in the subsequent comparisons and analyses. It is possible that this effect is due to plasticisation of the polymer by the penetrant even at the low concentrations of penetrant involved (~0.2% by weight), and slight deformation of the membrane under the pressure differences employed may also contribute to the observed increases.

Permeabilities at 30°C and pseudo-activation energies are given in table 4.2. E_P for propane is in good agreement with a previously reported value (120) although the permeability is significantly (20%) higher. This difference may be due to differences between the two samples or to systematic errors introduced by the different apparatus employed, and is thought unlikely to affect any comparisons made in the present study.

Table 4.2 PDMS Permeabilities (30°C)

	$P \times 10^7$	E_P
	$cm^3(STP)\,cm\,cm^{-2}(cm\ Hg)^{-1}s^{-1}$	$kJ\ mol^{-1}$
methane	1.32	7.3
propane	6.59	-2.9
n-butane	15.1	-6.8
iso-butane	8.10	-5.3

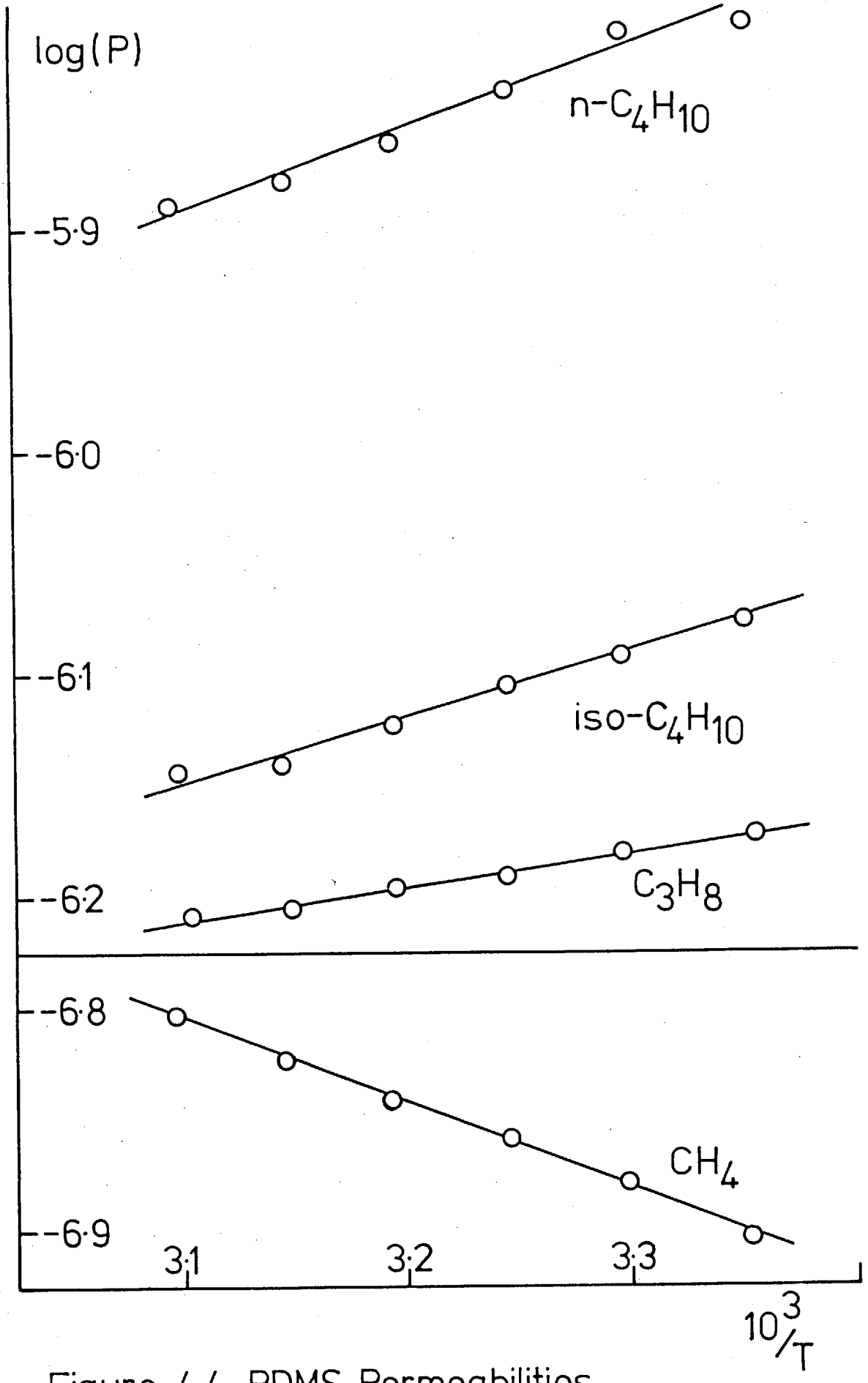

Figure 4.4: PDMS Permeabilities

Diffusion coefficients for propane, n-butane, and iso-butane were obtained from the initial rates of sorption and desorption of these gases. As stated previously, this method was not applicable to methane due to the rapid sorption rates and the difficulty in desorbing to zero pressure. D_s values from the rates of sorption were found to increase slightly with increasing concentration, and the D_d values from the conjugate desorption to decrease. The mean diffusion coefficient, $\overline{D}$, was independent of concentration, within the experimental error, and for this reason the variations of D_s and D_d are thought to be due to the method of measurement, rather than a real effect, and may be associated with the effect of the balance response time as discussed in appendix B.

Arrhenius plots of the diffusion coefficients are shown in figure 4.5, and in table 4.3 the interpolated values of $\overline{D}$ at 30°C are compared with the values obtained from the permeation time lag, D_L, and steady-state diffusion coefficients determined from $D_S = P/S$.

$\overline{D}$ values are consistently higher than the corresponding D_S, and D_L values are generally lower. It is believed that the D_S values are the most accurate although all values are subject to errors due to edge effects. $\overline{D}$ is obtained from equation 1.17 in which diffusion is assumed to occur only through the faces of the sheet. In practice diffusion also occurs through the edges of the sheet and, to a first approximation, $\overline{D}$ will be increased in proportion to the total surface area (121). Permeabilities, and consequently estimates of D_S, are affected by the portion of the membrane which is clamped under the glass faces of the diffusion cell. The internal radius of the diffusion cell was typically 1.3 cm and the width of the ground glass rim

Table 4.3 PDMS Diffusion Coefficients (30°C)

($D \times 10^6/cm^2s^{-1}$)

	$\overline{D}$	D_L	D_S
methane	-	17.12	20.5
propane	7.81	5.96	6.34
n-butane	6.33	4.70	4.70
iso-butane	4.90	3.50	3.68

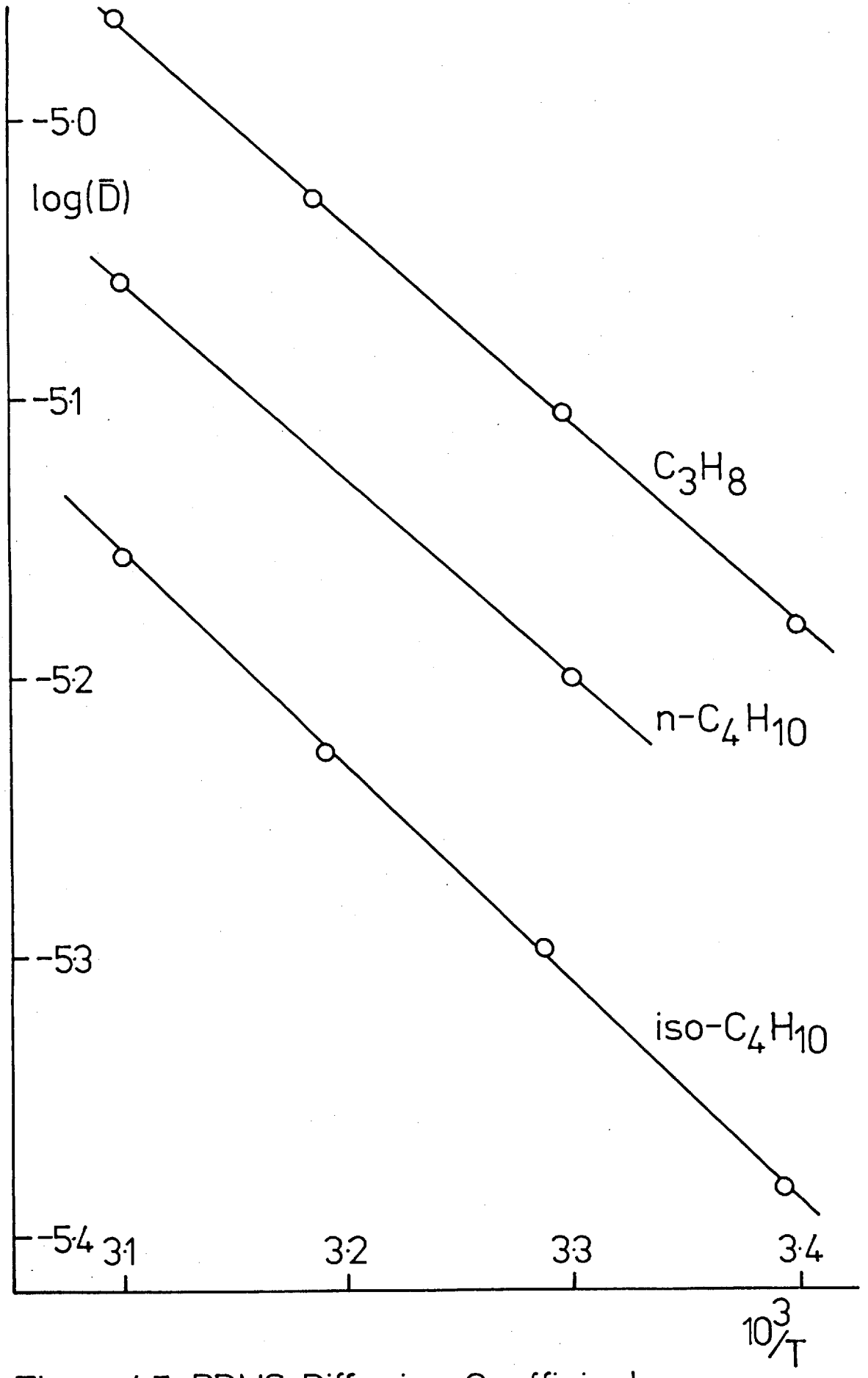

Figure 4.5: PDMS Diffusion Coefficients

approximately 0.2 cm. Thus the area of membrane clamped under the glass faces is of the order of 30% of the measured area, and can be expected to contribute significantly to the steady-state flux. An approximate solution to this problem has been given by Barrer et al (122) which, from the figures given above, predicts an increase in the steady-state flux of approximately 5% for the 0.2 cm thickness PDMS membrane employed. The time lag and derived diffusion coefficient, D_L, are related to the total amount of penetrant within the membrane and the edge effect may thus be expected to be larger for these parameters, and may be of the same order as the "neglected" fraction of the membrane.

The decrease in D with increasing molecular weight and hence molecular size of the penetrant is well illustrated by the values given in table 4.3 as is the additional effect of the branched iso-butane molecule. The activation energies for diffusion listed in table 4.4, however, show little variation due to the high segmental mobility of PDMS chains. E_D is essentially constant for each penetrant and independent of the method of measurement, within the experimental error, although a definite trend of increasing E_D with increasing penetrant size is apparent. Both D_L and E_D are in reasonable agreement with previously reported values for propane (120).

Table 4.4 Activation Energies of Diffusion

	$(E_D/kJ\ mol^{-1})$		
	$E_{\overline{D}}$	E_{D_L}	$E_P - \Delta\overline{H}_S$
methane	-	11.7	13.7
propane	13.7	12.0	14.0
n-butane	13.7	13.3	15.1
iso-butane	14.7	14.6	15.0

4.2 Polystyrene

At the temperatures used in this investigation (30°C and 50°C) polystyrene is well below its T_g of 101°C and exhibits dual mode

sorption characteristic of a glassy polymer. The methane sorption isotherms of figure 4.6 show only slight curvature, indicating that the pressure range studied corresponds to the initial linear region of the isotherm. In addition, the measured or effective diffusion coefficients obtained from the initial rates of sorption were constant, within the experimental error, and showed no significant trend. The results are summarised in table 4.5.

The initial linear region of the dual mode sorption isotherm is given by equation 2.13 and the solubility coefficient under these conditions by $S = k_D + c'_H.b$. The heat of sorption obtained is thus a composite term involving ΔH_D, ΔH_H, and the temperature coefficient of c'_H. $\Delta \overline{H}_S$ is significantly more negative than the heat of sorption of methane in PDMS and other elastomers, and this may be ascribed to the more exothermic contribution of ΔH_H.

The relationship between the effective diffusion coefficient, D_{eff}, and the diffusion coefficient of the mobile dissolved penetrant may be derived from a consideration of the flux, as follows. In terms of the total concentration the flux is given by:

$$J = -D_{eff} \cdot \frac{\partial c}{\partial x} \qquad \ldots (4.1)$$

and, assuming the Langmuir component of sorption to be totally immobilised, the flux in terms of the mobile concentration is given by:

$$J = -D \cdot \frac{\partial c_D}{\partial x} \qquad \ldots (4.2)$$

Table 4.5 Methane Sorption

T / ^oC	$S \times 10^3$ / $cm^3 STP cm^{-3} cm\ Hg^{-1}$	$D_{eff} \times 10^8$ / $cm^2 s^{-1}$
30	6.9	1.27
50	4.4	3.3

$$E_{D_{eff}} = 39\ kJ\ mol^{-1}$$

$$\Delta \overline{H}_S = -18\ kJ\ mol^{-1}$$

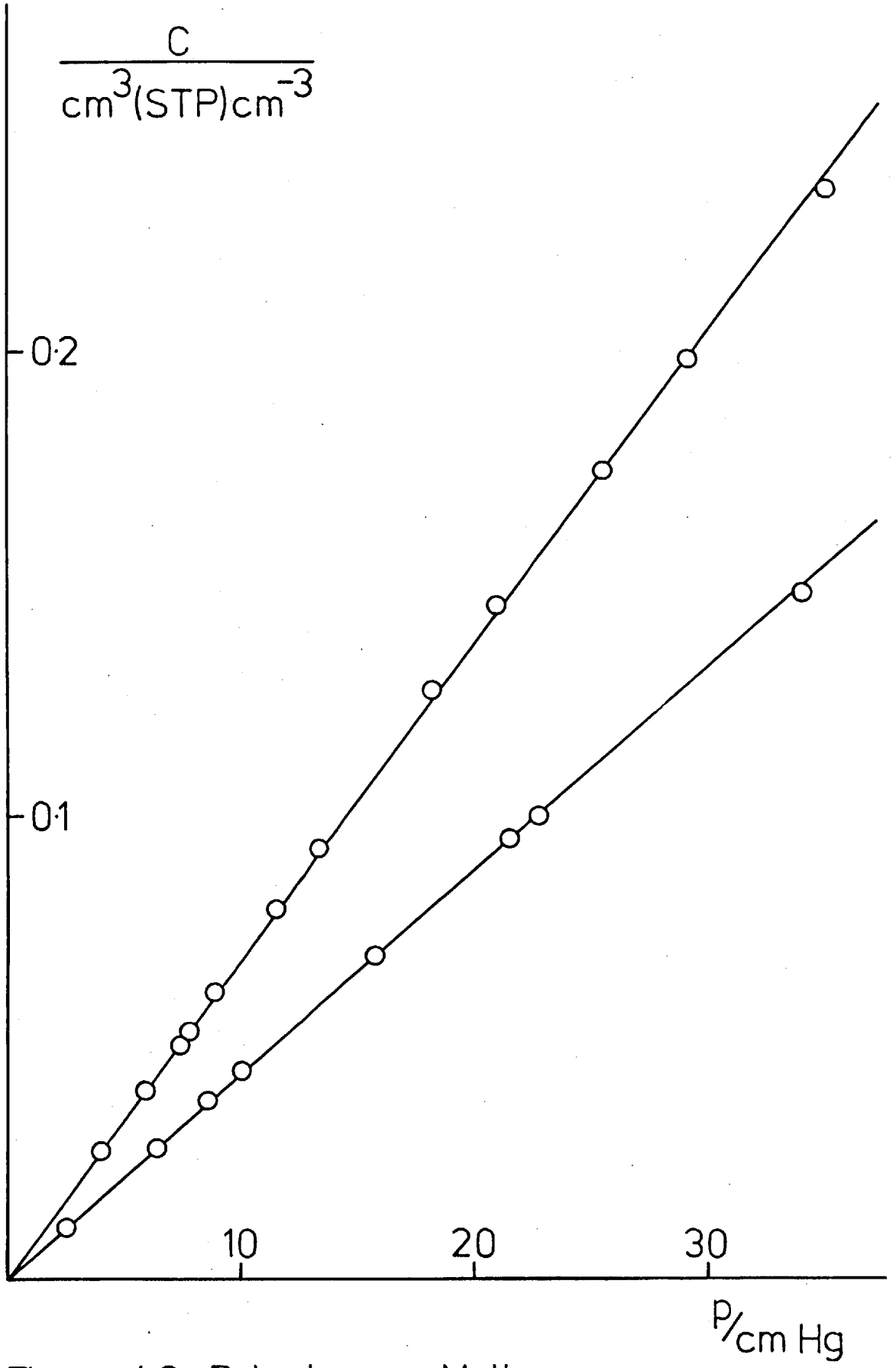

Figure 4.6 : Polystyrene Methane Sorption Isotherms

equating these two expressions leads to:

$$D_{eff} = D.\frac{\partial c_D}{\partial c} \qquad \ldots (4.3)$$

and thus D_{eff} is a function of concentration. At low pressures, however, both c_D and c obey Henry's law and $\partial c_D/\partial c$ is constant, given by k_D/S. The results can thus be compared with the dual sorption parameters and diffusion coefficients given by Vieth et al (123), and reasonable agreement is obtained for the solubilities although D_{eff} values are approximately four times larger than those calculated from Vieth's data. The reason for this discrepancy is not immediately apparent. The method used by Vieth to determine D involved the use of an empirical correlation involving the dual sorption parameters. Some doubt has been cast upon the accuracy of the graphical method used to determine these parameters (111), and the general applicability of the correlation has not been proven. The constant value of D at high pressures was also determined by Vieth using the solution to the diffusion equation given by Crank (18). It is reported that the two values differed by a factor of two, although good agreement was obtained in this way for the system upon which the correlation was based (124).

The propane sorption isotherms shown in figure 4.7 exhibit significant curvature, typical of dual mode sorption, in the pressure range investigated. A computer program was written to determine the "best fit" dual sorption parameters by a least squares regression analysis based upon a trial and error method. This method was found to be preferable to the iterative method described by Koros et al (125) which converges only slowly, and gives no indication of the convergence limits. The mathematical basis of the program used is described in a recent paper (126) (which is included as an addendum) and the method of estimation of the uncertainties is outlined. It should be stressed that the method of estimation is non-rigorous and that the uncertainties have no statistical significance, although it is felt that the estimates provide a useful guide as to the uncertainties in the individual parameters. The interdependence of the dual sorption parameters means that composite terms, such as $c'_H.b$, can be determined more accurately than either of the individual parameters. A full investigation of the uncertainties of experimentally determined dual sorption parameters and their interdependence has been reported by Koros et al (125).

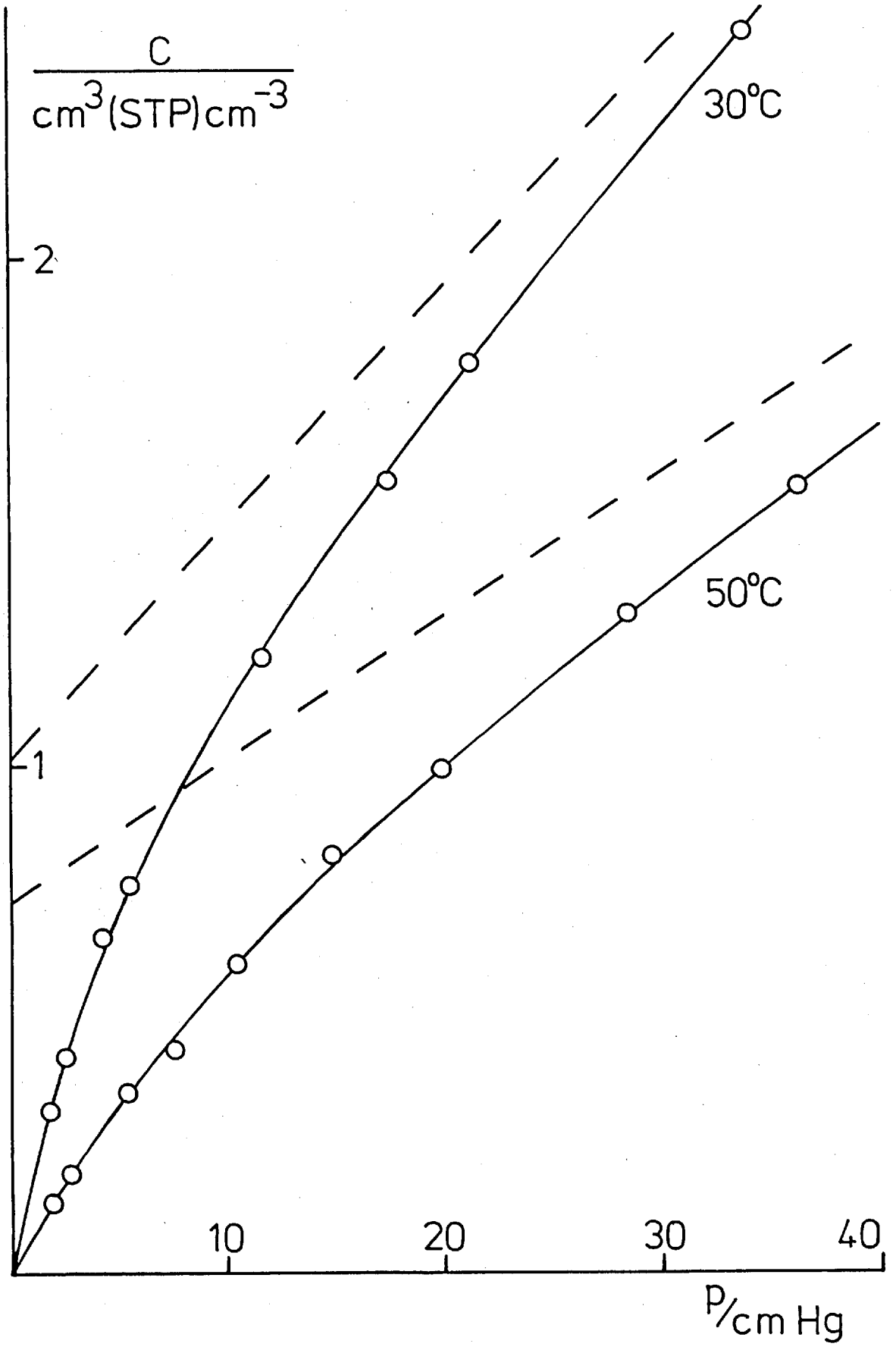

Figure 4.7: Polystyrene Propane Sorption Isotherms

The solid lines of figure 4.7 represent the best fit isotherms constructed from the dual sorption parameters of table 4.6, and the dashed lines show the limiting high pressure asymptotes (equation 2.14). It is clear that the isotherms lie well below their respective asymptotes in the pressure range investigated. The apparent linearity of the isotherms in the upper half of the pressure range indicates the difficulty in ascertaining when the asymptote is truly reached, and the subsequent inaccuracies inherent in the graphical method of analysis. The heats of sorption quoted in table 4.6 were calculated from the temperature dependence of the isotherm parameters and are subject to large degrees of uncertainty, since only two temperatures were investigated. They do, however, illustrate the typical features of heats of sorption in glassy polymers. ΔH_D is comparable to the heat of sorption of propane in elastomers, for example, -14 kJ mol^{-1} in natural rubber (120), and -17 kJ mol^{-1} in PDMS from the present work. ΔH_H, the enthalpy of the hole filling process is significantly more exothermic although the true interpretation of this parameter is uncertain, and awaits a more complete understanding of the dual mode sorption process. The limiting value of the heat of sorption at zero concentration, $(\Delta \bar{H}_S)_{c=0}$, is the most exothermic of the heats of sorption, and is a composite term involving ΔH_D, ΔH_H, and the temperature dependence of c'_H. The interpretation of this parameter is thus complex, and the explanation offered by Meares (65) is now seen to be true only in an approximate qualitative sense.

Figure 4.8 shows a test of the Langmuir component of the sorption

Table 4.6 Polystyrene Propane Dual Sorption Parameters

T	$k_D \times 10^2$	c'_H	b
^oC	$cm^3 STP cm^{-3} cm\ Hg^{-1}$	$cm^3 STP cm^{-3}$	$cm\ Hg^{-1}$
30	4.7 (±5%)	1.01 (±8%)	0.18 (±8%)
50	2.8 (±8%)	0.74 (±16%)	0.071 (±13%)

$$\Delta H_D = -21 \text{ kJ mol}^{-1}$$
$$\Delta H_H = -38 \text{ kJ mol}^{-1}$$
$$(\Delta \bar{H}_S)_{c=0} = -43 \text{ kJ mol}^{-1}$$

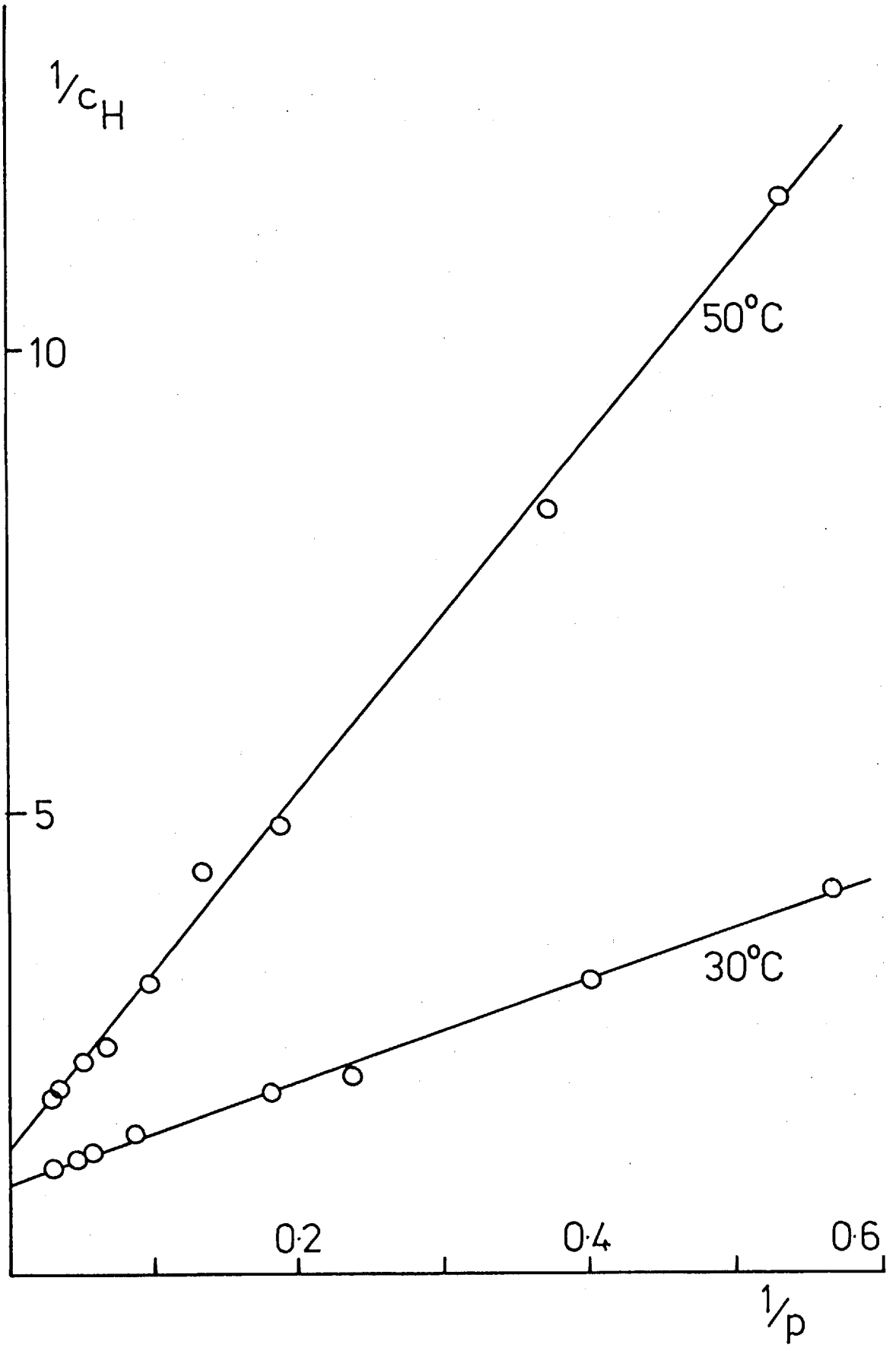

Figure 4.8: Polystyrene Propane
Langmuir Sorption

isotherms according to the more stringent conditions of equation 2.16. It is clear that a good fit is obtained to the parameters of table 4.6 and the dual mode sorption equation is an accurate representation of the experimentally determined isotherms. It does not follow, however, that the model from which the isotherm equation is derived is necessarily correct, and a number of features of this model require further elucidation. In particular, the physical nature of the microvoids within a glassy polymer has not been established, and if these "holes" or microvoids are assumed to be the physical space of the polymer free volume then this begs the question of where the dissolved penetrant resides. A tentative quantitative relationship has recently been proposed (112) between the Langmuir saturation constant, c'_H, and the "excess" free volume given by the difference between the polymer specific volume and the specific volume obtained by extrapolation from the liquid state. This is in accord with the views of the author which are that sorption takes place into the free volume of a polymer, and in a glassy polymer only part of that free volume is at any one time associated with the molecular motions of the polymer. This fraction of the free volume may be regarded as instantaneously "mobile", and the sorption into this free volume to be, to a first approximation, a direct extrapolation from the rubbery state, Sorption into the remaining "immobile" free volume can reasonably be expected to follow a Langmuir type of isotherm, typical of sorption into a porous solid.

The main feature of the proposed model is that it is the sorption sites, rather than the penetrant molecules, which are in equilibrium between the two states. It is evident that any molecular motion within a polymer leads to a local redistribution of free volume, and it is the molecular motions remaining within the glassy state that give rise to the mobility of free volume. Thus, if the molecular motion within a glassy polymer is given by an extrapolation from the rubbery state, a direct correlation is obtained between c'_H and the "excess" free volume as defined above.

Diffusion coefficients for propane were determined by conjugate sorption and desorption rate measurements at four pressures at each temperature investigated. Crank (18) has shown that if D is only weakly dependent upon c then equation 1.14 ie:

$$\overline{D} = \frac{1}{c_o} \int_0^{c_o} D(c)dc \qquad \ldots (4.4)$$

is a reasonable approximation. If it is assumed that the Langmuir component of sorption is totally immobilised, then substituting from equation 4.3:

$$\overline{D} = \frac{1}{c_o} \int_0^{c_o} D.\frac{\partial c_D}{\partial c}.dc \qquad \ldots (4.5)$$

where D is assumed constant, and thus:

$$\overline{D} = D.\frac{c_D}{\overline{c}_o}$$

$$= D.\frac{k_D.p}{k_D.p + c'_H.\frac{b.p}{1 + b.p}} \qquad \ldots (4.6)$$

By use of equation 4.6 and the dual sorption parameters of table 4.6 the value of D was determined at each concentration. No significant trends were observed, and average values of D, given in table 4.7, were used to determine the theoretical lines of figure 4.9 which shows the variation in $\overline{D}$ with concentration. The large experimental error evident is thought to be due to temperature variations (caused by the removal of the water bath for these experiments) and because of this it is not possible to test the assumption of total immobilisation of the Langmuir component.

The concentration dependence of the effective diffusion coefficient

Table 4.7 Polystyrene Propane Diffusion Coefficients

$(D \times 10^{11}\ cm^2 s^{-1})$

$T(^oC)$	D	$D_{c=0}$
30	8	1.6
50	18	6.3

$E_D = 33\ kJ\ mol^{-1}$

$E_{D_{c=0}} = 55\ kJ\ mol^{-1}$

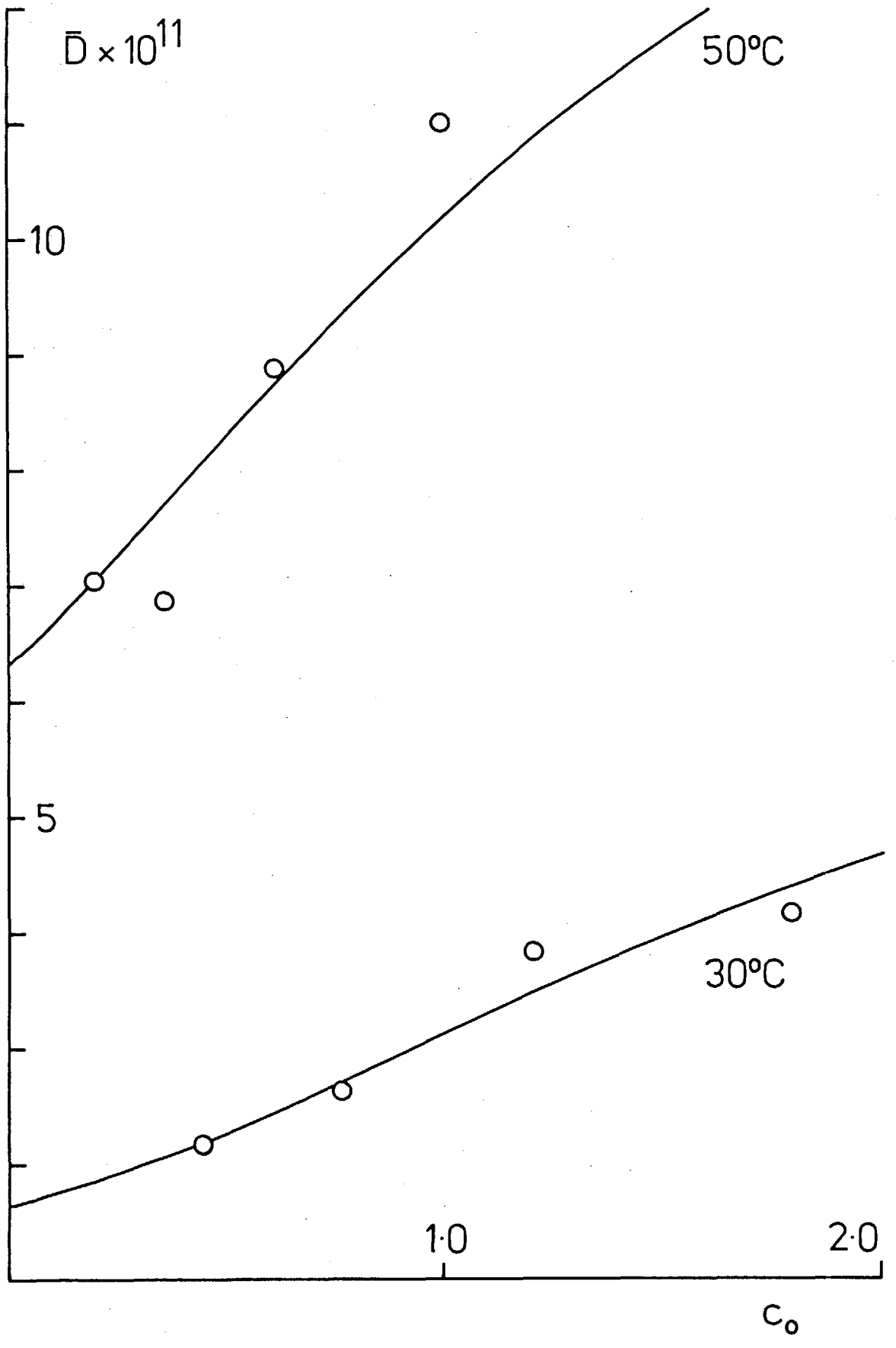

Figure 4.9: Polystyrene Propane Diffusion Coefficients

may be readily obtained from equation 4.3. Since $c_D = k_D.p$, this equation may be re-written as:

$$D_{eff} = D.k_D.\frac{\partial p}{\partial c} \qquad \ldots (4.7)$$

Then solving the dual sorption isotherm equation for p and differentiating w.r.t. c leads to:

$$D_{eff} = D.\tfrac{1}{2}\{1 + (k_D - c'_H.b + b.c).[(k_D + c'_H.b - b.c)^2 + 4k_D.bc]^{-\frac{1}{2}}\} \qquad \ldots (4.8)$$

It is easily shown that this equation reduces to the correct expression at zero concentration ie:

$$D_{c=0} = D.\frac{k_D}{k_D + c'_H.b} = \frac{D.k_D}{S} \qquad \ldots (4.9)$$

As only two temperatures were investigated the activation energies for diffusion given in table 4.7 should be regarded as estimates only, and are subject to large degrees of uncertainty. E_D represents the "true" activation energy for the diffusion of mobile penetrant molecules, and is lower than E_D for propane in most elastomers (eg 41 kJ mol^{-1} in natural rubber (120), and 52 kJ mol^{-1} in polyethylene (127)). This behaviour is not uncommon, and reflects the increased temperature dependence of the diffusion coefficient in polymers above T_g, as discussed in chapter 1.

4.3 Copolymers : Equilibrium Sorption

4.3.1 Graft Copolymers

The propane sorption isotherms of the graft copolymers studied are shown in figures 4.10 to 4.14. It is evident that the degree of curvature of the isotherms increases with increasing polystyrene content of the polymer, and is due to the dual mode sorption behaviour of polystyrene. The electron micrographs of the copolymers (appendix C) show the polystyrene to be present in discrete domains dispersed within the darker coloured PDMS continuum, and these domains may be expected to exhibit properties similar to those of bulk polystyrene.

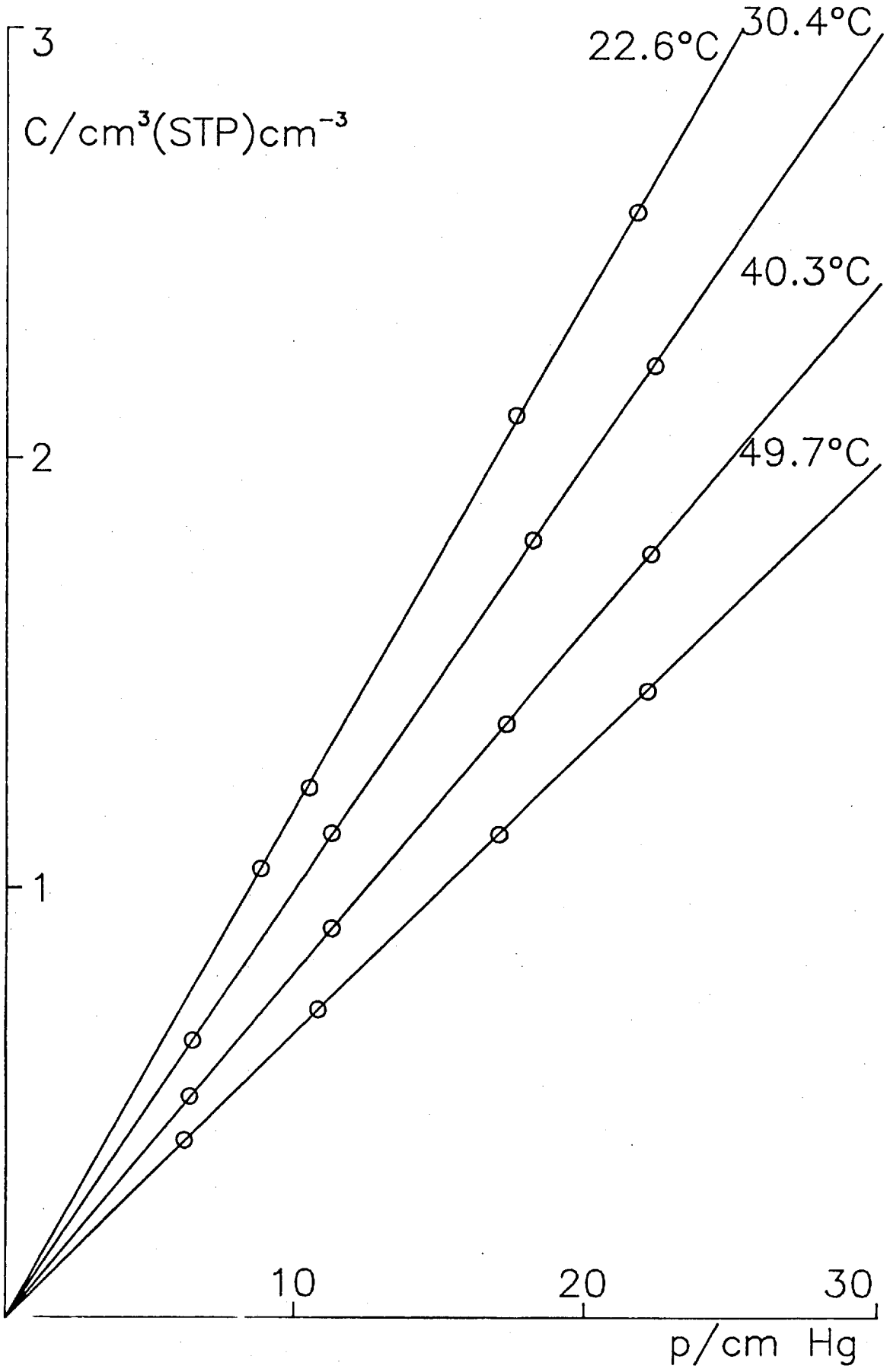

Figure 4.10: 4.9% Graft Propane Sorption Isotherms

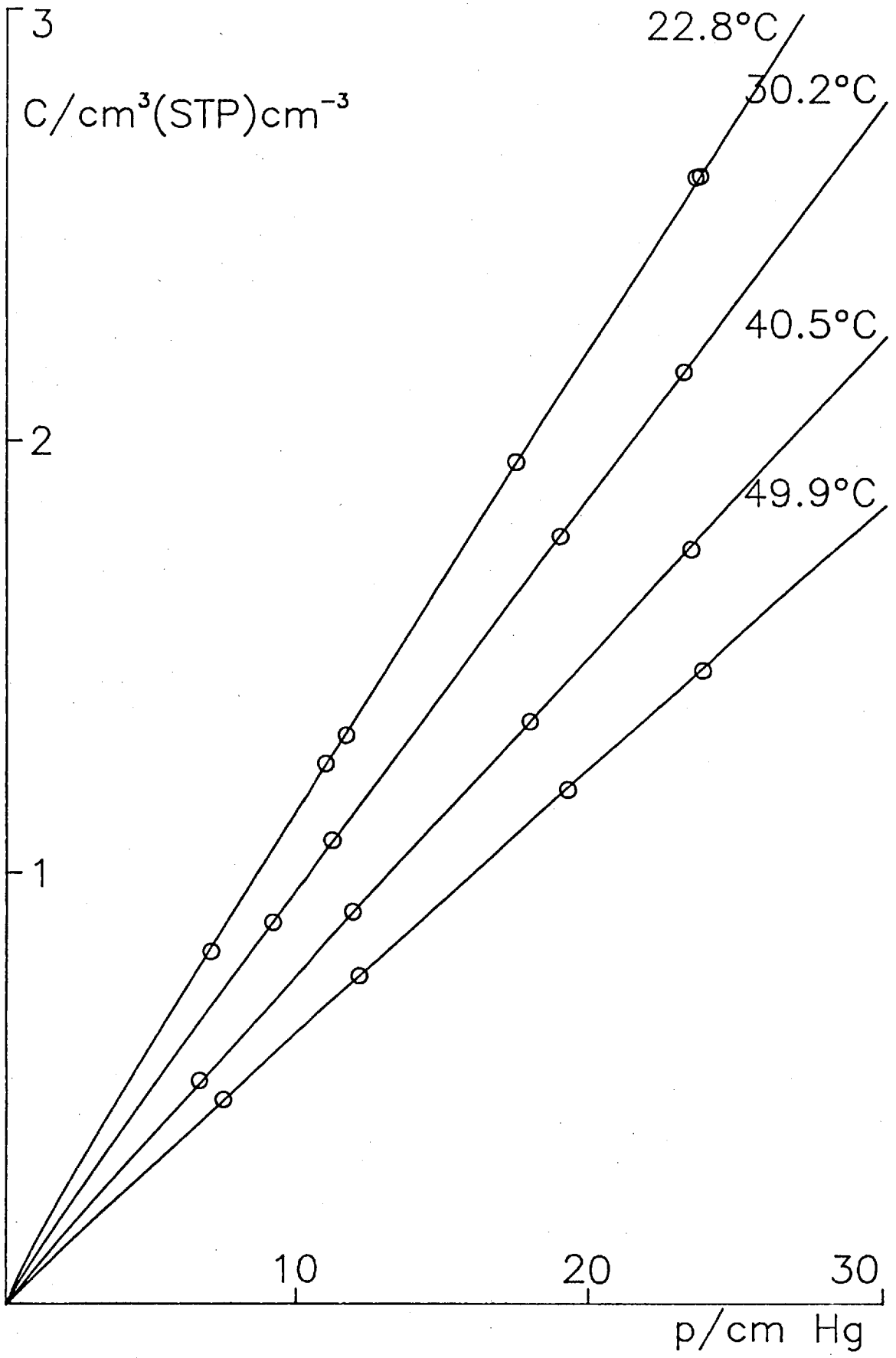

Figure 4.11: 15.5% Graft Propane Sorption Isotherms

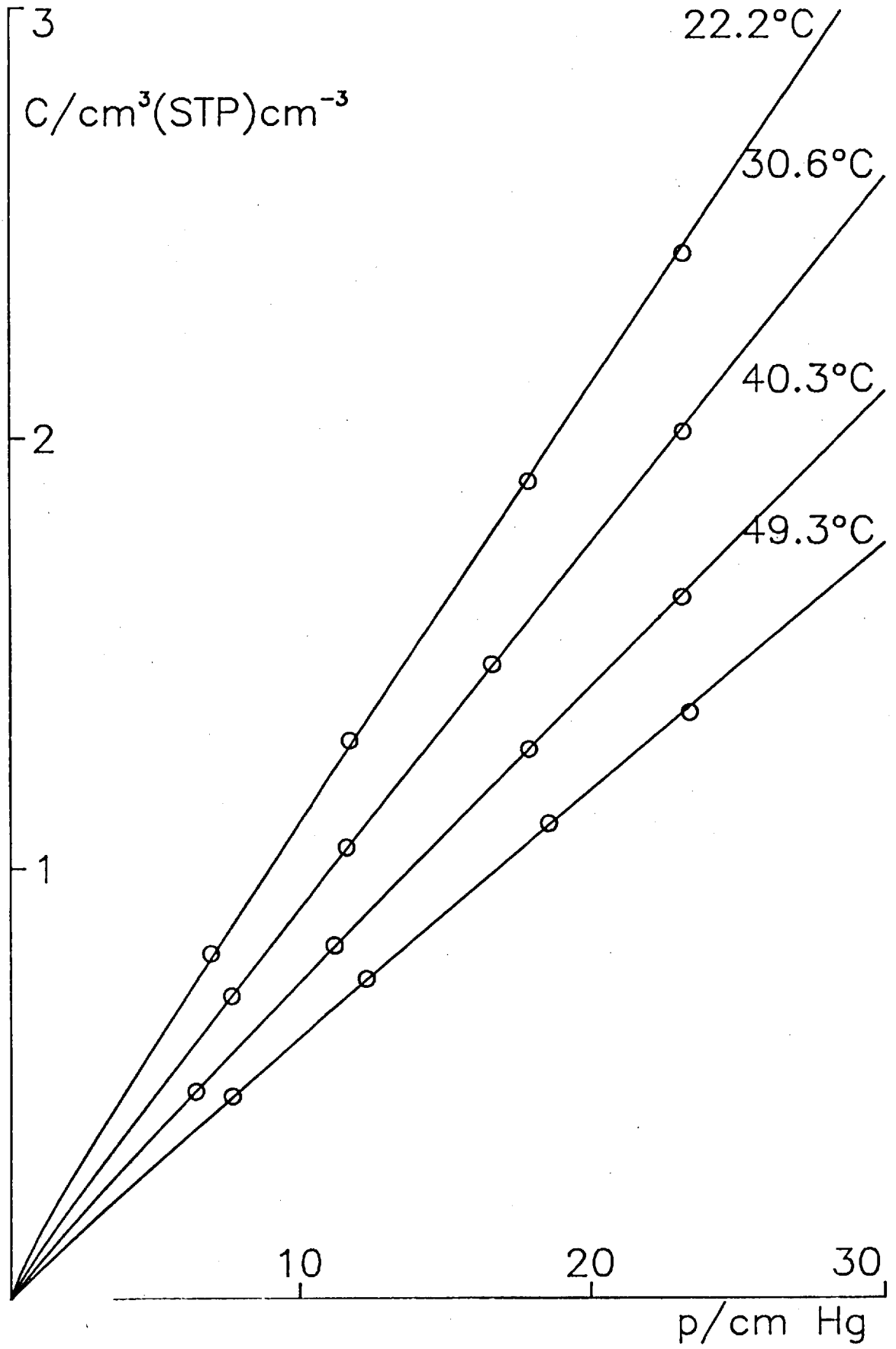

Figure 4.12: 26.2% Graft Propane Sorption Isotherms

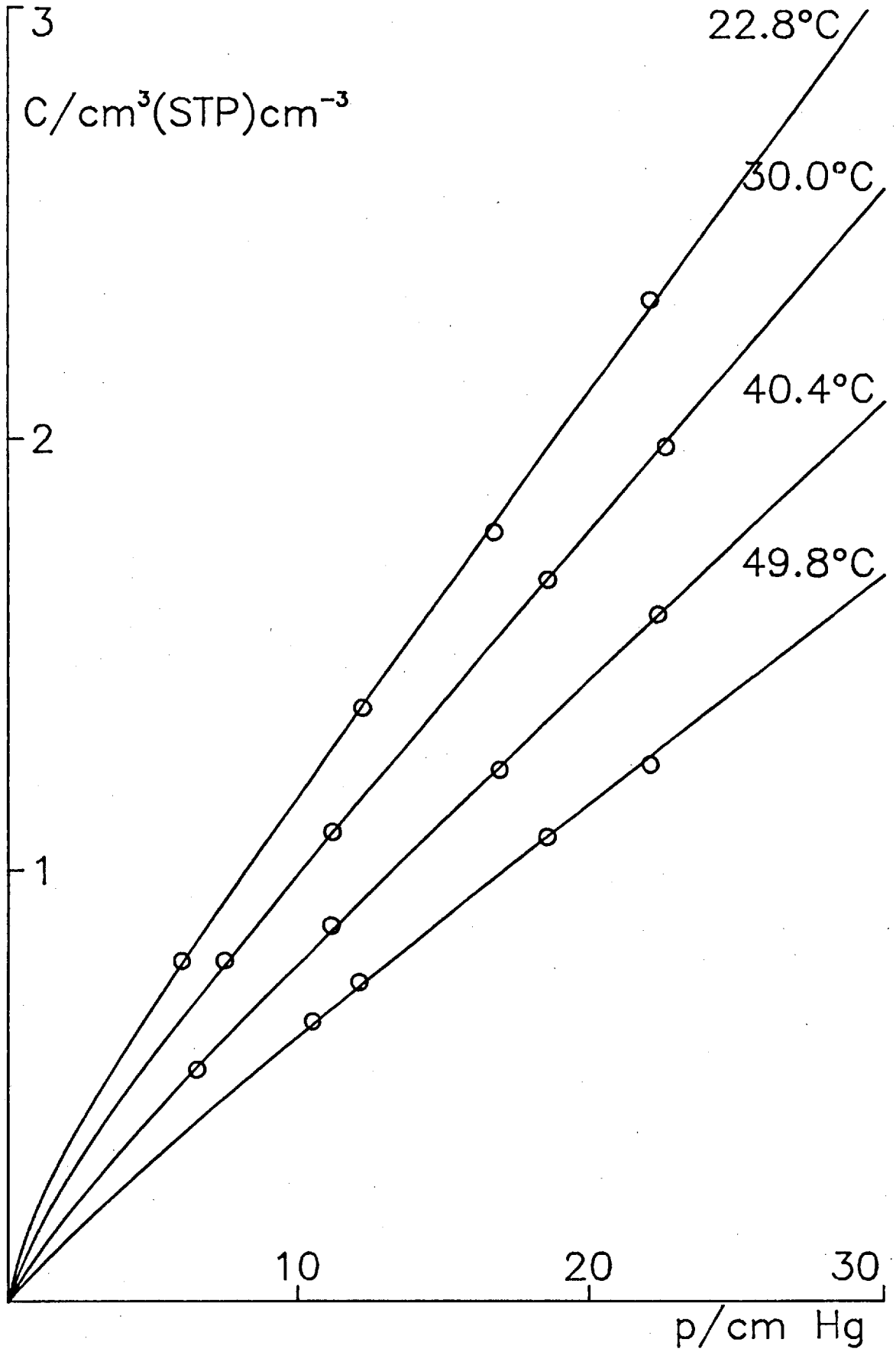

Figure 4.13: 38.2% Graft Propane Sorption Isotherms

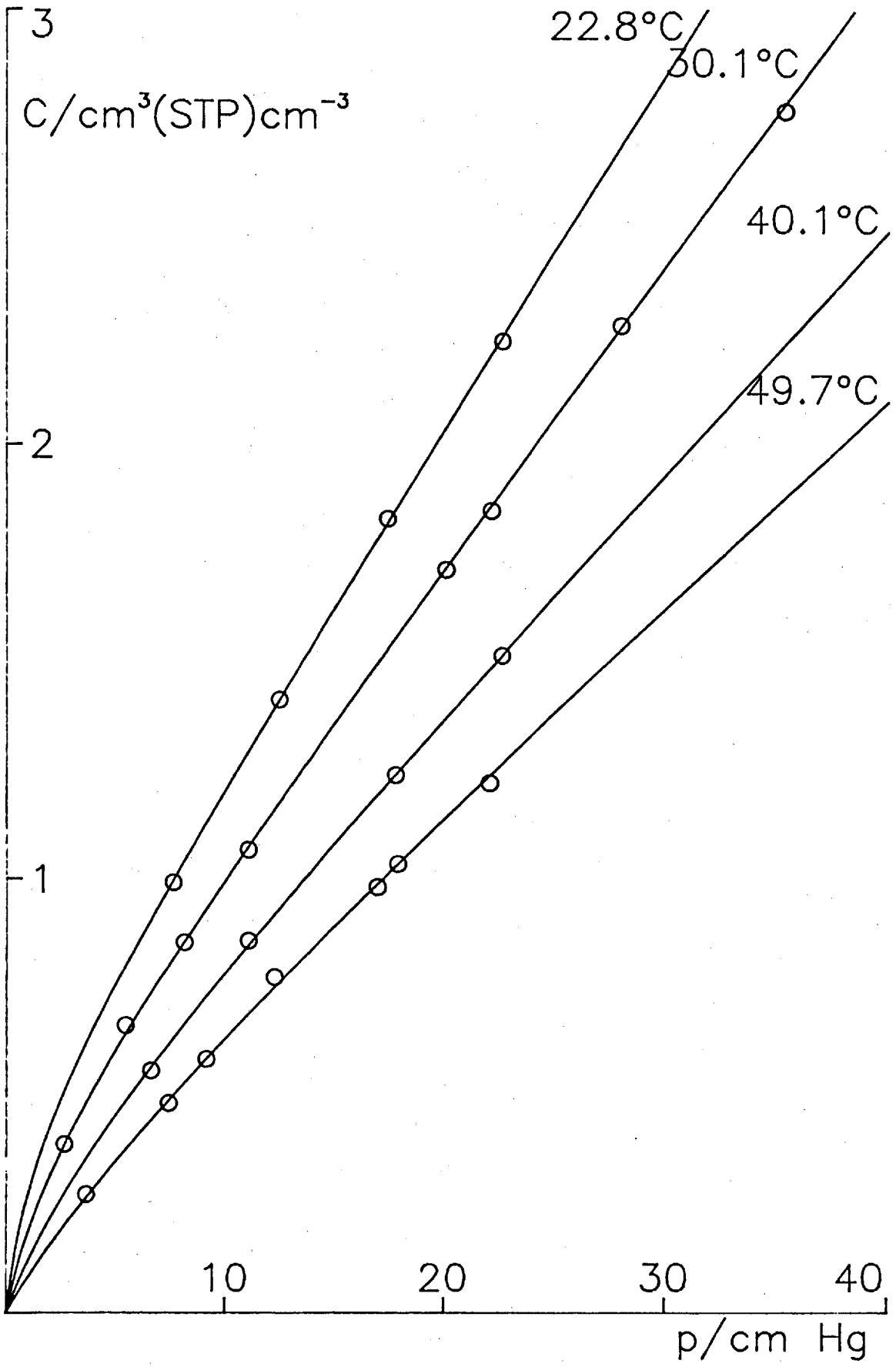

Figure 4.14: 56.3% Graft Propane Sorption Isotherms

The iso-butane sorption isotherms illustrated in figures 4.15 to 4.19 show the same features as the propane isotherms with levels of sorption somewhat higher, as expected for a more easily condensable vapour.

The heat of dissolution, ΔH_D, as determined from the temperature dependence of the Henry's law dissolution constant is the only readily accessible heat of sorption for these copolymers. Levels of Langmuir sorption are too low to allow any reasonable estimate of the Langmuir sorption parameters for the majority of the membranes studied, and for this reason k_D values were estimated from the slope of the linear region of the sorption isotherms. The isotherm parameters for the 56.3% polystyrene copolymer were also obtained from the dual mode sorption computer program, and k_D values obtained in this way were in good agreement with the graphical estimates. The k_D values for the two penetrants are shown in the form of van't Hoff plots in figures 4.20 and 4.21, and the heats of dissolution obtained from the best fit straight lines are given in table 4.8. The almost constant values of ΔH_D obtained indicate that, as for PDMS, there are no strong interactions between polystyrene and these penetrants, and the heat of sorption is due largely to the heat of condensation of the gases.

Table 4.8 Graft Copolymer Solubilities

(k_D: $cm^3(STP)cm^{-3}cmHg^{-1}$, ΔH_D: $kJ\ mol^{-1}$)

		Propane		iso-Butane	
	V_{PS}	k_D (30°C)	ΔH_D	k_D (30°C)	ΔH_D
PDMS	0	.104	-17.0	.220	-20.3
4.9% PS	.046	.100	-17.1	.209	-20.4
15.5% PS	.146	.0912	-16.6	.190	-20.2
26.2% PS	.248	.0852	-17.1	.169	-19.5
38.2% PS	.365	.0786	-17.2	.151	-19.6
56.3% PS	.545	.0686	-16.7	.225	-19.4

4.3.2 Block Copolymers

Sample sorption isotherms at approximately 30°C for the block copolymer membrane CM (compression moulded) are shown in figure 4.22,

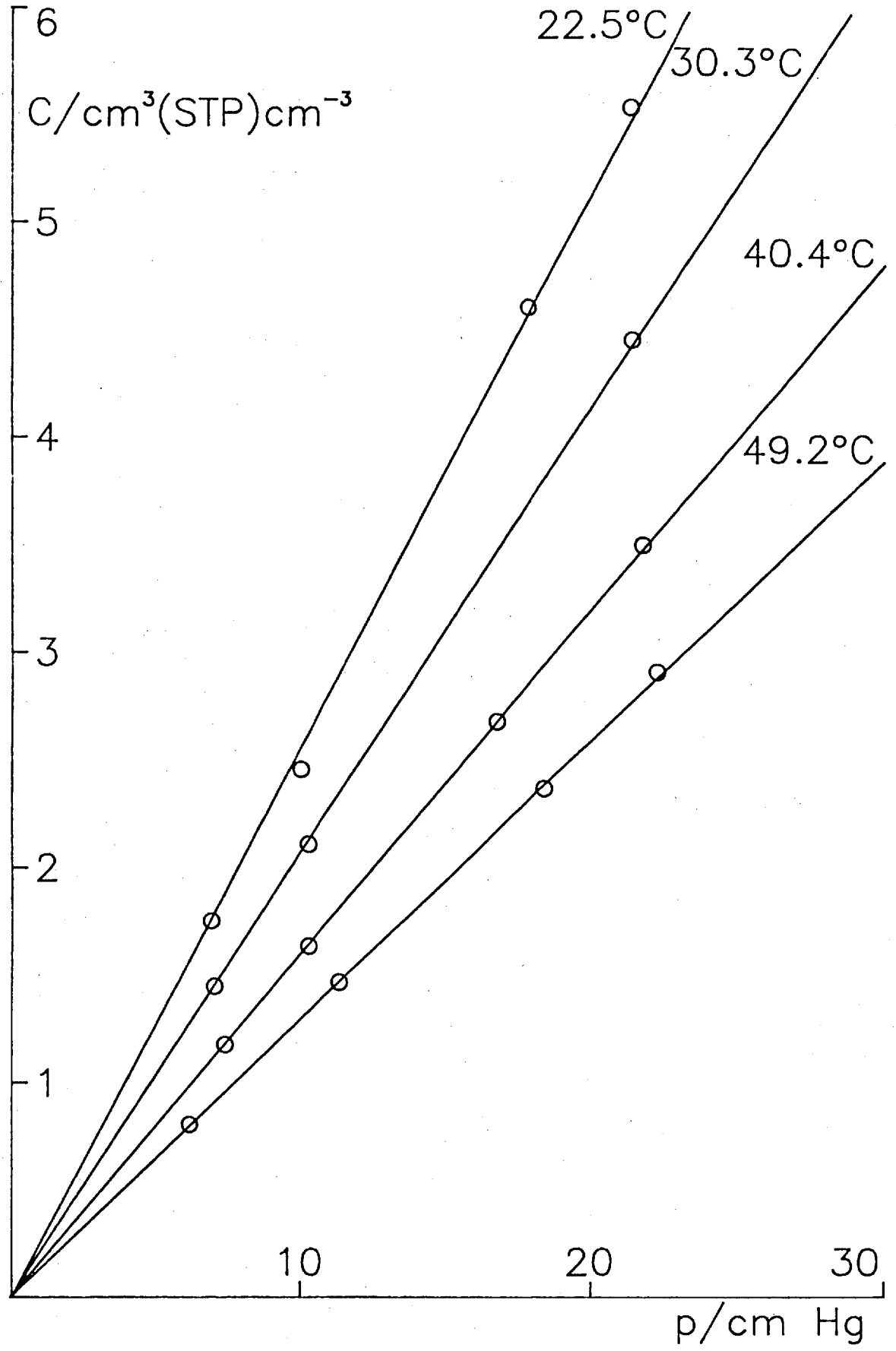

Figure 4.15: 4.9% Graft iso–Butane Sorption Isotherms

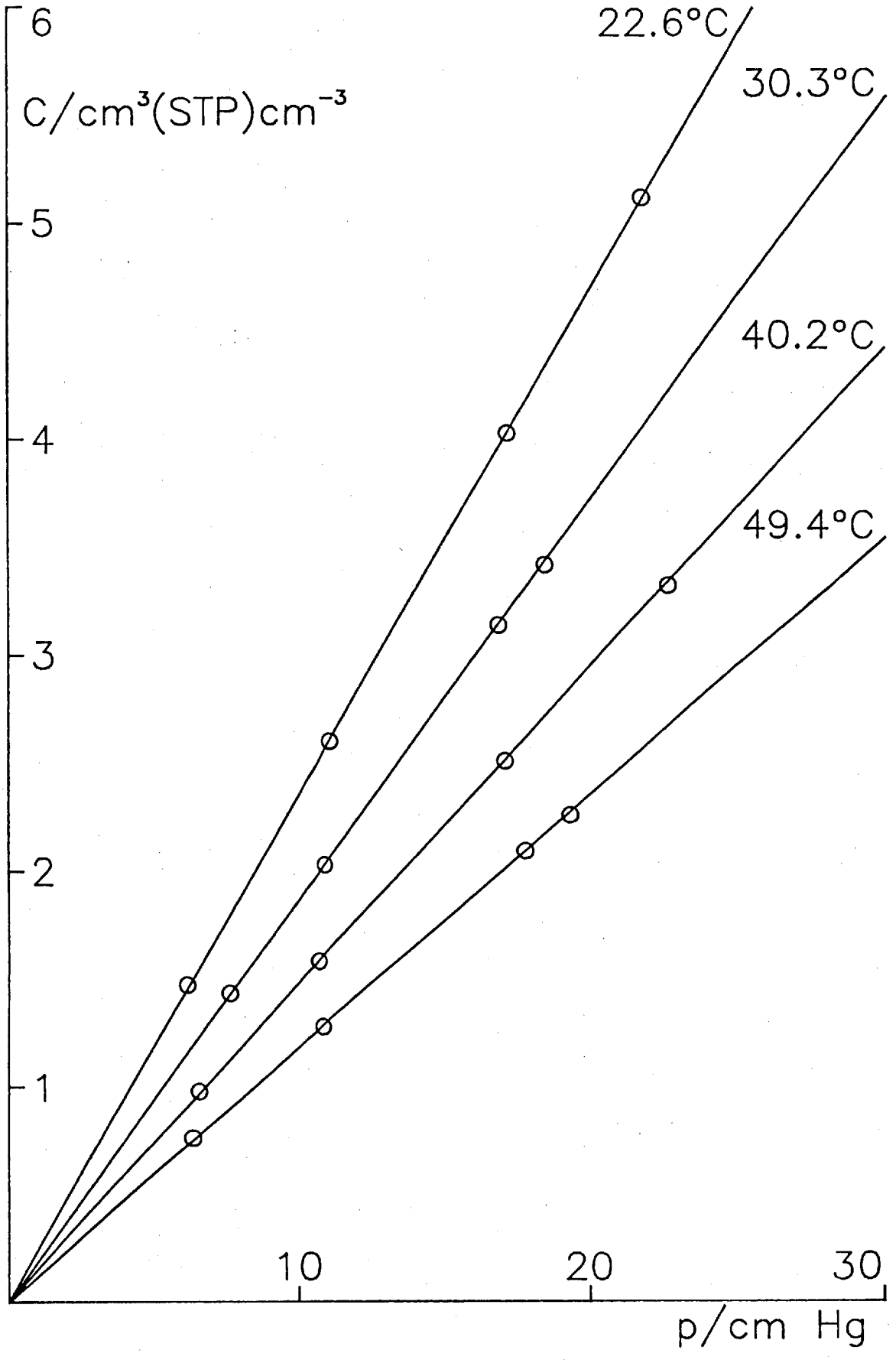

Figure 4.16: 15.5% Graft iso–Butane Sorption Isotherms

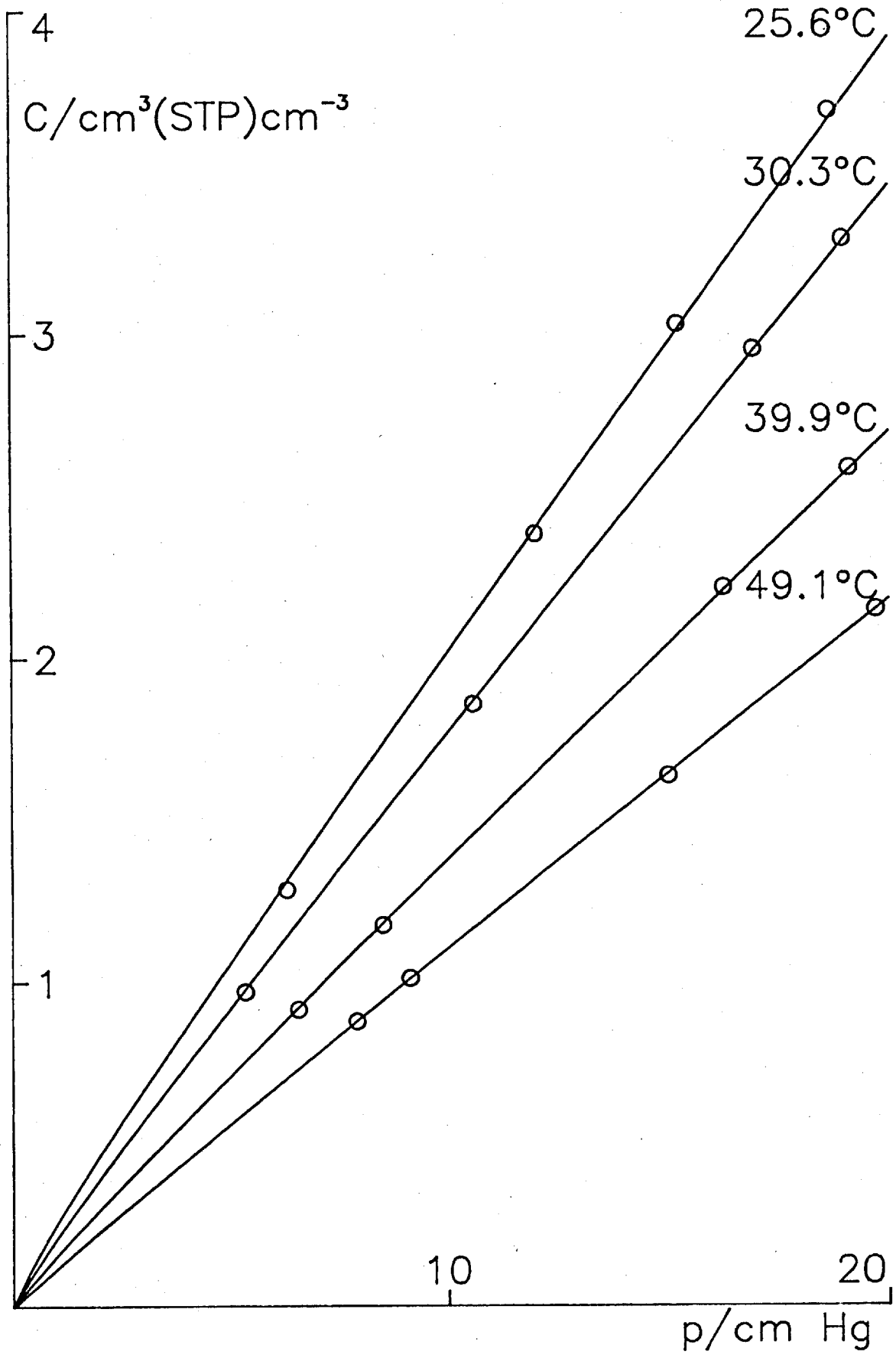

Figure 4.17: 26.2% Graft iso–Butane Sorption Isotherms

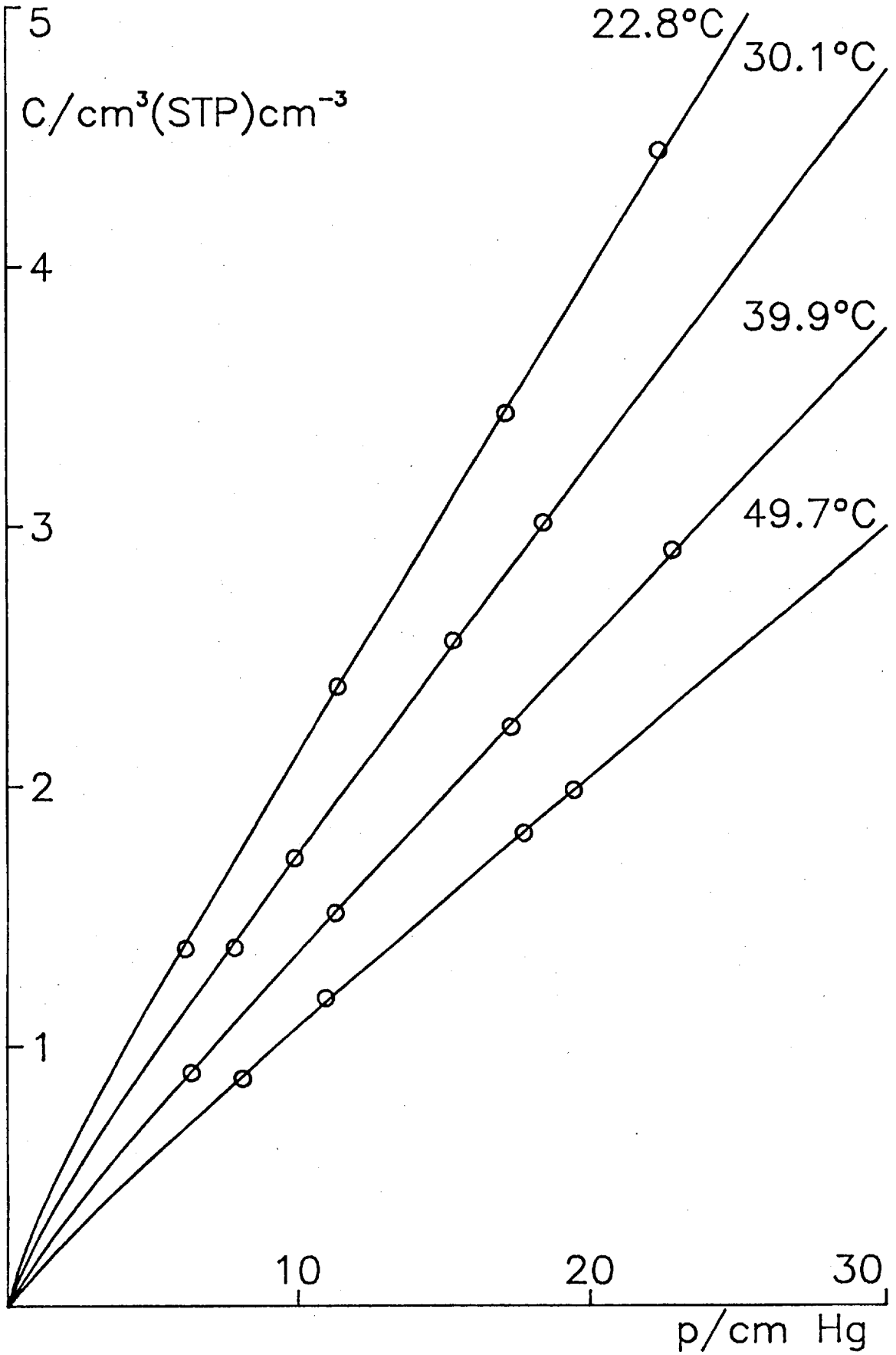

Figure 4.18: 38.2% Graft iso–Butane Sorption Isotherms

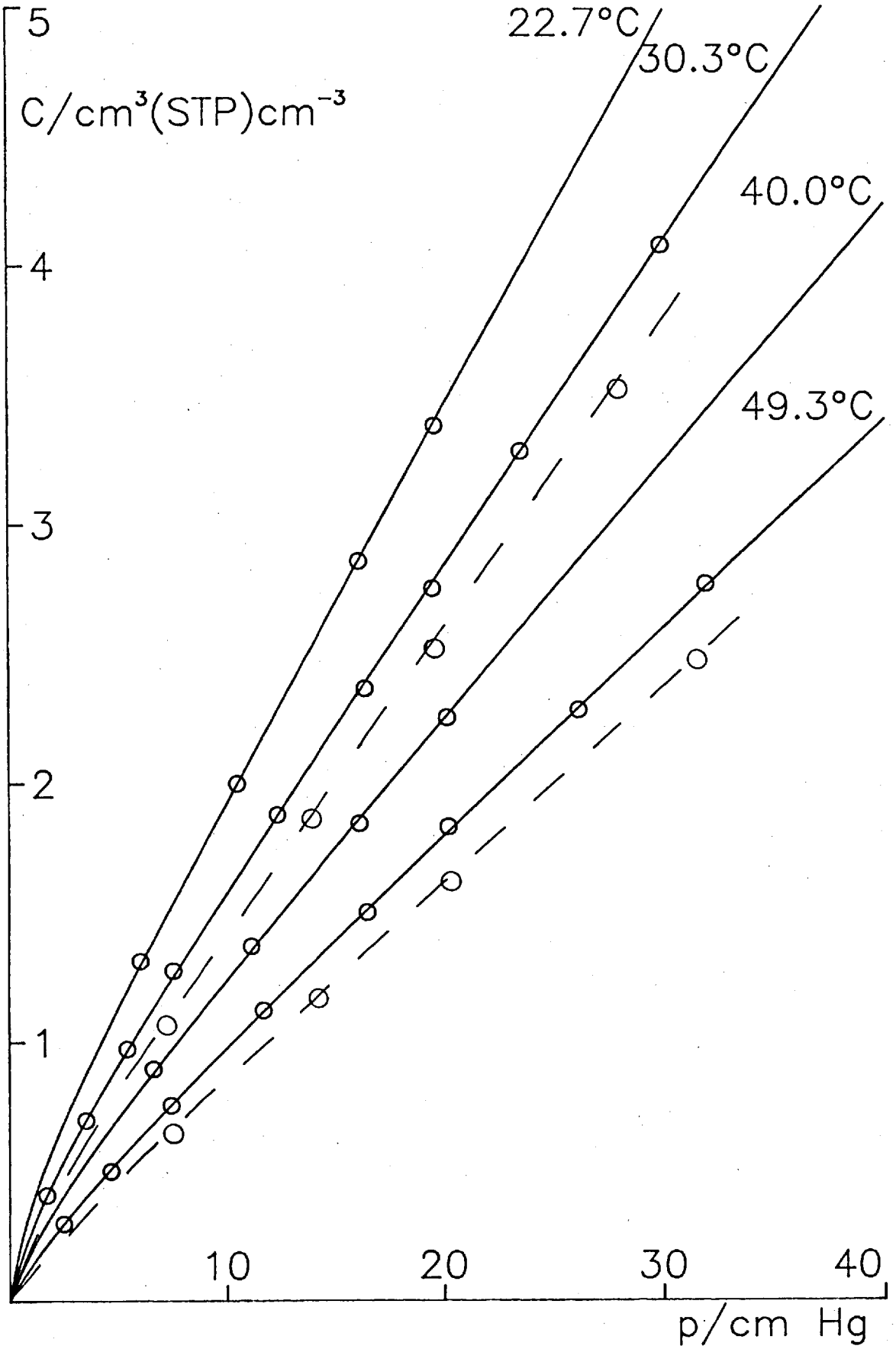

Figure 4.19: 56.3% Graft iso-Butane Sorption Isotherms

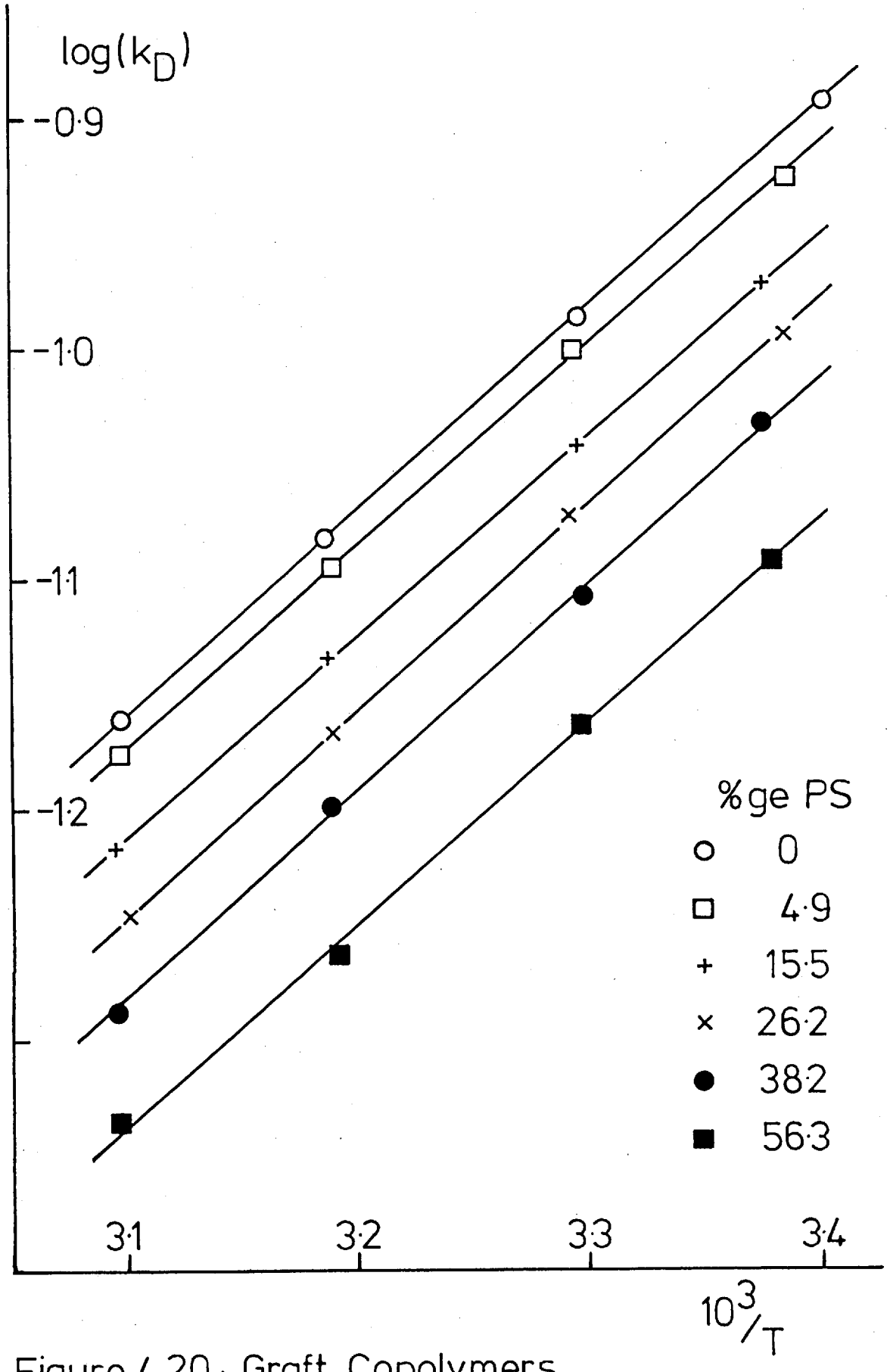

Figure 4.20 : Graft Copolymers
Propane Solubilities

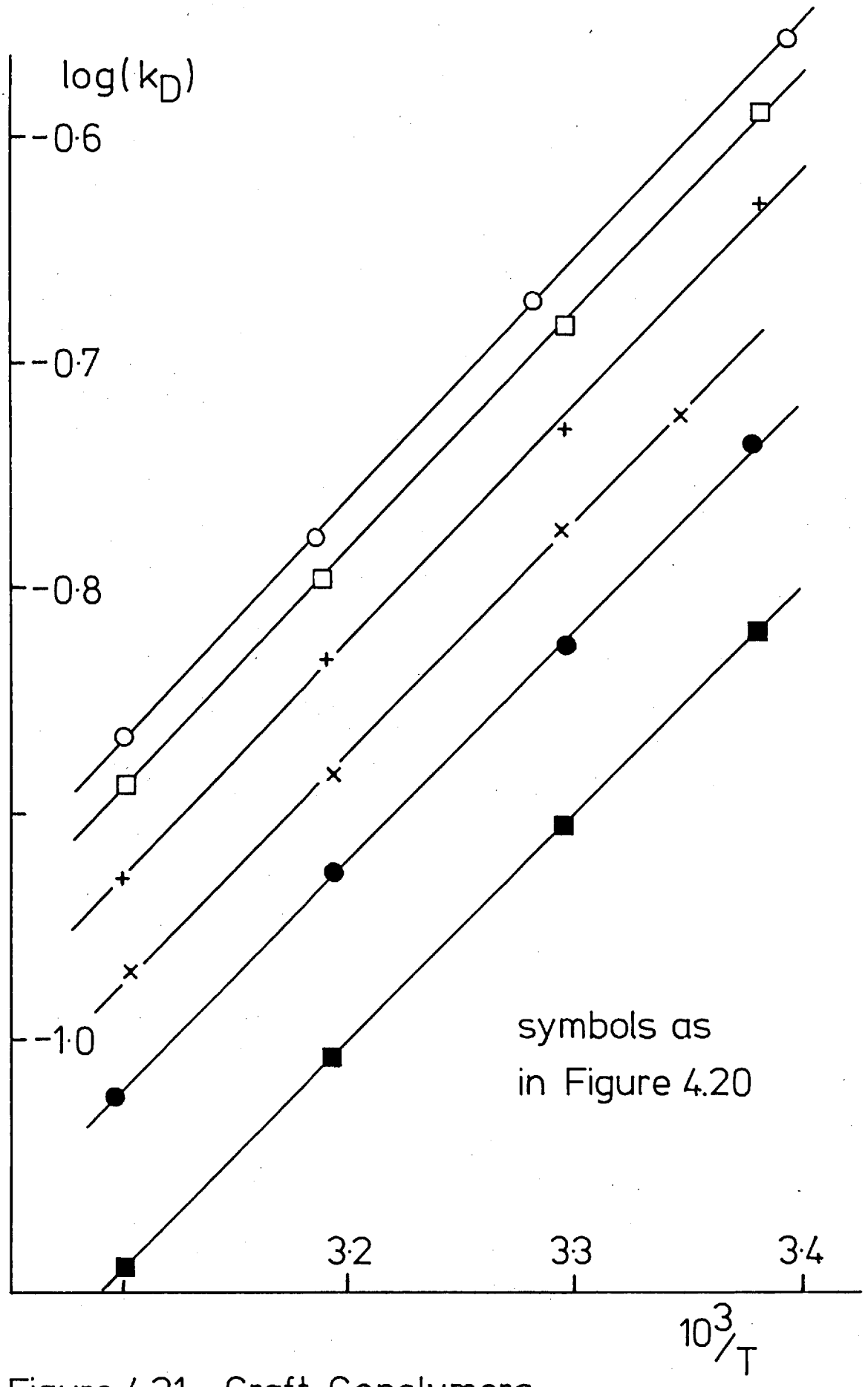

Figure 4.21: Graft Copolymers
iso-Butane Solubilities

and are all linear over the pressure range studied. Comparisons with the polystyrene propane sorption isotherms and with the isotherms of a graft copolymer of a similar composition (38.2% PS, figure 4.13 and 4.18) indicate, however, that significant curvature is to be expected for propane and higher hydrocarbons. The possible causes of this anomaly will be discussed later.

Figure 4.23 shows van't Hoff plots of the solubilities of the four gases, and includes the solubilities of propane and iso-butane in membranes CC (cyclohexane cast) and SC (styrene cast). These solubilities are in good agreement with those in membrane CM, and indicate that the method of sample preparation has negligible effect upon the block copolymer solubilities. Heats of sorption obtained from the van't Hoff plots are given in table 4.9. $\Delta\bar{H}_S$ shows little change from the values for PDMS given in table 4.1, and good agreement is obtained with ΔH_D for propane and iso-butane in the graft copolymers. $\Delta\bar{H}_S$ is determined from the temperature dependence of the solubility constant (equation 1.3), and ΔH_D from the temperature dependence of the Henry's law dissolution constant k_D. It was shown in section 4.2 that heats of sorption which include a Langmuir component of sorption are significantly more exothermic than ΔH_D and thus the close correspondence of $\Delta\bar{H}_S$ for the block copolymers and ΔH_D for the graft copolymers may be taken as evidence that there is no Langmuir sorption in the block copolymers, and that the sorption process is that of the Henry's law sorption in the graft copolymers.

The lack of any Langmuir sorption is also shown by the methane and propane solubilities. If simple additivity of the concentrations within the two phases is assumed as given by equation 4.10:

Table 4.9 Block Copolymer Solubilities

	$S\ (30^{o}C)$	$\Delta\bar{H}_S$
	$cm^3(STP)cm^{-3}cmHg^{-1}$	$kJ\ mol^{-1}$
methane	5.32×10^{-3}	-7.5
propane	8.41×10^{-2}	-17.1
n-butane	2.55×10^{-1}	-22.1
iso-butane	1.68×10^{-1}	-20.0

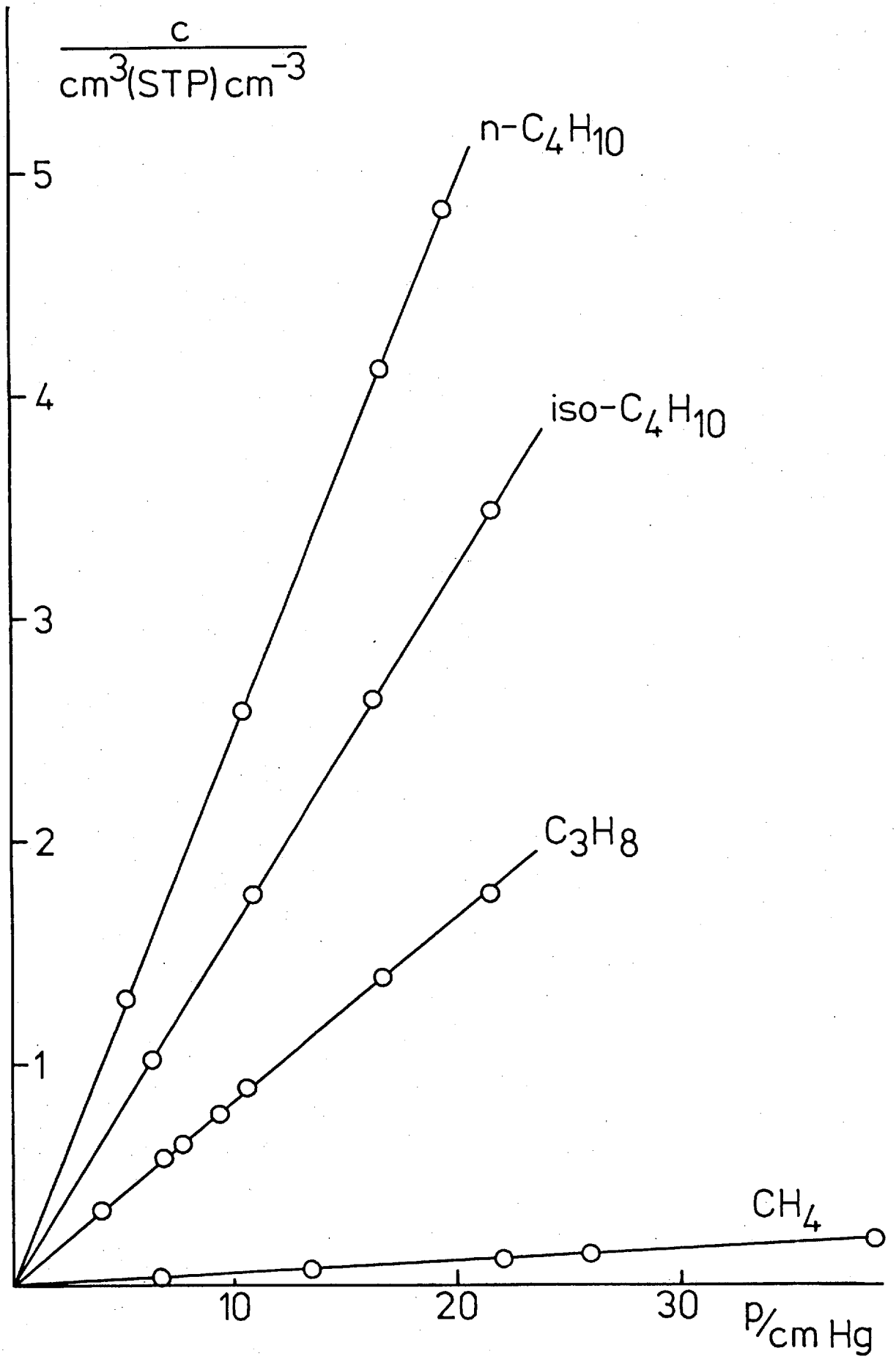

Figure 4.22: Membrane CM Sorption Isotherms

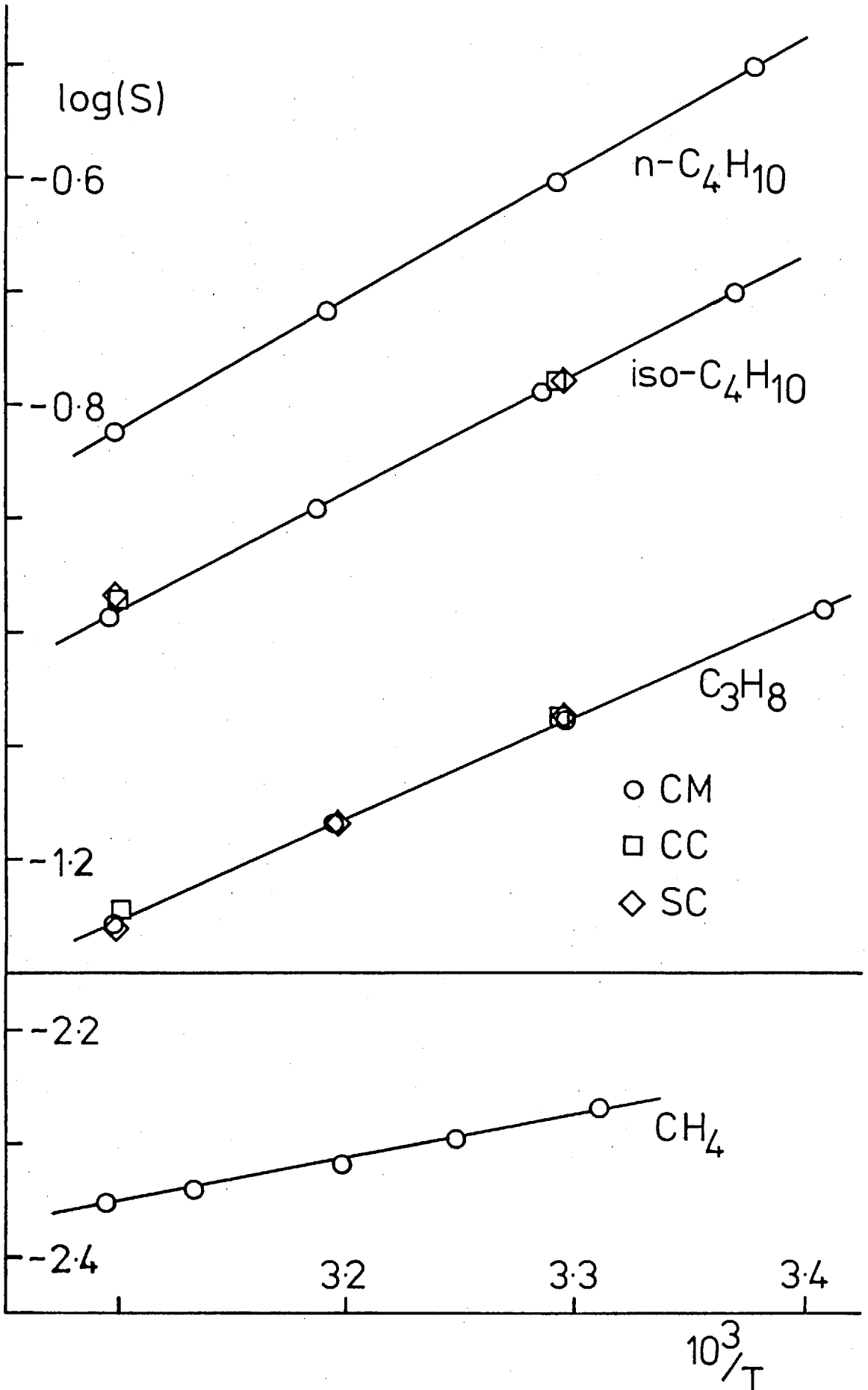

Figure 4.23: Block Copolymer Solubilities

$$c_M = V_C \cdot c_C + V_D \cdot c_D \quad \ldots (4.10)$$

then the solubility will be a weighted mean of the solubilities in the component polymers. Use of the solubilities of methane in PDMS and polystyrene given in tables 4.1 and 4.5 respectively, results in a value of 6.6×10^{-3} $cm^3 STP cm^{-3} cm\ Hg^{-1}$ for the solubility in the block copolymer at 30^oC, significantly higher than the experimentally determined value of 5.32×10^{-3}. The data of Vieth (123) allow the interpolation of k_D at 30^oC for methane in polystyrene, and use of this value (2.44×10^{-3}) leads to a solubility of 5.1×10^{-3} in the block copolymer, in good agreement with the experimentally determined value. Similarly, using the k_D for propane at 30^oC from table 4.6, good agreement is obtained between the predicted (8.48×10^{-2}) and experimentally determined (8.41×10^{-2}) solubilities.

4.3.3 Discussion

The absence of any Langmuir component of the sorption in the block copolymers is thought to be due to two factors:

1. the T_g of the polystyrene phase in the block copolymer ($\sim 70^oC$) is much lower than that in the graft copolymers ($\sim 100^oC$);
2. the polystyrene domains in the block copolymer are somewhat smaller than domains in the graft copolymers ($\sim$40 nm as compared to 50-100 nm).

From the data for the block copolymer supplied by the manufacturer the molecular weight of the polystyrene end blocks may be calculated as approximately 18,000. Homopolystyrene of this molecular weight would be expected to have a T_g some 5 or 6^oC below that of polystyrene of an infinite molecular weight (128). Clearly some other factor must be responsible for the lower T_g, and it is believed that incomplete phase separation, giving an interfacial region consisting of both polymers, may be responsible for this effect. The presence of an interfacial region may be inferred from the broad transitions obtained by DSC, and from the lack of a distinct phase boundary in the electron micrographs as is observed for polymer blends prepared from mixtures of discrete particulate emulsions. Although the properties of this miscible region are not accurately known, it is to be expected that the sorption

properties will be intermediate between those of the two homopolymers. Also, since the T_g of a miscible polymer system lies between those of its components, Langmuir sorption is likely to be absent from most of the interfacial region.

The smaller size of the domains in the block copolymer is expected to accentuate this effect, since smaller domains will have a larger total surface area and the interfacial region will account for a larger proportion of the polystyrene than in the larger domains of the graft copolymers.

The data also suggest that the graft copolymers exhibit enhanced Langmuir sorption due to the method of preparation. If, as suggested in section 4.2, the Langmuir saturation constant is directly related to the "excess" free volume in a glassy polymer, then the method of sample preparation will have a large effect upon levels of Langmuir sorption. The dashed lines of figure 4.19 show the iso-butane sorption isotherms at 30.3°C and 49.3°C obtained after heating the 56.3% polystyrene copolymer at 150°C for 24 hours in a vacuum oven. It is evident that the Langmuir sorption capacity has been significantly reduced by the heat treatment, although the Henry's law sorption, as given by the high pressure asymptote, is relatively unaffected. The polystyrene domains of the graft copolymer become highly swollen during the extraction with ethyl acetate (a good solvent for polystyrene) and it is thought that the domains are left in an expanded configuration upon desorption of the solvent. In this way the free volume within the domains, and hence the Langmuir sorption capcity, is significantly higher than that of an equilibrium polystyrene sample. On heating above T_g relaxation to an equilibrium configuration becomes possible, and this is shown by the lower sorptive capacity of the copolymer.

The Henry's law solubilities of propane and iso-butane at 30°C are plotted as a function of copolymer composition in figure 4.24. Clearly, simple additivity is not applicable to the graft copolymers and the solid lines represent an empirical correlation deduced from the spacing of the van't Hoff plots of figures 4.20 and 4.21, and given by equation 4.11;

$$\log k_{D(M)} = V_C . \log S_C + V_D . \log k_{D(D)} \qquad \ldots (4.11)$$

The subscripts used above are M for the copolymer, C for the continuous

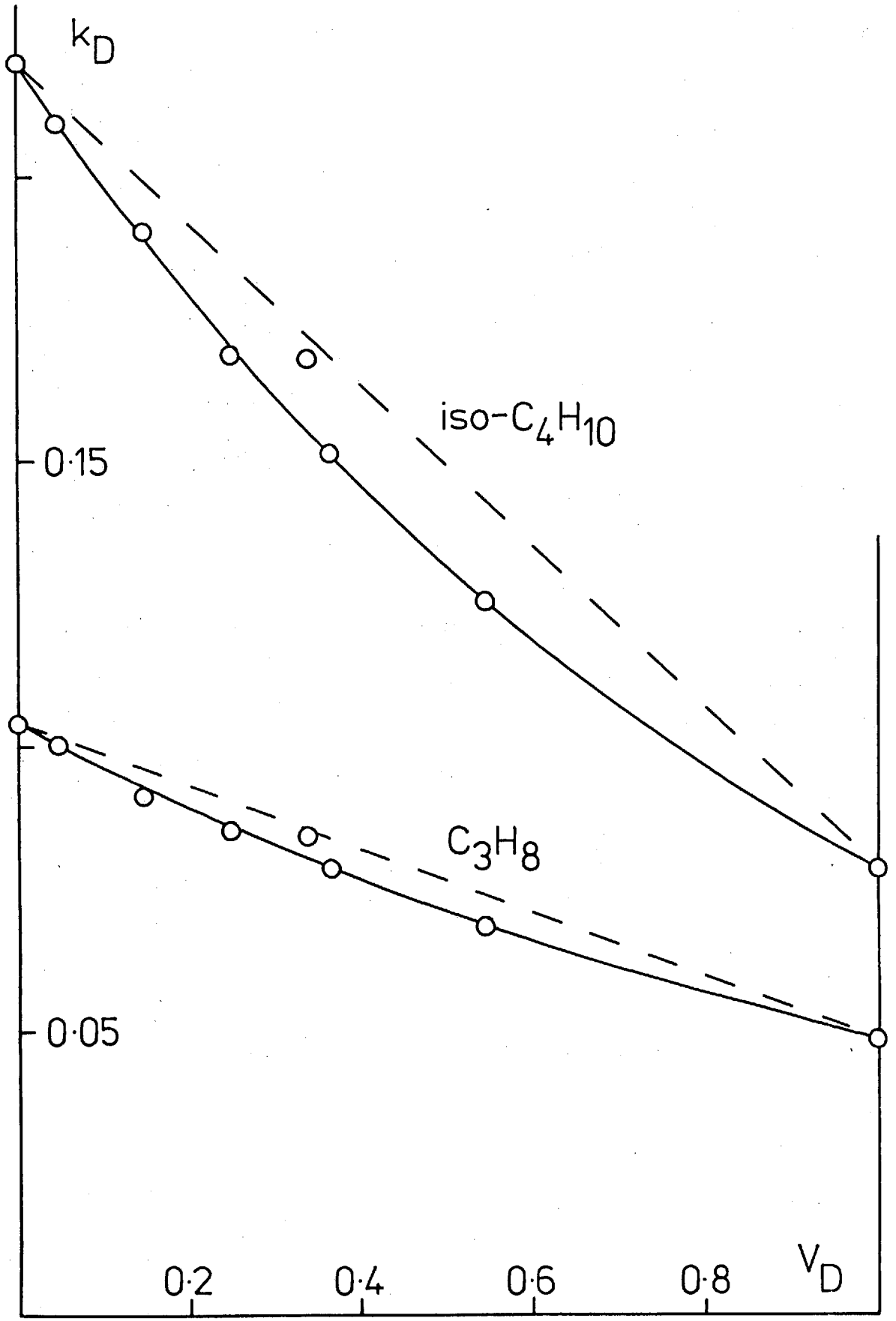

Figure 4.24: Copolymer Solubilities at 30°C

PDMS phase, and D for the disperse polystyrene phase. Similar behaviour has been reported by Toi et al (15) for polyethylene grafted with styrene, although in this case simple additivity of the component polymer solubilities was observed after soxhlet extraction with benzene. No explanation of this effect is offered by Toi.

A possible cause of the departure from simple additivity may be found from the examination of similar effects observed for other physical properties of polymer composites. The thermal expansion coefficients of filled polymers are found to vary in the same manner (129), and an equation of the form of equation 4.11 has been proposed to represent this behaviour. Wang and Kwei (130) attribute the deviations from a linear rule of mixtures to induced thermal stresses in the polymer, and it is possible that stresses caused by the inclusion of polystyrene domains into the cross-linked PDMS network may be responsible for the departure from linearity of the graft copolymer solubilities. The block copolymer is not cross-linked and is therefore expected to be stress-free, and the solubilities of the block copolymer lie close to the linear tie-lines. (The k_D for iso-butane in polystyrene was estimated as 7.8×10^{-2} from the extrapolation of the empirical correlation.)

4.4 Copolymers: Steady State Permeation

4.4.1 Block Copolymers

The permeabilities of the four penetrants in the block copolymer membrane CM were measured in the temperature range $25^{o}C$ to $50^{o}C$, and the results are shown in the form of Arrhenius plots in figure 4.25. The permeabilities were independent of ingoing pressure, except for a slight trend towards increasing permeability for the more soluble penetrants as noted for PDMS. E_P and P at $30^{o}C$ obtained from the Arrhenius plots are given in table 4.10 which includes comparisons with the continuous (PDMS) phase values. Within the experimental error the permeability ratio, P/P_C, is independent of the penetrant, as is expected for a relatively impermeable disperse phase. (The permeability of propane in polystyrene, for example, may be estimated from the diffusion and solubility coefficients as $\sim 3.4 \times 10^{-12}$). When $P_D << P_C$ the models reviewed in chapter 2 can all be reduced to:

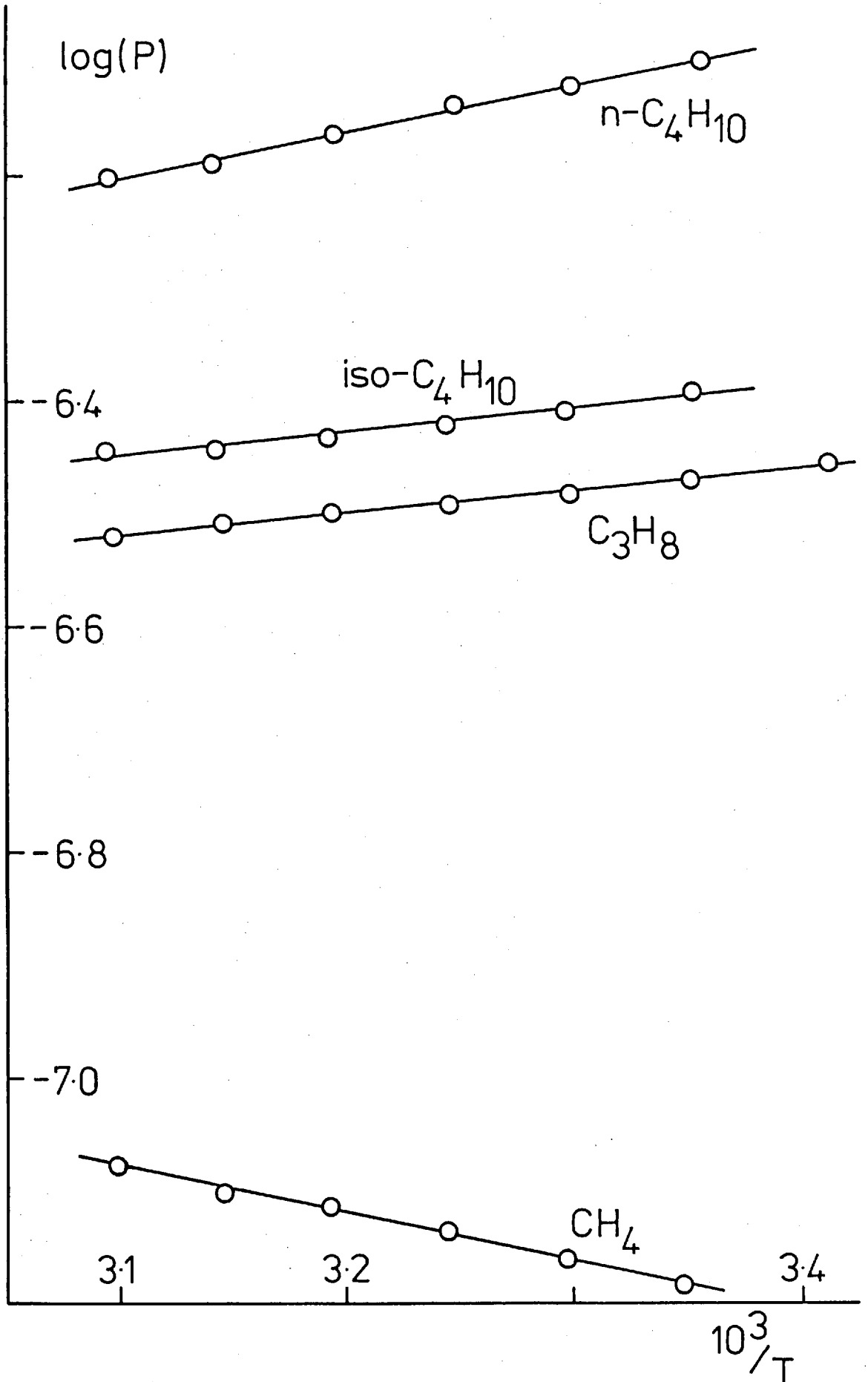

Figure 4.25: Membrane CM Permeabilities

Table 4.10 Block Copolymer (CM) Permeabilities

($P \times 10^7$ $cm^3(STP)cm\ cm^{-2}(cm\ Hg)^{-1}s^{-1}$; E_P $kJ\ mol^{-1}$)

	$P\ (30^0C)$	P/P_C	E_P	E_{P_C}
methane	0.689	0.52	7.9	7.3
propane	3.32	0.50	-3.8	-2.9
n-butane	7.57	0.50	-7.9	-6.8
iso-butane	3.92	0.48	-4.5	-5.3

$$P_M = P_C.F(V_D) \qquad \ldots (4.12)$$

where the form of the function $F(V_D)$ is specific to each model. Thus the permeability ratio is dependent only upon the volume fraction of each phase, and since V_D is virtually independent of temperature, E_P for the copolymer is equal to that of the continuous phase. This is shown by the last two columns of table 4.10 where the small differences between the values are well within the experimental error.

The permeabilities of propane and iso-butane in the block copolymer membranes CC and SC were also determined and the results are summarised in table 4.11. Although E_P values are approximately the same for the two membranes, and again approximately equal to E_P for PDMS, there is a marked difference in the permeabilities. The permeabilities of membrane CC are little different from those of the compression moulded (CM) membrane and it seems reasonable to infer from this that the two have similar morphologies. The electron micrographs confirm the basic similarity although the sample CC is seen to have regions of a lamellar type of structure. Some inferences concerning the morphology of membrane SC may also be made from the permeability data. The constant value of E_P for the three block copolymer membranes and for PDMS implies that all have a continuous phase consisting of essentially pure PDMS. The lower permeability of membrane SC must therefore be due to a difference in domain shape which produces a more effective barrier to permeation, the most probable being a plate-like or lamellar type of structure. The electron micrograph of membrane SC shows that this is indeed the case, and long continuous regions of the paler polystyrene are clearly visible.

It is pertinent at this point to discuss briefly the reasons for

the different morphologies observed by preparing samples of the same copolymer by different methods. The phase separation of a block copolymer in solution is thought to occur via the formation of micelles of the least soluble component at some critical concentration (131). In the case of the membrane cast from cyclohexane, which is a better solvent for PDMS, micelles of polystyrene will be formed, and upon further evaporation these micelles are left as the disperse phase within the membrane. Styrene monomer is a better solvent for polystyrene and hence the formation of PDMS micelles will be favoured when casting from this solvent. The volume fraction of polystyrene (0.337) is insufficient to form a totally continuous phase, although the polystyrene remains in large lamellar-like regions.

Table 4.11 Block Copolymer (CC and SC) Permeabilities

($P \times 10^7$ $cm^3(STP)cm\ cm^{-2}(cm\ Hg)^{-1}s^{-1}$, E_p $kJ\ mol^{-1}$)

	$P(30^oC)$	P/P_C	E_P	E_{P_C}
Membrane CC				
propane	3.25	0.49	-1.9	-2.9
iso-butane	3.84	0.47	-4.1	-5.3
Membrane SC				
propane	1.01	0.15	-1.9	-2.9
iso-butane	1.23	0.15	-3.7	-5.3

4.4.2 Graft Copolymers

The propane and iso-butane permeabilities of the graft copolymers are shown in the form of Arrhenius plots in figures 4.26 and 4.27, and the results are summarised in table 4.12. The permeabilities were again independent of ingoing pressure, except for the slight trend noted previously. As for the block copolymer membranes E_p is seen to be constant within experimental error for each penetrant, and indicates that PDMS forms the continuous phase in all of the membranes studied.

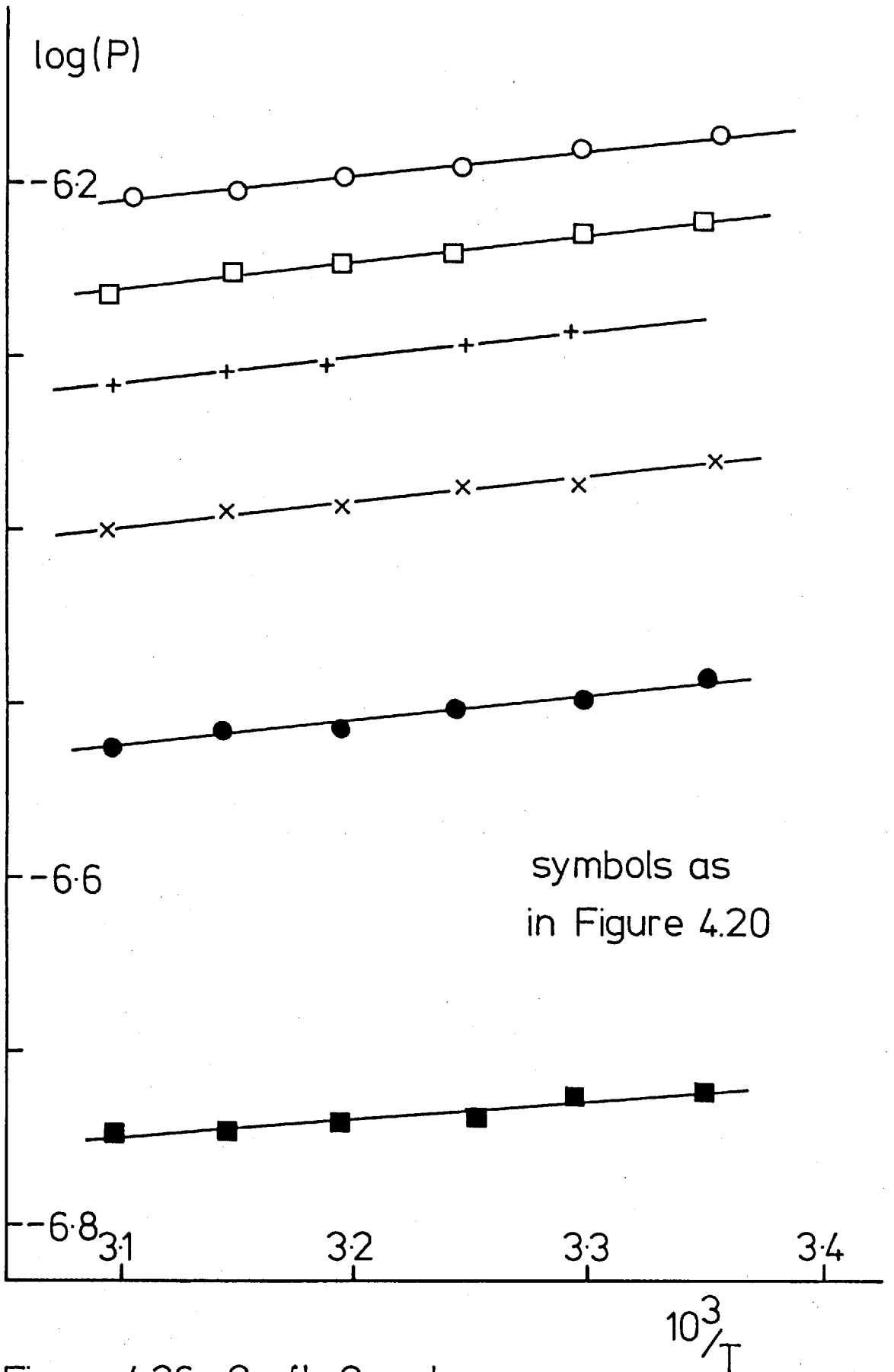

Figure 4.26: Graft Copolymers
Propane Permeabilities

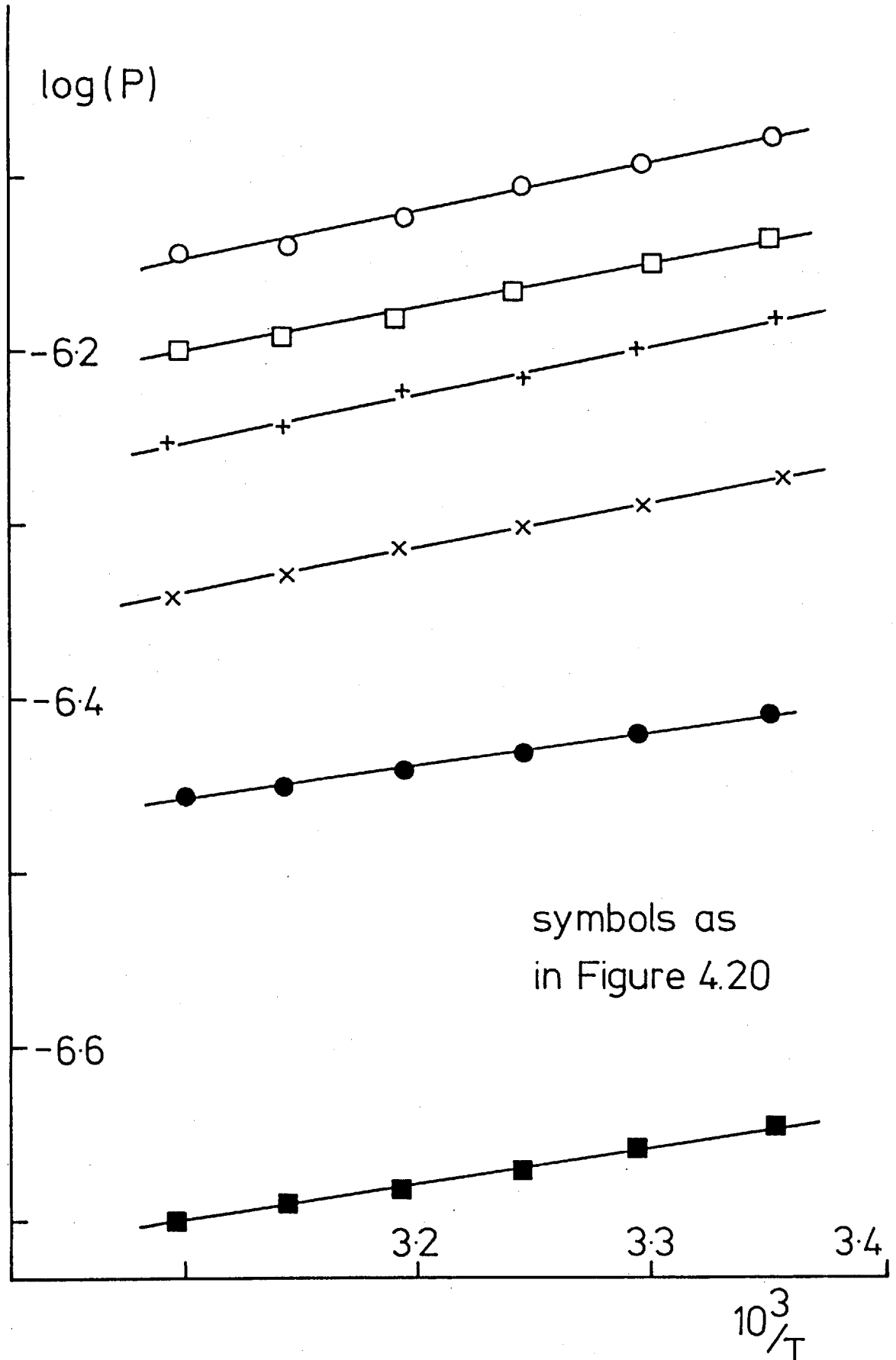

Figure 4.27: Graft Copolymers
iso-Butane Permeabilities

Table 4.12 Copolymer Permeabilities

($P \times 10^7$ $cm^3(STP)cm\ cm^{-2}(cm\ Hg)^{-1}s^{-1}$, E_P $kJ\ mol^{-1}$)

Membrane	V_D	P (30°C)	P/P_C	E_P
propane				
PDMS	0	6.59	1.00	-2.9
4.9% PS	.046	5.89	0.89	-3.1
15.5% PS	.146	5.19	0.79	-3.1
26.2% PS	.248	4.27	0.65	-2.8
CM	.337	3.32	0.50	-3.8
38.2% PS	.365	3.20	0.49	-3.2
56.3% PS	.545	1.87	0.28	-2.0
iso-butane				
PDMS	0	8.10	1.00	-5.3
4.9% PS	.046	7.08	0.87	-5.0
15.5% PS	.146	6.34	0.78	-5.1
26.2% PS	.248	5.15	0.64	-5.1
CM	.337	3.92	0.48	-4.5
38.2% PS	.365	3.80	0.47	-3.8
56.3% PS	.545	2.20	0.27	-4.0

4.4.3 Discussion

The permeability ratios are plotted against volume fraction of disperse phase in figure 4.28. The solid lines show the predictions of four of the models which, for the case when $P_D << P_C$ reduce to the following forms:

Maxwell (42) $$P_M = P_C \cdot \frac{2V_C}{2 + V_D} \quad \ldots (4.13)$$

Bruggeman (49) $$P_M = P_C \cdot (V_C)^{3/2} \quad \ldots (4.14)$$

Higuchi (54) $$P_M = P_C \cdot \frac{1.61\ V_C}{1.61 + 1.39\ V_D} \quad \ldots (4.15)$$

Böttcher (51) $$P_M = P_C \cdot (1 - \frac{3V_D}{2}) \quad \ldots (4.16)$$

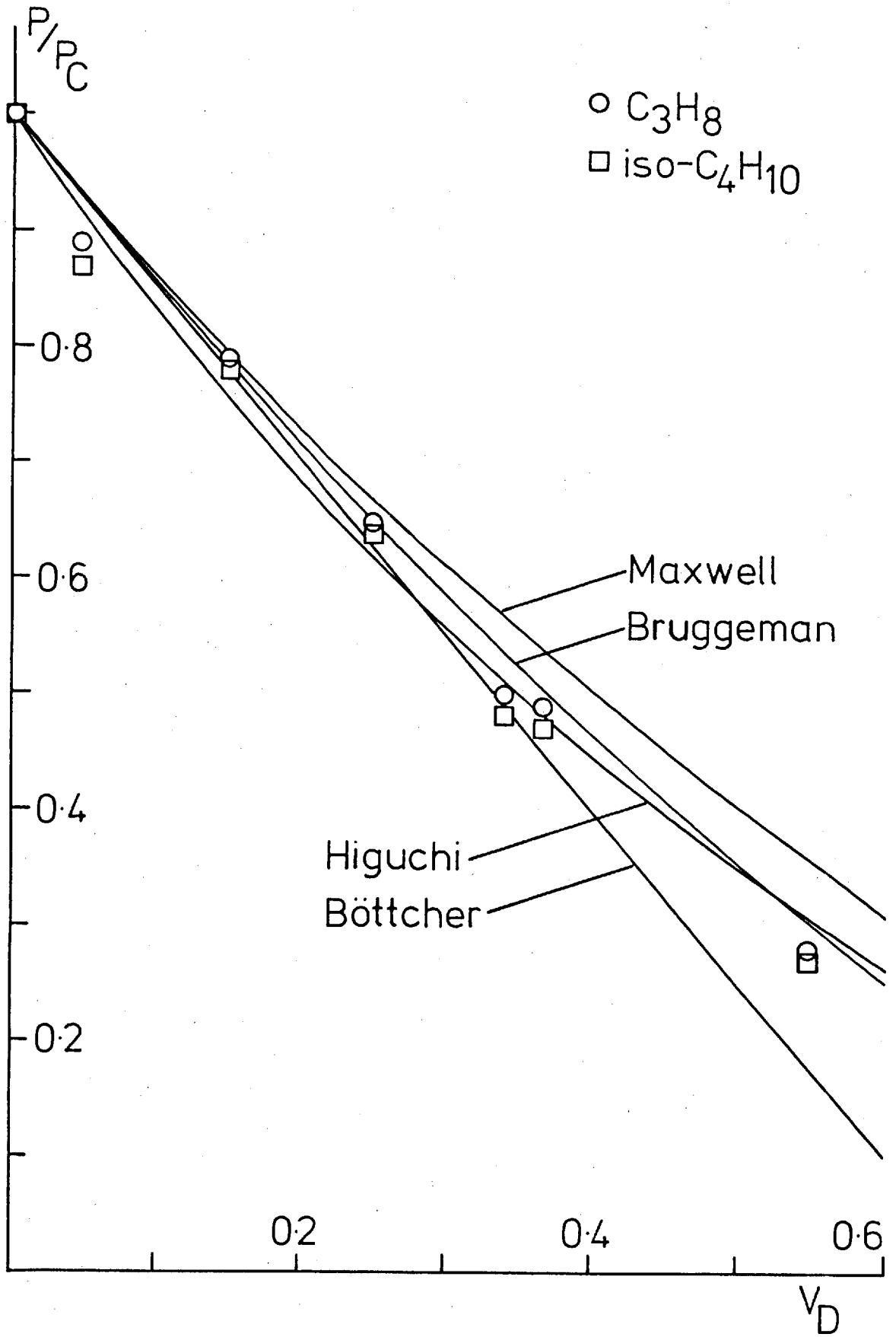

Figure 4.28: Copolymer Permeability Ratios

The Bruggeman, Higuchi, and Böttcher models represent the most successful predictions for the PDMS-PVAc graft copolymers studied by Sheer (81), and the Maxwell model is included for comparative purposes. The effect of neighbouring spheres, not included in the Maxwell model, is seen to cause a significant lowering in P at high volume fractions of the disperse phase. The Böttcher model (for the particular case of $P_D \approx 0$) is also clearly inadequate in this region, although the agreement with the experimental results and with the other models at low V_D is surprisingly good in view of the simple linear form of this expression. The Higuchi model is thought to provide a good representation of the data, with the experimental points randomly scattered about this line, and for this reason the Higuchi expression is used as the basis for the theoretical curves in the remaining analysis. The scatter of the experimental results is such that the Bruggeman model is an equally good representation and the two curves are not widely different over the range of volume fraction studied. The final choice of a suitable model is thus based upon a personal preference in favour of the semi-empirical formulation of Higuchi.

Only a brief mention will be made here of the remaining models reviewed in chapter 2. Use could be made of the extensions to the Maxwell model for simple lattices of dispersions (45-48), since P is relatively insensitive to the arrangement of the disperse phase. The expressions are highly complex, however, and give no better fit than the simple models discussed above. The modification to the Bruggeman model proposed by Meredith and Tobias (50) does not deviate significantly from the original except as the limit for close packing of spheres is approached, and similarly offers no advantages to offset the greater complexity. Finally, the only other suitable model not involving arbitary or experimentally determined parameters is that of Prager (60) which, in the form given in chapter 2 for the permeability, predicts permeabilities slightly higher than those given by the Maxwell model, and much reduced permeabilities if the proposed correction is not made.

4.5 Copolymers: Diffusion

It has been shown in the previous section that the polystyrene domains of the copolymers act only as impermeable filler particles towards the steady-state permeability of the membranes. The diffusion

coefficient, however, relates the flux to the concentration gradient within the membrane and is hence affected by the sorptive capacity of the disperse phase. Higuchi (54) gives the condition for Fickian behaviour of this type of system and, despite the large difference between the diffusion coefficients of the two phases, the domains are sufficiently small to allow rapid equilibriation and Fickian diffusion in all of the samples studied.

4.5.1 Block Copolymers

The block copolymers represent the simplest of the copolymer membranes since P, S, and consequently D are all independent of concentration. The block copolymer is thus effectively a filled rubber in which the filler absorbs penetrant according to Henry's law, and provides the simplest example of diffusion with immobilisation. The flux, J, can be related to the diffusion coefficient and concentration gradient within the membrane:

$$J = -D_M \cdot \frac{\partial c}{\partial x} \qquad \ldots (4.17)$$

or, since the flux is controlled only by the continuous phase, J can be related to the concentration gradient within that phase only:

$$J = -D_F \cdot \frac{\partial c_C}{\partial x} \qquad \ldots (4.18)$$

D_F is the diffusion coefficient of a membrane containing an equal volume fraction of a non-sorbing filler, and may be obtained from the models for the permeability of a filled membrane since $P_F/P_C = D_F \cdot V_C/D_C$. Equating the two expressions for J gives an equation for the diffusion coefficient of the membrane:

$$D_M = D_F \cdot \frac{\partial c_C}{\partial c} \qquad \ldots (4.19)$$

and since the solubilities are independent of concentration:

$$D_M = D_F \cdot \frac{V_C \cdot S_C}{S_M} \qquad \ldots (4.20)$$

where $V_C \cdot S_C$ is the solubility of the continuous phase per unit volume of the membrane. (It is apparent that equation 4.20 could also have been derived from a consideration of the membrane permeabilities.)

Since D_M is independent of c the simple time lag expression (equation 1.12) is applicable to the block copolymer. Diffusion coefficients obtained from the time lag are included in table 4.13 which gives a comparison of the diffusion coefficients of the four penetrants in membrane CM. The close correspondence between $\overline{D}$ and D_S obtained for this copolymer is due to the use of aluminium foil to blank off the edges of the sample used on the sorption balance. A thin strip of foil was stuck around the edge of the sample by first moistening the edge with solvent (1,1,1 trichloroethane). Good adhesion was obtained in this way, and the aluminium foil was found to be effective in preventing diffusion from occurring through the edges of the sample, thus eliminating the edge effect. This procedure was not applicable to the cross-linked samples since poor adhesion and no measurable change in D was observed when this was attempted.

The diffusion coefficients of table 4.13 were interpolated from the corresponding Arrhenius plots and those for $\overline{D}$ are shown in figure 4.29. The activation energies of diffusion obtained from these plots are given in table 4.14 which shows that E_D is constant for each penetrant, within the experimental error, and independent of the method of measurement. A theoretical expression for E_D may be derived from equation 4.20 by taking logarithms and differentiating w.r.t. 1/T, which leads to:

$$E_{D_M} = E_{D_F} + \Delta\overline{H}_{S_C} - \Delta\overline{H}_{S_M} \qquad \ldots (4.21)$$

Since D_F depends only upon D_C and the volume fraction of filler we also have $E_{D_F} = E_{D_C}$, and hence:

Table 4.13 Block Copolymer (CM) Diffusion Coefficients

($D \times 10^6$ $cm^2 s^{-1}$ at 30^0C)

	$\overline{D}$	D_L	D_S
methane	-	10.0	13.0
propane	4.06	3.13	3.95
n-butane	3.07	2.59	2.97
iso-butane	2.38	2.03	2.33

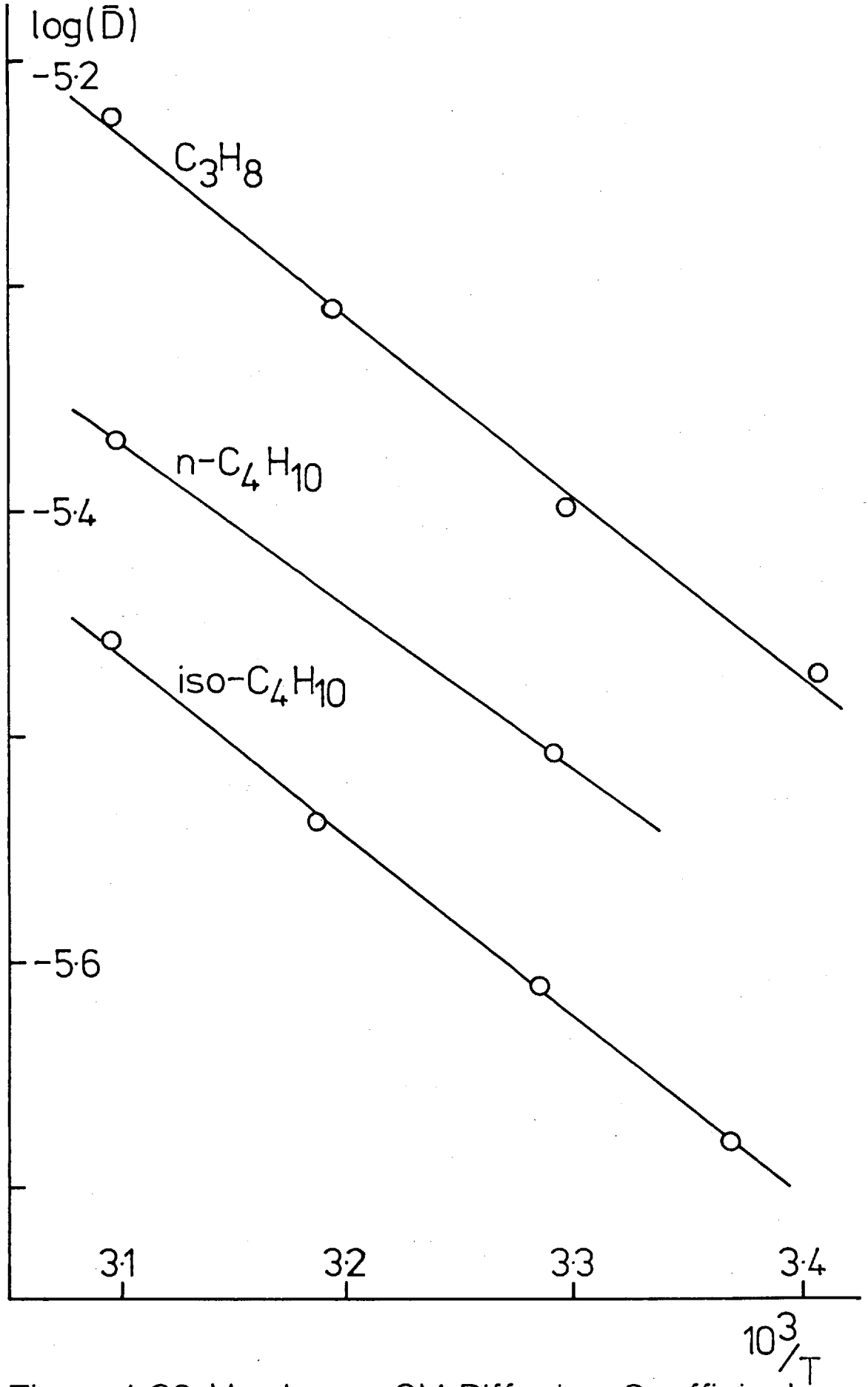

Figure 4.29: Membrane CM Diffusion Coefficients

Table 4.14 Block Copolymer (CM) Activation Energies of Diffusion

	(E_D kJ mol^{-1})		
	$E_{\overline{D}}$	E_{D_L}	$(E_P - \Delta\overline{H}_S)$
methane	-	13.1	15.4
propane	15.3	14.5	13.3
n-butane	13.8	14.4	14.2
iso-butane	15.4	15.1	15.5

$$E_{D_M} = E_{D_C} + \Delta\overline{H}_{S_C} - \Delta\overline{H}_{S_M} \qquad \ldots (4.22)$$

It is apparent then that the close correspondence between E_D for the block copolymer and for PDMS is fortuitous, and due to the similarity of the heats of sorption in the two polymers.

4.5.2 Graft Copolymers

Although permeabilities were also independent of ingoing pressure for the graft copolymers, the non-linear isotherms obtained for these samples means that the measured diffusion coefficients are concentration dependent. In this respect the graft copolymers are examples of dual mode sorption in which the concentration of immobile penetrant is given by the total concentration within the polystyrene domains, and not solely by the Langmuir component of the sorption. However, by following the normal dual mode sorption analysis a concentration independent diffusion coefficient, D*, is obtained which relates the flux to the total Henry's law concentration within the membrane, c*, and is thus comparable to the D_M obtained for the block copolymer. From equation 1.14:

$$\overline{D} = \frac{1}{c_o} \int_0^{c_o} D_M(c).dc \qquad \ldots (4.23)$$

and from a consideration of the flux:

$$D_M(c) = D^*.\frac{\partial c^*}{\partial c} \qquad \ldots (4.24)$$

D* is the theoretical limiting value of the diffusion coefficient at

Table 4.15 Example Calculation of D*

($D \times 10^6$ $cm^2 s^{-1}$, c_o $cm^3(STP)cm^{-3}$, p_o cm Hg)

p_o	c_o	$\bar{D}$	D*
7.54	1.275	1.44	1.95
12.33	1.877	1.59	1.94
16.37	2.365	1.72	1.99
19.47	2.752	1.84	2.08

high concentration and is equal to the steady-state diffusion coefficient defined by $D_S = P/k_D$. (In practice, D is expected to increase further at high concentration due to plasticisation of the polymer.) Combining the two equations gives:

$$\bar{D} = \frac{1}{c_o} \int_0^{c_o} D^* dc^* = D^* . \frac{c^*}{c_o}$$

$$D^* = \bar{D} . \frac{c_o}{k_D \cdot p_o} \qquad \ldots (4.25)$$

Table 4.15 gives, as an example the experimentally determined $\bar{D}$ and D* values for iso-butane sorption in the 56.3% PS copolymer at 30.3°C (k_D = 0.1245). Although a small trend of increasing D* with increasing c remains, this is not felt to be significant, and parallels the trend observed for the permeabilities.

Interpolated values of D* at 30°C for the series of graft copolymers are compared with the steady-state diffusion coefficients in table 4.16. The values of D* are larger than the corresponding D_S values by a nearly constant factor, and this is attributed to edge effects during sorption. The time lag for these copolymers is dependent upon the ingoing pressure and has not been included in the analysis. It is to be expected that the time lag will be given by an expression similar to that of Paul (73) for dual mode sorption, and this has recently been verified for the system used in the present study (132). (See appendix C.3)

Table 4.16 Graft Copolymer Diffusion Coefficients

($D \times 10^6$ $cm^2 s^{-1}$ at 30^oC)

		propane		iso-butane	
Membrane	V_D	D*	D_S	D*	D_S
4.9% PS	.046	6.98	5.89	3.86	3.39
15.5% PS	.146	6.50	5.69	3.80	3.34
26.2% PS	.248	5.65	5.01	3.60	3.05
38.2% PS	.365	4.61	4.07	2.90	2.52
56.3% PS	.545	3.04	2.73	1.98	1.76

4.5.3 Discussion

Equation 4.20 is also applicable to D* and the correlation of diffusion coefficients is shown in the form of plots of the diffusion coefficient ratio, D/D_C, against the volume fraction of polystyrene in figures 4.30 and 4.31. The theoretical lines in these figures were obtained from the use of the Higuchi expression for D_F and the additivity rule (equation 4.10) for the Henry's law solubility of the copolymers. The points have also been scaled to give the best fit to the theoretical curves and to remove the dependence upon the experimental values of D_C. The steady-state value of D_C was used for both diffusion coefficient ratios for the membrane CM (V_D = 0.337), since edge effects during sorption were eliminated for this sample. The close correspondence of the diffusion coefficient ratios determined from D* and D_S for each sample may well indicate that the scatter of the experimental data is due largely to the uncertainties in the determination of the membrane dimensions. This is further shown by the similarity in the scatter of the points in the two figures, and the similarity with the scatter of the permeability ratios (figure 4.28).

Estimates of the activation energy of diffusion associated with D* are presented in table 4.17. In many cases these values have been derived from measurements at only two temperatures and the uncertainty in E_D is consequently large. Despite this fact it is evident that the change in E_D remains small, as predicted by the earlier analysis for the block copolymers (equation 4.22).

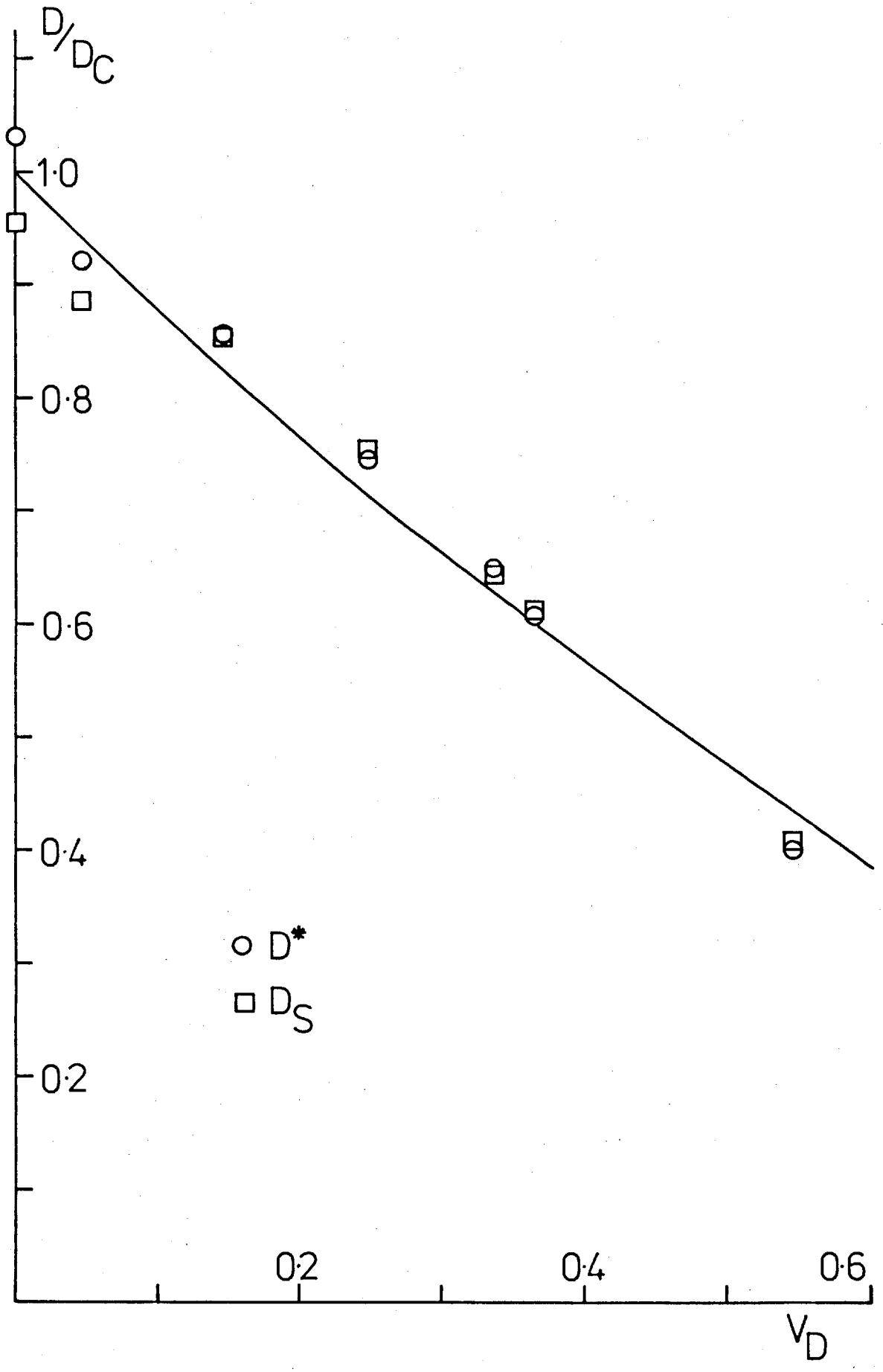

Figure 4.30: Propane Diffusion Coefficient Ratios

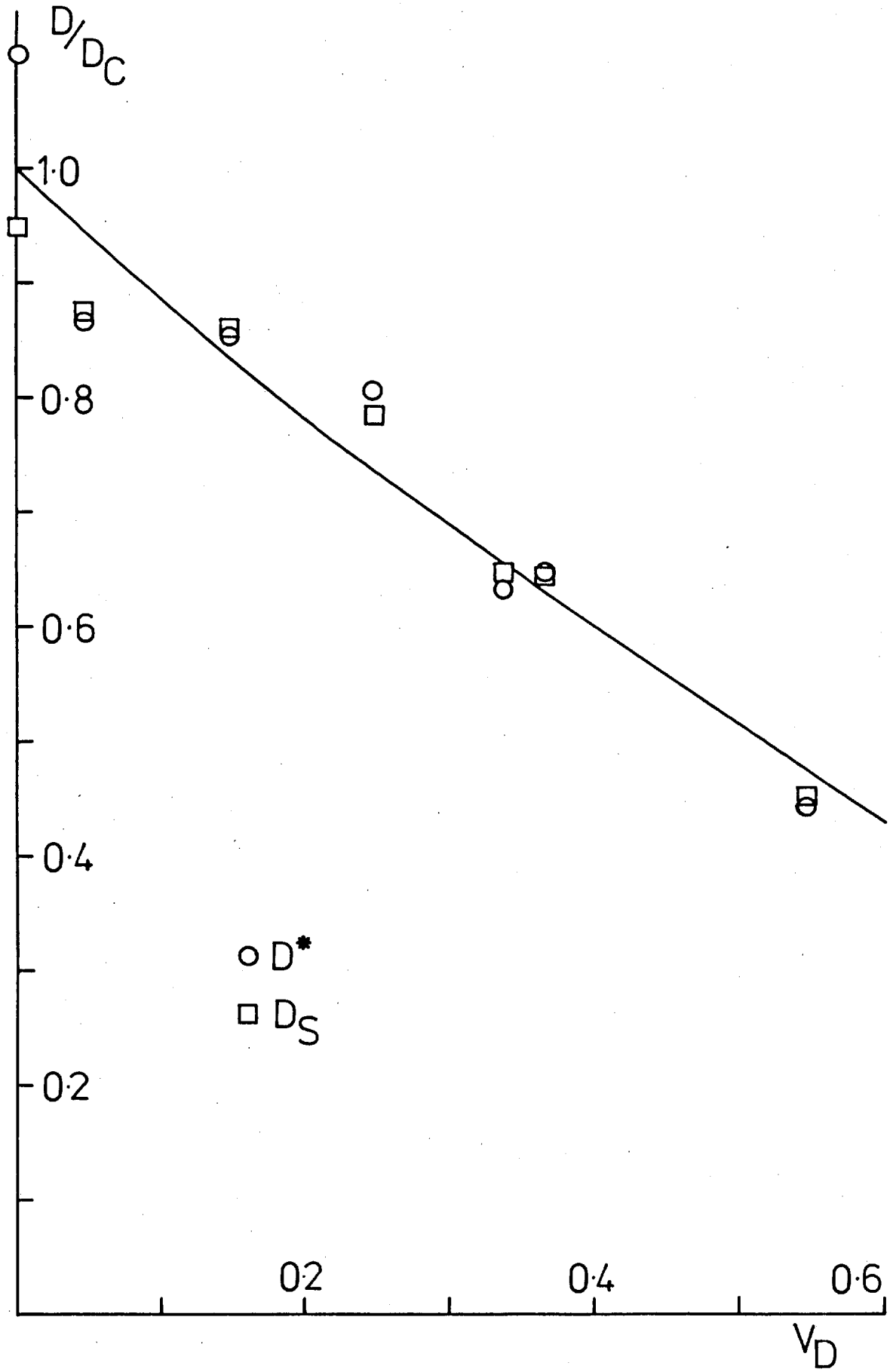

Figure 4.31: iso-Butane Diffusion Coefficient Ratios

Table 4.17 Copolymer Activation Energies of Diffusion

(E_D kJ mol^{-1})

	propane		iso-butane	
	E_{D*}	$(E_P - \Delta\bar{H}_S)$	E_{D*}	$(E_P - \Delta\bar{H}_S)$
4.9% PS	14.4	14.0	14.2	15.4
15.5% PS	13.5	13.5	14.8	15.1
26.2% PS	15.1	14.3	13.4	14.4
CM	15.3	13.3	15.4	15.5
38.2% PS	13.5	14.0	12.3	15.8
56.3% PS	12.5	14.7	15.2	15.4

Finally, it should be noted that the use of the standard dual mode sorption analysis for the diffusion coefficients of the graft copolymers means that the equations derived for the diffusion of propane in polystyrene (section 4.2) are also applicable to the copolymers. In particular, the effective, concentration dependent, diffusion coefficient is given by equation 4.8 with $D = D^*$. This equation is also applicable to the block copolymers ($D = D_M$) since, for the case of $c'_H = 0$, the equation correctly reduces to the trivial expression $D_{eff} = D_M$.

CHAPTER 5

CONCLUSIONS

5.1 Graft Copolymers

The preparation of the graft copolymers presented no great problems and was easily achieved by following the standard procedures for radiation grafting. This work was, however, based upon earlier erroneous results (133), and it is likely that much shorter irradiation times than the 18 hours used may prove sufficient for the grafting process. The phenyl group is an efficient absorber of radiation, and as the major reaction of both PDMS and polystyrene on irradiation is that of cross-linking, the longer irradiation times used are not thought likely to affect any of the later results.

Although the block copolymers were translucent, as expected from their domain sizes, the graft copolymers were opaque and white in colour even at the lowest levels of grafting. Red light from a white light source was faintly visible through the 4.9% PS copolymer, which is consistent with the opacity being due to the scattering of light, since scattering is proportional to the fourth power of the frequency of the radiation. The normal criteria for the scattering of light from this type of heterogeneous system are that the domains have a different refractive index from the continuum, and are larger than the wavelength of light. As domain sizes in the graft copolymers are an order of magnitude lower than the wavelength of visible light the scattering must be presumed to be due to localised "clusters" of domains as shown in the electron micrographs. (The block copolymers contain more uniform dispersions of domains and are not subject to this effect.)

5.2 Summary of Results

The correlation of transport properties with the morphology of the copolymers has proved successful, and the permeabilities are well predicted by the models of Higuchi (54) and Bruggeman (49) for a membrane containing an impermeable disperse phase. E_p for this type of system is shown to be equal to that of the continuous phase, and

this may prove to be a reliable test for phase separation when the E_p values of the component polymers are markedly different.

The copolymer solubilities showed some unexpected effects, in particular the lack of any Langmuir component of sorption in the block copolymers. The suggestion that this is due largely to incomplete phase separation seems to be at variance with the permeability results. However, it is possible that the inclusion of relatively small amounts of PDMS acting as a plasticiser in the polystyrene domains may be sufficient to lower the T_g of the domains without significantly affecting membrane permeabilities.

If the T_g of the block copolymers as obtained by DSC represents the T_g of a central core of relatively pure polystyrene which accounts for only a fraction of the total polystyrene content, then the sorption isotherms of the block copolymer should be compared to those of a graft copolymer of a lower polystyrene content. This contention is further supported by the fact that the graft copolymers have been shown to exhibit enhanced Langmuir sorption. Comparisons of the Langmuir component of sorption should also be made at an equivalent temperature below T_g. Thus at the lowest temperatures investigated (approx. 20^oC) the polystyrene domains of the block copolymer are $\sim 50^oC$ below T_g and the Langmuir saturation constant may be expected to be comparable to that of a graft copolymer at 50^oC below T_g (ie 50^oC). Although this reasoning may be sufficient to explain the absence of any detectable Langmuir sorption in the block copolymers, clearly further work is required to provide a complete explanation of this phenomenon.

The departure from simple additivity of the solubilities of the component phases of the graft copolymers is also worthy of further study. The proposed explanation that this is due to internal stresses caused by the inclusion of polystyrene domains into the cross-linked PDMS network is based upon the similar behaviour of other physical properties of polymer composites. An investigation of this effect would be of interest and might shed further light upon its causes.

Despite the anomalous solubility behaviour, the diffusion coefficients of the copolymers can be predicted with reasonable accuracy by a combination of the Higuchi model and simple additivity of the concentrations of the component phases. Thus the copolymers are well represented by a model of diffusion with immobilisation in which the polystyrene

domains act as impermeable absorptive filler particles to the transport of hydrocarbons.

5.3 Further Study

In addition to the suggestions for further work with regard to the solubility behaviour of the copolymers, several other areas which may be worthy of further study have become apparent during the course of this work.

The transport properties of homogeneous polymer systems have received some attention but a definitive test of the Lichtenecker rule (equation 2.3) seems long overdue. In this respect it would be of interest to examine the variations of the diffusion coefficient with composition, since simple relationships have been proposed both for the dependence of log D upon free volume, and for the variation of free volume with composition. Whilst diffusion coefficients may differ by several orders of magnitude the solubilities of penetrants in any two polymers often differ by only a factor of two or three. Thus the general agreement of P with the Lichtenecker rule may reflect the fact that the variation of P is determined largely by that of D in these cases.

Although the dual mode sorption theory has proved successful in explaining a large volume of experimental data, there is little experimental evidence to support the underlying assumptions of the theory. The nmr study by Assink (117) of ammonia sorbed in polystyrene is the only investigation of dual mode sorption on a molecular level. The single concentration dependent relaxation time observed was interpreted as evidence for the rapid exchange of penetrant between the two modes of sorption, but no direct evidence of the two sorption modes is available. It is difficult to envisage any means by which the assumption may be tested reliably, although further theoretical work following the proposal of Koros and Paul (112) may lead to a verifiable hypothesis.

APPENDIX A

SAMPLE CALCULATIONS AND ESTIMATES OF ERROR

A.1 Sorption

A point (p,c) on a sorption isotherm was determined as shown in the following example (PDMS-g-38.2% PS propane sorption at 30°C):

Sample temperature (T) 30.0°C = 303.2K
Sample volume (V) 0.474 cm^3
Volume of Cu counterweight (V_1) 0.0579 cm^3
Volume of Pt support wire (V_2) 0.0017 cm^3
Molecular weight of propane 44.11 g mol^{-1}
Transducer reading (R) 16.02 mV
Transducer calibration constant (K) 1.158 cm Hg mV^{-1}
Equilibrium weight increase (Δw) 1385 μg

Pressure (p) = R x K = 18.55 cm Hg

$$\text{Buoyancy correction (B)} = (V + V_2 - V_1) \times \frac{44.11}{22,414} \times \frac{p}{76} \times \frac{273.2}{T}$$

$$= 182 \text{ μg}$$

$$\text{Concentration (c)} = \frac{(\Delta w + B)}{V} \times \frac{22,414}{44.11}$$

$$= 1.674 \text{ } cm^3(STP)cm^{-3}$$

The major cause of uncertainties in the measured parameters is temperature fluctuations in both the air and water thermostats. The magnitude of the uncertainty in each parameter is estimated below:

T = 30.0 (±0.1) °C
V = 0.474 (±1%) cm^3
V_1, V_2 negligible uncertainty
R = 16.02 (±0.03) mV
K = 1.158 (±1%) cm Hg mV^{-1}
Δw = 1385 (±1%) μg

For typical values (R = 10 mV, Δw = 1,000 μg) the reproducibility is estimated as ±1%, and the absolute accuracy as ±3%.

Values of the diffusion coefficient ($\bar{D}$) were determined from the initial rates of sorption and desorption. The calculation of D_s from the initial rate of sorption is illustrated below for the previous

example:

Sample thickness (ℓ) 0.119 cm

Slope of M_t/M_∞ vs. $\sqrt{t}$ (I) 3.83×10^{-2} $s^{-\frac{1}{2}}$

$$D_s = \frac{\pi}{16} \times I^2 \times \ell^2 = 4.10 \times 10^{-6} \text{ cm}^2\text{s}^{-1}$$

The uncertainties are estimated as:

$\ell = 0.119$ ($\pm 1\%$) cm

$I = 3.83 \times 10^{-2}$ ($\pm 2\%$) $s^{-\frac{1}{2}}$

where the uncertainty in I is again largely due to temperature fluctuations. The reproducibility of $\bar{D}$ is estimated as $\pm 5\%$, and the absolute accuracy as $\pm 7\%$, plus errors introduced by edge effects and the effect of the balance response time, as discussed elsewhere.

A.2 Permeation

Permeability and time lag diffusion coefficients were determined as shown in the following example (PDMS propane permeation at 30.2°C):

Membrane temperature 30.2°C

Average room temperature (T_r) 23.7°C = 296.9K

Membrane area (A) 5.94 cm^2

Membrane thickness (ℓ) 0.194 cm

Downstream volume (V) 2,282 cm^3

Transducer reading (R) 4.40 mV

Transducer calibration constant (K) 1.208 cm Hg mV^{-1}

Steady-state rate of pressure increase (dp/dt) 3.90×10^{-5} mm Hg s^{-1}

Time lag (L) by extrapolation 1053 s

Ingoing pressure (p_o) = R x K = 5.32 cm Hg

$$\text{Steady-state flux (J)} = \frac{dp}{dt} \times \frac{V}{760} \times \frac{273.2}{T_r}$$

$$= 1.077 \times 10^{-4} \text{ cm}^3\text{(STP)}\text{s}^{-1}$$

$$\text{Permeability (P)} = \frac{J \times \ell}{A \times p_o}$$

$$= 6.61 \times 10^{-7} \text{ cm}^3\text{(STP)cm cm}^{-2}\text{(cm Hg)}^{-1}\text{s}^{-1}$$

$$\text{Diffusion coefficient } (D_L) = \frac{\ell^2}{6L}$$

$$= 5.95 \times 10^{-6} \text{ cm}^2\text{s}^{-1}$$

The uncertainties in the measured parameters are estimated below:

T_r = 23.7 (±0.2) ^{o}C

A = 5.94 (±2%) cm^2

ℓ = 0.194 (±1%) cm

V = 2,282 (±0.5%) cm^3

R = 4.40 (±0.03) mV

K = 1.208 (±1%) cm Hg mV^{-1}

dp/dt = 3.90 x 10^{-5} (±0.5%) mm Hg s^{-1}

L = 1053 (±2%) s

The reproducibility is estimated as ±1.5% for P, and ±2% for D_L, and the uncertainties in the absolute values are estimated as ±6% for P, and ±5% for D_L, plus errors introduced by edge effects. The uncertainty in the relative permeability of two membranes is somewhat smaller, since errors in factors such as volume and transducer calibrations remain constant for each sample. The uncertainty in relative permeability is estimated as ±4%.

APPENDIX B

THE EFFECT OF BALANCE RESPONSE TIME ON SORPTION KINETICS

The electronic microbalance and recorder used for the sorption measurements in this work were found to have a finite response time to a change in weight. The response to an instantaneous increase in weight of w_o was found to be of the form:

$$w(t) = w_o.(1 - e^{-kt}) \qquad ...(B.1)$$

where $w(t)$ is the weight indicated by the balance. The value of k was determined from plots of $\ln(w_o - w)$ against t, and was found to be a constant (0.78), independent of the balance range in use if w_o and w are expressed in terms of the full scale of the recorder. Equation B.1 is more conveniently expressed in terms of the rate of change of weight:

$$\frac{dw}{dt} = k.(w_o - w) \qquad ...(B.2)$$

During the initial stages of a sorption experiment the true weight is given by:

$$w_o = A.t^{\frac{1}{2}} - B \qquad ...(B.3)$$

where $A = \frac{4.}{M_\infty}\left(\frac{D}{\pi.\ell^2}\right)^{\frac{1}{2}}$

and B = buoyancy correction. Thus at any time during the initial stages:

$$\frac{dw}{dt} = k.(A.t^{\frac{1}{2}} - B - w) \qquad ...(B.4)$$

and the solution of equation B.4 predicts the weight indicated by the balance during the "$\sqrt{t}$ region" of the sorption. Multiplying through by the integrating factor e^{kt} gives:

$$\frac{d}{dt}\left(\frac{w.e^{kt}}{k}\right) = (A.t^{\frac{1}{2}} - B) \qquad ...(B.5)$$

and integrating from 0 to t w.r.t. t leads to:

$$w = -B.(1 - e^{-kt}) + \frac{A.k}{e^{kt}}.\int_0^t t^{\frac{1}{2}}.e^{kt}.dt \qquad ...(B.6)$$

Substituting $x = t^{\frac{1}{2}}$ in the integral of equation B.6 gives:

$$\int t^{\frac{1}{2}}.e^{kt}.dt = \int 2x^2.e^{kx^2}.dx$$

$$= \frac{1}{k}.(x.e^{kx^2} - \int e^{kx^2}.dx) \qquad ...(B.7)$$

Then expanding e^{kx^2} as a power series:

$$e^{kx^2} = 1 + \frac{kx^2}{1!} + \frac{k^2x^4}{2!} + \frac{k^3x^6}{3!} + ...$$

and integrating term by term:

$$\int e^{kx^2}.dx = x + \frac{kx^3}{3.1!} + \frac{k^2x^5}{5.2!} + \frac{k^3x^7}{7.3!} + ...$$

Substituting back into equation B.7 then leads to:

$$\int_0^t t^{\frac{1}{2}}.e^{kt}.dt = \left|\frac{t^{\frac{1}{2}}.e^{kt}}{k} - \frac{t^{\frac{1}{2}}}{k}.\left(1 + \frac{kt}{3.1!} + \frac{(kt)^2}{5.2!} + ...\right)\right|_0^t$$

$$= \frac{t^{\frac{1}{2}}.e^{kt}}{k}.f(t) \qquad ...(B.8)$$

where $f(t) = 1 - e^{-kt}\sum_{i=0}^{\infty} \frac{(kt)^i}{(2i+1).i!}$

and finally:

$$w = -B.(1 - e^{-kt}) + A.t^{\frac{1}{2}}.f(t) \qquad ...(B.9)$$

The summation term of f(t) is convergent, and it is readily shown that, for n+1>kt, the error in summing to n terms is given by:

$$E_n < \frac{A_{n+1}}{\{1-kt/(n+1)\}} \qquad ...(B.10)$$

where A_{n+1} is the next term of the series.

The solution to equation B.9 can be easily determined by computer methods to any given degree of accuracy, and the early time results (solid line) are compared with the true weight (dashed line) in figure B.1. The solid line of this figure is an accurate representation of recorder traces obtained during sorption, and offers a strong argument in support of the preceeding analysis. It is evident that the observed rate of change of weight (after the minimum weight has been passed) is significantly higher than the true rate of

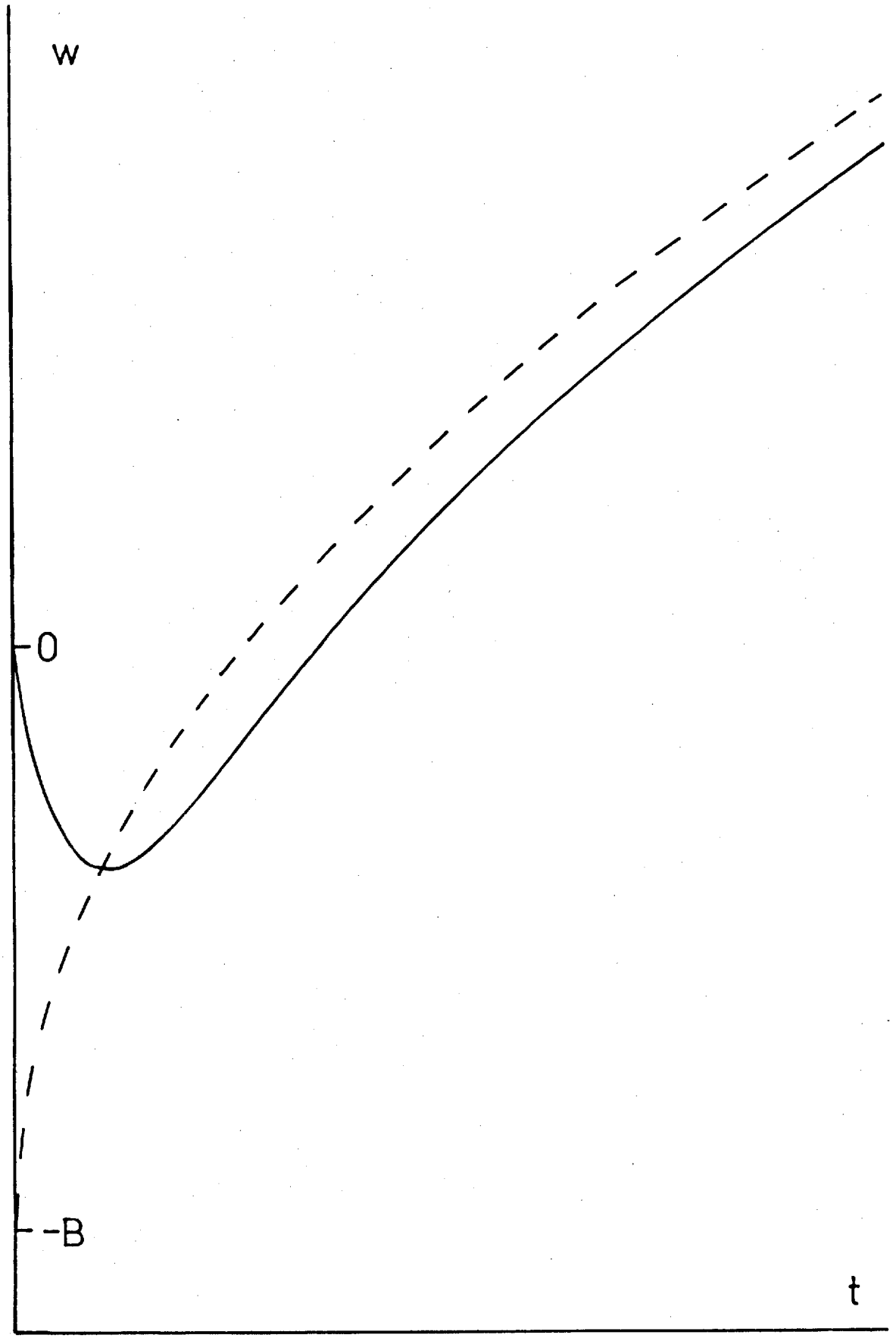

Figure B.1 Effect of balance response time

change. A computer program was used to determine the error introduced by the effect of the balance response time in the determination of the diffusion coefficient from initial rates of sorption. The error was found to increase with increasing buoyancy and with decreasing time span of the $\sqrt{t}$ region, but no simple relationships could be established. Under typical experimental conditions (B = 10-20% of M_∞) and for the worst case ($\sqrt{t}$ region of 100 s) the value of D determined would be approximately 5% higher than the true value. Thus the error in D due to the effect of the balance response time is less than 5% for all of the reported values.

APPENDIX C

EXPERIMENTAL DATA

The symbols and corresponding units used in the following tables are given below:

- p pressure (cm Hg)
- c concentration (cm^3STP cm^{-3})
- D diffusion coefficient ($cm^2 s^{-1}$)
- P permeability coefficient (cm^3STP cm cm^{-2}cm $Hg^{-1} s^{-1}$)
- L time lag (s)
- T temperature (^oC)

C.1 Sorption Results

PDMS Methane

T	p	c
29.5	6.69	.0430
	14.84	.0954
	21.05	.1352
	27.67	.1783
	33.48	.2157
34.8	6.50	.0403
	13.15	.0822
	20.38	.1267
	28.60	.1783
40.6	6.65	.0395
	14.49	.0858
	21.30	.1264
	28.40	.1684
	33.45	.1984
45.5	6.49	.0369
	13.50	.0770
	20.31	.1161
	29.93	.1708
	32.60	.1857
49.5	7.58	.0416
	14.36	.0789
	21.84	.1203
	28.61	.1578
	36.41	.2011

PDMS Propane

T	p	c	$\bar{D}x10^6$
21.0	5.53	.701	6.57
	8.09	1.025	6.54
	10.24	1.304	6.52
	16.31	2.113	6.72
	19.92	2.565	6.67
30.2	5.68	.584	7.84
	9.09	.935	7.86
	13.15	1.354	7.85
	19.22	1.985	7.95
	20.22	2.098	7.85
40.7	5.49	.454	9.03
	11.03	.909	9.47
	16.51	1.365	9.51
	20.59	1.705	9.47
49.6	4.65	.322	11.90
	9.54	.659	10.89
	15.75	1.087	10.94
	21.09	1.459	10.84

PDMS n-Butane

T	p	c	$\overline{D}x10^6$
22.7	2.72	1.077	
	4.60	1.806	
	8.36	3.316	
	11.05	4.435	
29.9	5.39	1.715	6.28
	6.39	2.047	6.21
	10.22	3.293	6.34
	13.86	4.519	6.45
40.0	4.17	.995	
	8.67	2.074	
	13.36	3.249	
	16.61	4.061	
49.2	8.34	1.586	8.69
	9.28	1.763	8.78
	17.27	3.321	8.68
	21.66	4.190	8.85

PDMS iso-Butane

T	p	c	$\overline{D}x10^6$
21.5	6.98	1.908	4.12
	8.99	2.468	4.09
	13.14	3.649	4.13
	16.00	4.492	4.23
31.5	7.17	1.514	5.05
	10.86	2.293	5.03
	16.08	3.417	5.01
	19.93	4.262	5.11
40.7	7.46	1.232	5.91
	10.35	1.716	5.96
	15.89	2.651	5.95
	20.52	3.447	5.94
49.3	8.03	1.076	7.02
	10.43	1.403	7.00
	16.18	2.193	6.93
	20.52	2.780	6.96

Polystyrene Methane

T	p	c	$D_S \times 10^8$
30	4.07	.0277	1.34
	5.84	.0410	1.20
	7.42	.0510	1.19
	7.78	.0537	1.29
	8.85	.0623	1.22
	11.48	.0800	1.26
	13.40	.0931	1.23
	18.20	.1273	1.31
	20.97	.1457	1.26
	25.51	.1740	1.36
	29.13	.1986	1.31
	34.95	.2350	-
50	2.53	.0116	3.34
	6.36	.0287	3.27
	8.53	.0390	3.25
	10.04	.0454	3.23
	15.73	.0703	3.43
	21.52	.0950	3.28
	22.72	.1003	3.09
	33.90	.1481	-

Polystyrene Propane

T	p	c	$\bar{D} \times 10^{11}$
30	1.77	.324	
	2.50	.431	2.13
	4.22	.666	
	5.51	.766	2.64
	11.65	1.204	3.84
	17.45	1.561	
	21.26	1.795	4.18
	33.79	2.448	
50	1.88	.139	
	2.69	.197	7.05
	5.36	.358	6.87
	7.54	.442	
	10.43	.612	8.89
	14.89	.826	
	19.89	.994	11.0
	28.43	1.301	
	36.20	1.549	

Block Copolymer (CM) Methane

T	p	c
28.9	6.73	.0362
	13.56	.0728
	22.10	.1196
	25.92	.1413
	38.46	.2085
34.7	6.21	.0316
	13.47	.0680
	20.96	.1062
	29.23	.1483
	35.03	.1776
	37.55	.1899
39.5	6.95	.0334
	14.23	.0688
	25.73	.1234
	33.23	.1590
	38.62	.1853
46.0	5.99	.0280
	12.83	.0590
	18.30	.0836
	24.60	.1119
	31.58	.1445
	37.08	.1693
50.0	7.45	.0328
	13.93	.0626
	22.13	.0985
	26.93	.1201

Block Copolymer (CM) Propane

T	p	c	$\bar{D}x10^6$
20.3	5.39	.587	3.19
	11.02	1.175	3.34
	17.72	1.853	3.47
	21.25	2.199	3.48
30.1	3.97	.348	3.88
	6.81	.580	4.03
	7.64	.648	3.89
	9.26	.780	4.03
	10.52	.885	3.98
	16.63	1.387	4.08
	21.39	1.767	4.09
39.9	2.91	.209	
	5.41	.377	4.87
	6.34	.440	
	10.09	.690	4.92
	10.82	.734	
	10.88	.740	4.89
	17.34	1.171	
	21.70	1.459	
49.7	5.29	.297	5.88
	10.95	.609	
	17.36	.961	5.93
	21.93	1.213	6.06

Block Copolymer (CM) n-Butane

T	p	c	$\bar{D}x10^6$
22.9	6.13	1.914	
	11.02	3.464	
	16.56	5.172	
	22.43	7.149	
30.7	5.13	1.296	2.95
	10.39	2.585	3.06
	16.59	4.122	3.18
	19.38	4.838	3.27
40.2	6.18	1.186	
	10.60	2.023	
	17.23	3.291	
	23.58	4.541	
49.6	4.57	.686	4.23
	8.38	1.250	4.25
	15.73	2.365	4.27
	20.55	3.083	4.39

Block Copolymer (CM) iso-Butane

T	p	c	$\bar{D}x10^6$
23.6	5.38	1.093	1.96
	10.97	2.195	2.08
	16.72	3.321	2.15
	21.50	4.310	2.18
31.2	6.25	1.026	2.33
	10.80	1.760	2.41
	16.19	2.636	2.54
	21.51	3.486	2.51
40.6	6.30	.817	2.83
	10.81	1.380	2.86
	16.93	2.171	2.93
	21.70	2.789	2.99
49.9	6.09	.638	3.51
	10.47	1.082	3.47
	16.39	1.693	3.45
	21.27	2.201	3.52

Block Copolymer (CC) Propane

T	p	c
30.6	6.13	.539
	10.64	.924
	17.50	1.471
	22.25	1.868
49.4	6.47	.379
	10.56	.611
	17.14	.979
	22.33	1.266

Block Copolymer (CC) iso-Butane

T	p	c
30.7	6.22	1.061
	10.71	1.790
	16.70	2.740
	20.64	3.463
49.5	5.39	.589
	10.64	1.135
	16.74	1.798
	21.17	2.258

Block Copolymer (SC) Propane

T	p	c
30.3	5.24	.472
	11.20	.964
	16.93	1.425
	22.32	1.859
39.7	6.10	.430
	10.84	.750
	16.70	1.138
	22.18	1.498
49.6	5.28	.298
	10.98	.605
	17.41	.951
	22.74	1.236

Block Copolymer (SC) iso-Butane

T	p	c
30.4	4.98	.860
	10.78	1.808
	15.95	2.659
	20.30	3.356
49.6	5.30	.578
	10.64	1.153
	16.67	1.778
	21.22	2.281

PDMS-g-4.9% PS Propane

T	p	c	$\bar{D}x10^6$
22.6	8.80	1.045	6.29
	10.48	1.233	6.13
	17.56	2.100	6.07
	21.68	2.573	6.36
30.4	6.47	.645	6.56
	11.26	1.127	6.65
	18.16	1.810	6.78
	22.30	2.217	7.09
40.3	6.38	.515	8.21
	11.28	.906	8.22
	17.26	1.383	8.92
	22.18	1.779	8.35
49.7	6.20	.413	10.1
	10.82	.718	9.89
	17.01	1.126	9.91
	22.07	1.460	10.2

PDMS-g-4.9% PS iso-Butane

T	p	c	$\bar{D}x10^6$
22.5	6.89	1.753	3.35
	9.99	2.456	3.27
	17.77	4.608	3.34
	21.28	5.540	3.41
30.3	7.01	1.445	3.87
	10.27	2.107	3.90
	21.35	4.456	-
40.4	7.41	1.179	4.76
	10.32	1.638	4.51
	16.77	2.683	4.77
	21.77	3.503	4.57
49.2	6.17	.803	5.41
	11.38	1.465	5.39
	18.40	2.367	5.38
	22.27	2.910	5.44

PDMS-g-15.5% PS Propane

T	p	c	$\bar{D}x10^6$
22.8	7.03	.819	
	10.98	1.254	
	11.68	1.319	
	17.46	1.953	
	23.55	2.613	
	23.70	2.616	
30.2	9.16	.886	6.06
	11.22	1.076	6.05
	18.97	1.781	6.33
	23.17	2.161	6.33
40.5	6.64	.517	
	11.91	.908	
	17.93	1.349	
	23.39	1.749	
49.9	7.44	.475	8.57
	12.12	.762	8.62
	19.21	1.193	8.90
	23.79	1.469	8.92

PDMS-g-15.5% PS iso-Butane

T	p	c	$\bar{D}x10^6$
22.6	6.17	1.466	
	11.08	2.595	
	17.15	4.022	
	21.73	5.113	
30.3	7.61	1.430	3.69
	10.89	2.026	3.75
	16.83	3.137	3.87
	18.43	3.417	3.95
40.2	6.55	.976	
	10.69	1.580	
	17.05	2.508	
	22.62	3.319	
49.4	6.36	.763	5.33
	10.86	1.279	5.41
	17.76	2.092	5.40
	19.29	2.257	5.48

PDMS-g-26.2% PS Propane

T	p	c	$\bar{D}x10^6$
22.2	6.93	.801	
	11.73	1.296	
	17.85	1.899	
	23.14	2.429	
30.6	7.65	.702	5.21
	11.63	1.048	5.38
	16.60	1.474	5.45
	23.14	2.015	5.63
40.3	6.42	.482	
	11.22	.821	
	17.86	1.277	
	23.09	1.630	
49.3	7.68	.471	7.43
	12.31	.743	7.60
	18.55	1.104	7.77
	23.35	1.362	7.93

PDMS-g-26.2% PS iso-Butane

T	p	c	$\bar{D}x10^6$
25.6	6.31	1.286	3.01
	11.99	2.385	3.16
	15.22	3.033	3.16
	18.65	3.693	3.23
30.3	5.34	.973	3.19
	10.57	1.861	3.58
	16.96	2.956	3.55
	18.97	3.296	3.56
39.9	6.57	.918	3.86
	8.52	1.179	3.94
	16.28	2.220	4.13
	19.11	2.589	4.20
49.1	7.92	.889	4.66
	9.13	1.015	4.74
	15.00	1.640	4.82
	19.70	2.153	4.94

PDMS-g-38.2% PS Propane

T	p	c	$\bar{D}x10^6$
22.8	6.00	.791	
	12.20	1.378	
	16.71	1.785	
	22.02	2.323	
30.0	7.48	.791	3.52
	11.19	1.089	3.72
	18.55	1.674	3.87
	22.55	1.983	4.06
40.4	6.55	.539	
	11.16	.873	
	16.91	1.235	
	22.31	1.594	
49.8	10.50	.650	5.32
	12.11	.741	5.36
	18.55	1.078	5.76
	22.04	1.246	5.74

PDMS-g-38.2% PS iso-Butane

T	p	c	$\bar{D}x10^6$
22.8	6.13	1.377	
	11.35	2.385	
	17.11	3.435	
	22.30	4.445	
30.1	7.81	1.381	2.42
	9.87	1.724	2.46
	15.30	2.561	2.64
	18.37	3.014	2.69
39.9	6.31	.898	
	11.26	1.513	
	17.25	2.229	
	22.74	2.909	
49.7	8.08	.875	3.42
	10.95	1.184	3.41
	17.70	1.819	3.56
	19.39	1.986	3.59

PDMS-g-56.3% PS Propane

T	p	c	$\bar{D}x10^6$
22.8	7.62	.992	
	12.46	1.412	
	17.38	1.828	
	22.57	2.236	
30.1	2.65	.390	
	5.45	.663	
	8.12	.854	2.02
	11.07	1.067	2.17
	20.03	1.711	2.42
	22.07	1.847	2.48
	27.96	2.272	
	35.34	2.765	
40.1	6.62	.559	
	11.08	.858	
	17.78	1.239	
	22.57	1.513	
49.7	3.66	.274	
	7.44	.484	
	9.17	.585	2.99
	12.27	.773	2.99
	16.97	.981	
	17.90	1.034	3.27
	22.02	1.220	3.41

PDMS-g-56.3% PS iso-Butane

T	p	c	$\bar{D}x10^6$
22.7	6.05	1.313	
	10.48	1.998	
	16.11	2.858	
	19.58	3.380	
30.3	1.72	.409	
	3.53	.698	
	5.43	.974	
	7.54	1.275	1.44
	12.33	1.877	1.59
	16.37	2.365	1.72
	19.47	2.752	1.84
	23.48	3.280	
	29.87	4.075	
40.0	6.63	.895	
	11.13	1.369	
	16.14	1.842	
	20.12	2.252	
49.3	2.51	.299	
	4.69	.501	
	7.45	.756	2.21
	11.70	1.122	2.34
	16.49	1.501	2.48
	20.20	1.830	2.50
	26.13	2.281	
	31.92	2.767	

C.2 Permeation Results

PDMS Methane

T	p	L	$Px10^7$	$D_L x10^5$
25.0	8.38	398	1.25	1.57
30.0	7.40	364	1.33	1.72
	13.22	367	1.32	1.71
34.9	5.07	333	1.39	1.88
	6.72	337	1.38	1.86
40.0	6.76	314	1.45	2.00
	7.43	317	1.44	1.98
44.8	7.50	298	1.52	2.11
	11.26	299	1.49	2.10
49.8	7.80	270	1.58	2.32

PDMS Propane

T	p	L	$Px10^7$	$D_L x10^6$
24.9	11.83	1123	6.72	5.59
30.2	5.32	1053	6.61	5.95
35.0	7.04	989	6.44	6.34
39.8	7.36	921	6.37	6.81
44.4	4.98	848	6.23	7.40
49.0	6.39	783	6.19	8.01

PDMS n-Butane

T	p	L	$Px10^6$	$D_L x10^6$
25.1	5.62	1450	1.56	4.33
30.1	6.19	1344	1.55	4.67
34.9	5.03	1221	1.45	5.14
39.8	5.68	1139	1.38	5.51
44.6	5.09	1048	1.32	5.98
49.8	4.92	965	1.29	6.50

PDMS iso-Butane

T	p	L	$P \times 10^7$	$D_L \times 10^6$
25.2	9.08	1945	8.39	3.22
30.2	7.52	1790	8.09	3.50
35.0	5.45	1652	7.86	3.80
39.8	6.41	1494	7.54	4.20
44.8	8.59	1394	7.25	4.50
49.6	4.84	1232	7.19	5.09
	5.32	1264	7.17	4.96

Block Copolymer (CM) Methane

T	p	L	$P \times 10^8$	$D_L \times 10^6$
25.4	4.61	361	6.53	9.18
30.0	3.91	332	6.93	9.99
	8.78	-	6.86	-
	13.00	-	6.96	-
30.1	4.37	327	6.84	10.13
	7.49	-	6.96	-
	9.25	-	7.00	-
35.0	4.69	307	7.31	10.80
40.0	4.64	277	7.67	11.98
44.7	4.95	257	7.86	12.87
49.5	5.01	245	8.35	13.53
	9.20	-	8.39	-
	12.17	-	8.44	-

Block Copolymer (CM) Propane

T	p	L	$Px10^7$	$D_L x10^6$
20.0	7.42	1282	3.51	2.59
25.2	8.99	1159	3.39	2.86
30.0	3.52	1116	3.24	2.97
	5.44	1118	3.27	2.96
	8.58	1077	3.30	3.08
	12.96	1029	3.34	3.22
	19.75	1007	3.40	3.29
35.0	9.35	951	3.23	3.48
39.9	6.28	880	3.17	3.78
44.8	6.97	821	3.11	4.03
49.7	3.34	739	3.02	4.49
	8.44	710	3.04	4.67
	12.64	720	3.09	4.60
	19.87	684	3.12	4.84

Block Copolymer (CM) n-Butane

T	p	L	$Px10^7$	$D_L x10^6$
24.9	4.61	1416	7.97	2.34
30.0	4.57	1270	7.55	2.61
34.8	4.40	1174	7.28	2.82
39.9	4.62	1063	6.84	3.12
45.2	5.26	973	6.44	3.41
49.9	4.62	903	6.27	3.67

Block Copolymer (CM) iso-Butane

T	p	L	$Px10^7$	$D_L x10^6$
25.1	4.91	1790	4.06	1.85
30.1	4.31	1623	3.89	2.04
	9.40	1551	4.04	2.14
	19.01	1469	4.25	2.26
	30.28	1428	4.48	2.32
35.1	4.34	1490	3.79	2.22
40.1	4.52	1349	3.69	2.46
45.0	4.46	1215	3.61	2.73
50.0	4.38	1133	3.52	2.92
	9.81	1125	3.59	2.94
	18.24	1064	3.66	3.11
	27.93	1042	3.75	3.18

Block Copolymer (CC) Propane

T	p	L	$Px10^7$	$D_L x10^6$
25.5	4.80	3428	3.30	2.71
	5.18	3490	3.32	2.66
	8.55	3324	3.33	2.79
29.9	4.97	3071	3.24	3.02
	6.13	3033	3.24	3.06
35.0	6.11	2795	3.23	3.32
	6.13	2764	3.19	3.36
39.7	5.08	2556	3.12	3.63
	5.14	2554	3.12	3.63
44.6	5.28	2364	3.10	3.93
	5.73	2362	3.10	3.93
49.9	4.46	2119	3.19	4.38
	4.46	2136	3.15	4.35

Block Copolymer (CC) iso-Butane

T	p	L	$Px10^7$	$D_L x10^6$
30.1	5.07	4767	3.82	1.95
	5.12	4772	3.84	1.94
35.2	4.84	4405	3.72	2.11
	7.52	4287	3.79	2.17
40.0	4.76	3960	3.63	2.34
	4.89	4009	3.64	2.32
45.0	4.55	3806	3.58	2.44
50.0	4.68	3299	3.47	2.81
	4.93	3299	3.46	2.81

Block Copolymer (SC) Propane

T	p	L	$Px10^7$	$D_L x10^6$
25.1	5.35	1134	1.02	0.98
	6.40	1113	1.02	1.00
	7.21	1103	1.03	1.01
30.0	4.33	1044	1.00	1.07
	5.26	1033	1.01	1.08
35.0	5.38	933	0.99	1.19
	5.93	937	1.00	1.19
39.8	4.91	849	0.98	1.31
	5.88	833	0.98	1.34
44.9	5.48	762	0.98	1.46
	5.49	783	0.99	1.42
50.0	4.72	687	0.95	1.62
	5.78	654	0.96	1.70
	5.97	703	0.97	1.59

Block Copolymer (SC) iso-Butane

T	p	L	$Px10^7$	$D_L x10^7$
25.4	4.98	1864	1.26	5.97
	5.47	1859	1.27	5.99
29.9	4.93	1648	1.22	6.75
	6.58	1647	1.24	6.75
34.7	4.54	1492	1.20	7.46
	5.08	1541	1.20	7.22
40.1	5.24	1419	1.18	7.84
	5.26	1391	1.18	8.00
44.8	4.99	1291	1.16	8.62
	6.00	1295	1.15	8.59
50.0	4.76	1195	1.12	9.31
	5.43	1181	1.14	9.42

PDMS-g-4.9% PS Propane

T	p	L	$Px10^7$	$D_L x10^6$
25.5	5.72	271	6.00	5.31
	5.89	273	6.00	5.28
30.2	5.89	247	5.89	5.84
	6.29	248	5.91	5.81
35.3	5.25	227	5.75	6.36
	6.35	227	5.73	6.36
39.9	4.21	206	5.67	6.99
	6.80	211	5.68	6.82
44.6	5.66	192	5.61	7.51
	6.52	194	5.60	7.42
49.8	4.31	168	5.47	8.56
	4.46	170	5.44	8.50
50.1	5.42	169	5.43	8.51

PDMS-g-4.9% PS iso-Butane

T	p	L	$Px10^7$	$D_L x10^6$
25.3	5.22	466	7.33	3.10
	5.47	462	7.32	3.12
29.8	4.98	427	7.10	3.38
	5.31	418	7.12	3.45
	5.96	422	7.09	3.42
35.3	4.08	375	6.82	3.84
	4.91	376	6.83	3.83
40.2	4.84	343	6.56	4.20
	5.08	346	6.61	4.17
45.0	4.98	323	6.41	4.46
	6.53	318	6.44	4.54
49.6	5.15	299	6.32	4.82
	5.18	298	6.32	4.84

PDMS-g-15.5% PS Propane

T	p	L	$Px10^7$	$D_L x10^6$
30.6	4.97	436	5.19	4.37
	5.07	436	5.18	4.38
	5.93	430	5.18	4.44
34.8	6.81	392	5.09	4.87
40.5	5.59	351	4.94	5.44
	6.03	350	4.95	5.46
44.9	8.99	318	4.90	5.99
49.8	4.49	295	4.80	6.46
	7.21	301	4.85	6.34

PDMS-g-15.5% PS iso-Butane

T	p	L	$Px10^7$	$D_L x10^6$
25.0	7.26	723	6.60	2.64
30.4	5.24	674	6.33	2.83
	6.52	663	6.31	2.88
34.9	5.09	629	6.06	3.03
39.9	6.41	559	5.98	3.41
	7.39	556	6.00	3.43
45.0	5.04	517	5.70	3.69
50.1	4.92	473	5.62	4.03
	5.94	469	5.60	4.07

PDMS-g-26.2% PS Propane

T	p	L	$Px10^7$	$D_L x10^6$
25.0	5.06	671	4.38	3.23
	6.75	653	4.35	3.32
30.3	5.24	582	4.21	3.72
	5.82	577	4.24	3.76
34.9	5.32	534	4.21	4.05
	5.80	532	4.22	4.07
39.9	5.13	469	4.09	4.62
	6.37	470	4.10	4.61
44.9	5.53	431	4.07	5.02
	7.79	432	4.09	5.01
50.0	6.32	391	3.99	5.54
	7.09	382	3.97	5.67

PDMS-g-26.2% PS iso-Butane

T	p	L	$P \times 10^7$	$D_L \times 10^6$
24.9	4.50	1031	5.30	2.10
	5.71	998	5.37	2.17
30.2	4.91	924	5.13	2.34
	5.20	907	5.13	2.39
35.1	5.48	809	4.96	2.68
	8.14	785	5.03	2.76
40.1	4.63	753	4.83	2.87
	6.25	724	4.83	2.99
45.0	5.13	683	4.69	3.17
	6.47	661	4.70	3.28
50.0	4.04	628	4.54	3.45
	5.43	605	4.55	3.58

PDMS-g-38.2% PS Propane

T	p	L	$P \times 10^7$	$D_L \times 10^6$
25.2	8.24	1139	3.27	2.07
30.0	5.76	1023	3.19	2.31
	6.17	1021	3.19	2.31
35.2	6.77	889	3.15	2.66
39.9	5.20	800	3.04	2.95
	5.97	798	3.07	2.96
45.0	5.54	720	3.06	3.28
49.8	5.10	637	2.97	3.70
	5.66	629	2.93	3.75

PDMS-g-38.2% PS iso-Butane

T	p	L	$Px10^7$	$D_L x10^6$
25.3	5.22	1627	3.91	1.45
30.4	4.87	1453	3.81	1.62
	6.00	1431	3.78	1.65
35.0	6.01	1297	3.71	1.82
39.9	4.90	1174	3.60	2.01
	7.18	1163	3.63	2.03
45.0	6.69	1042	3.54	2.26
49.3	6.25	953	3.47	2.48
	6.51	959	3.52	2.46

PDMS-g-56.3% PS Propane

T	p	L	$Px10^7$	$D_L x10^6$
25.3	6.07	2677	1.89	1.00
30.4	5.97	2348	1.88	1.14
	6.48	2299	1.88	1.17
34.4	5.22	2106	1.82	1.28
39.9	5.73	1842	1.81	1.46
	6.74	1772	1.81	1.52
44.8	6.65	1586	1.79	1.69
49.7	5.69	1429	1.79	1.88
	6.12	1424	1.79	1.89

PDMS-g-56.3% PS iso-Butane

T	p	L	$Px10^7$	$D_L x10^7$
25.1	5.31	3498	2.26	7.68
30.5	5.22	3092	2.19	8.69
	5.55	3081	2.20	8.73
35.1	5.08	2791	2.13	9.63
40.0	5.93	2447	2.08	11.0
	6.08	2401	2.07	11.2
44.9	6.84	2166	2.04	12.4
49.8	5.81	1996	2.00	13.5
	5.98	1994	2.01	13.5

C.3 Time Lag Data of D.C. Kuo

The diffusion time lag for propane has been measured in a membrane of PDMS grafted with 57.4% by weight of polystyrene in the pressure range 0 to 30 cm Hg (132). The results are tabulated below and the data are compared with the "best fit" to the equation of Paul (73) in figure C.1.

p	L (min)	p	L (min)
0.47	56.5	10.02	30.5
0.98	49.4	11.77	28.4
1.04	49.6	14.59	27.3
1.30	48.4	14.78	27.1
1.90	43.8	18.87	26.0
2.08	44.7	20.02	25.8
2.46	43.7	22.85	24.0
2.99	40.2	25.38	24.2
5.02	34.9	25.62	24.9
8.53	31.2	29.71	23.8

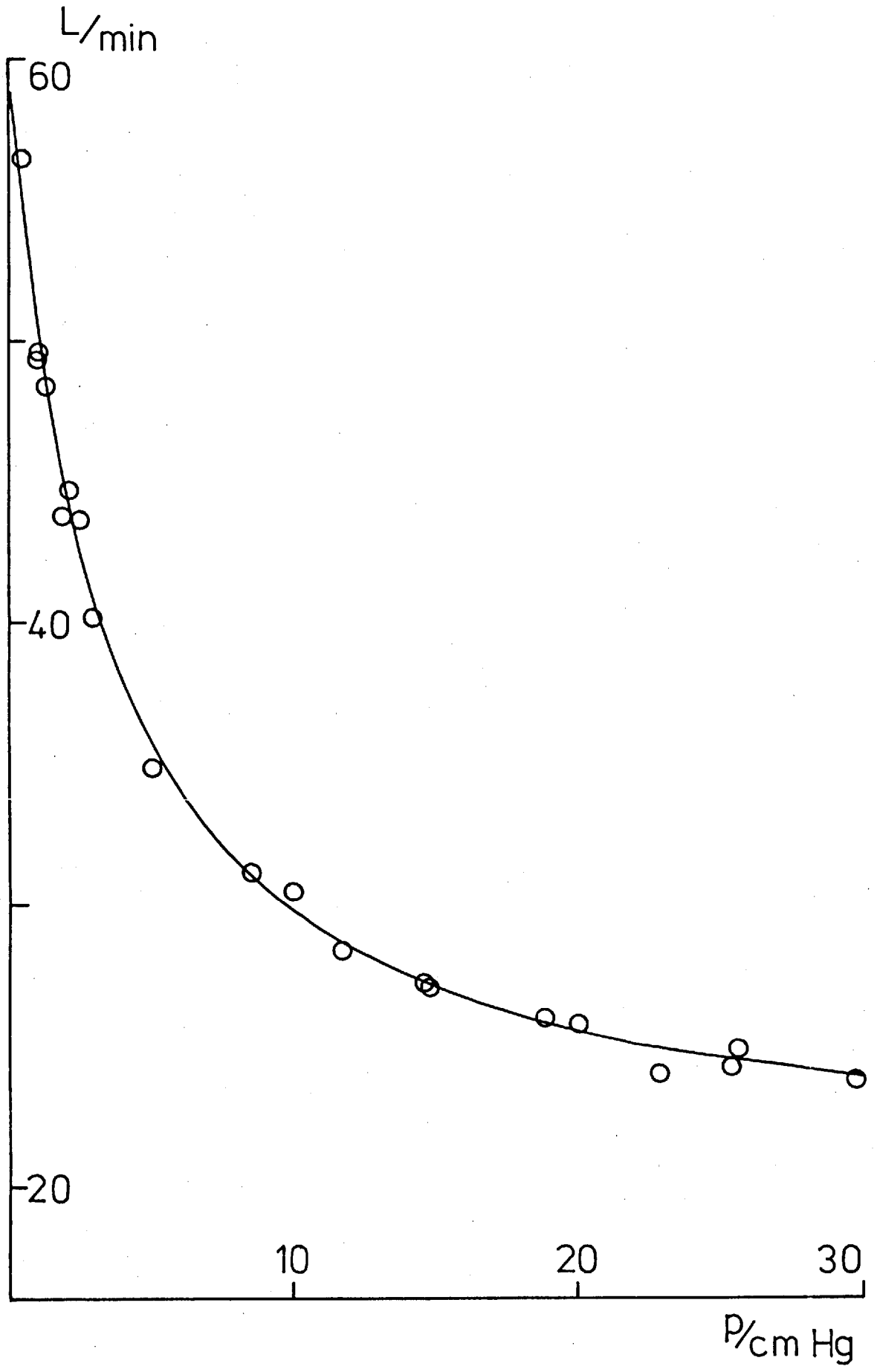

Figure C.1 : Time lag data of D.C. Kuo

C.4 Transmission Electron Micrographs

Transmission electron micrographs of some of the copolymer samples are shown on the following pages. The contrast in the micrographs is due to scattering of electrons by the Si atom of PDMS, and thus the lighter regions correspond to the polystyrene domains.

Figure	Sample	Magnification
C.2	SC	55,000
C.3	CM	55,000
C.4	CC	55,000
C.5	PDMS-g-26.2% PS	16,500
C.6	PDMS-g-38.2% PS	15,000

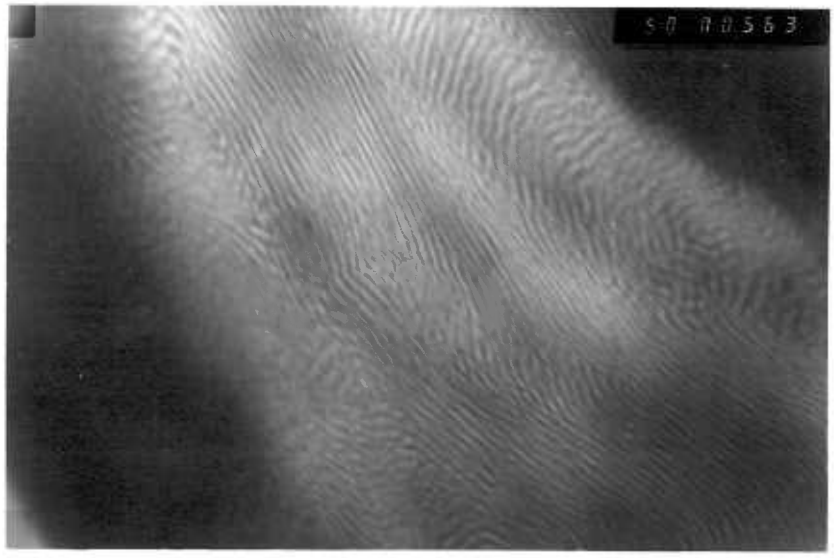

Figure C.2 Membrane SC

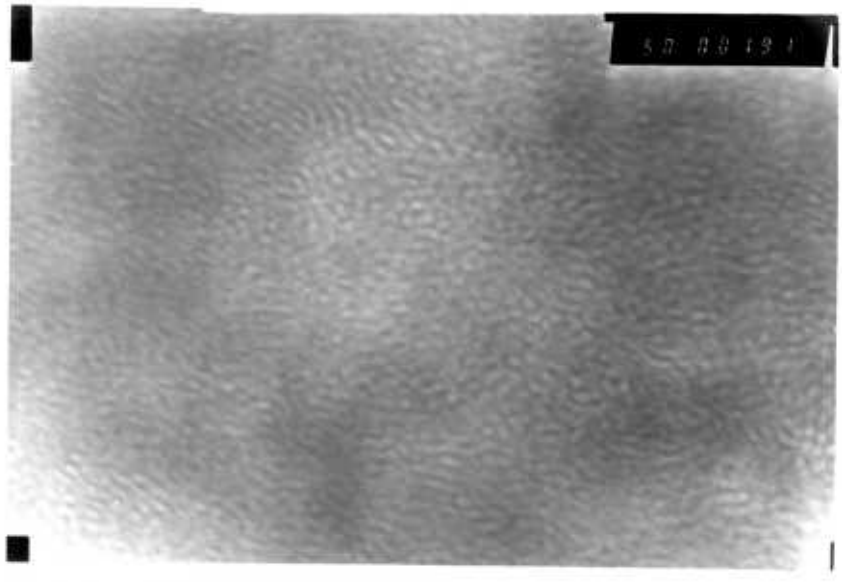

Figure C.3 Membrane CM

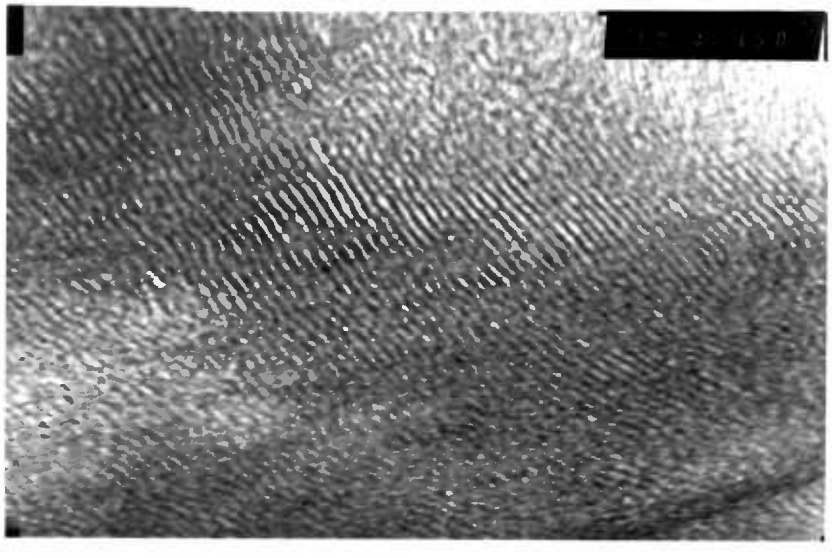

Figure C.4 Membrane CC

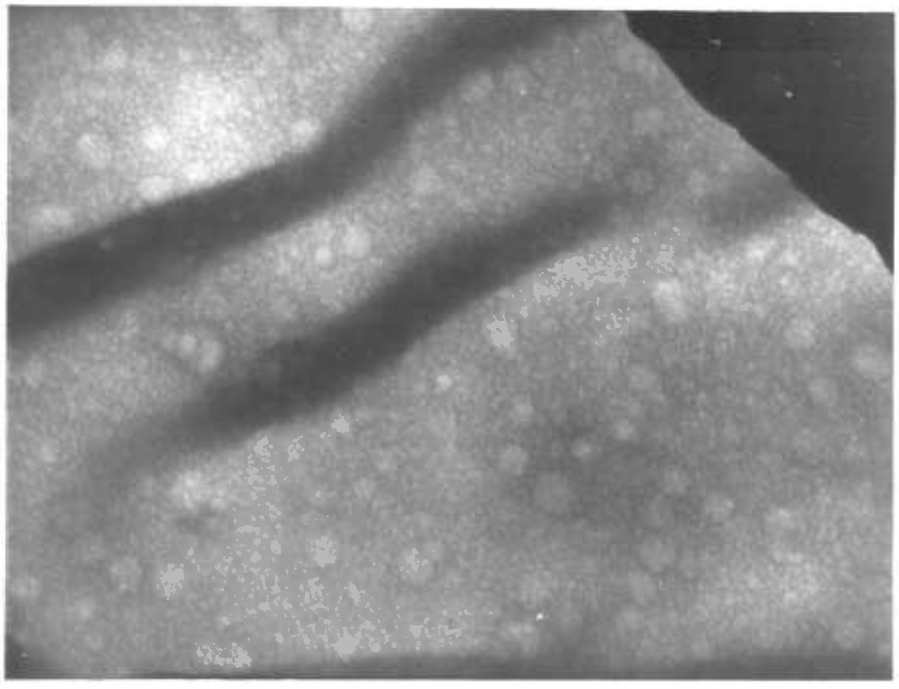

Figure C.5 PDMS-g-26.2% PS

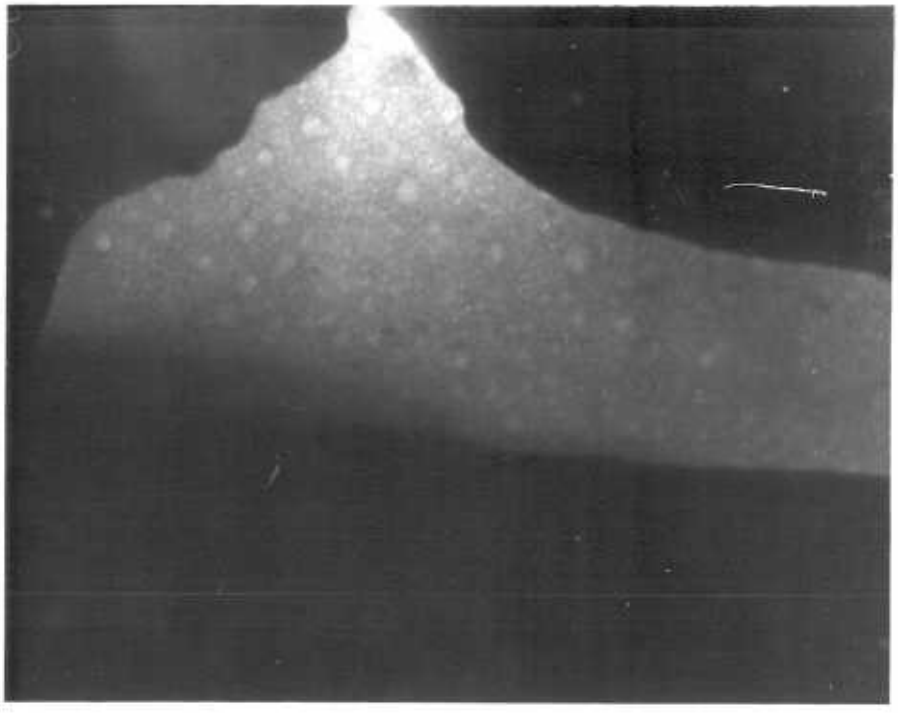

Figure C.6 PDMS-g-38.2% PS

REFERENCES

1. V. Stannett. chapter 2 in "Diffusion in Polymers", J. Crank and G.S. Park eds., Academic Press, London (1968).
2. C.A. Kumins. Ibid. chapter 4.
3. M.H. Cohen and D. Turnbull. J. Chem. Phys. 31, 1164 (1959).
4. R.M. Barrer. Trans. Faraday Soc. 39, 237 (1943).
5. R.M. Barrer. J. Phys. Chem. 61, 178 (1957).
6. C.E. Rogers. chapter 6 in "Physics and Chemistry of the Organic Solid State" Vol. 2, D. Fox, M.M. Labes and A. Weissberger eds., Interscience, New York (1965).
7. G.J. van Amerongen. J. Polymer Sci. 5, 307 (1950).
8. R.M. Barrer and G. Skirrow. J. Polymer Sci. 3, 564 (1948).
9. A.S. Michaels and H.J. Bixler. J. Polymer Sci. 50, 393 (1961).
10. G. Gee. Quart. Rev. 1, 265 (1947).
11. S. Prager and F.A. Long. J. Amer. Chem. Soc. 75, 1255 (1953).
12. S. Furuya. J. Polymer Sci. 17, 145 (1955).
13. A. Aitken and R.M. Barrer. Trans. Faraday Soc. 51, 116 (1955).
14. A.S. Michaels and R.B. Parker Jr. J. Polymer Sci. 41, 53 (1959).
15. E. Bagley and F.A. Long. J. Amer. Chem. Soc. 77, 2172 (1955).
16. P. Meares. Trans. Faraday Soc. 53, 1148 (1957).
17. A. Fick. Annln. Physik. (Leipzig) 170, 59 (1855).
18. J. Crank. "The Mathematics of Diffusion" (2nd Edition), Clarendon Press, Oxford (1975).
19. R.M. Barrer. Trans. Faraday Soc. 35, 628 (1939).
20. H.A. Daynes. Proc. Roy. Soc. (London), A97, 273 (1920).
21. H.L. Frisch. J. Phys. Chem. 61, 93 (1957).
22. J.A. Barrie and D. Machin. Trans. Faraday Soc. 67, 2970 (1971).
23. "Polymer Blends and Composites", J.A. Manson and L.H. Sperling eds., Plenum Press, New York (1976).
24. R.W. Lenz. "Organic Chemistry of Synthetic High Polymers", Interscience, New York (1967).
25. L.J. Fetters and M. Morton. Macromolecules, 2, 453 (1969).
26. Dow Corning Limited. Private communication.
27. M. Matsuo, T. Ueno, H. Horino, S. Chujyo and H. Asai. Polymer, 9, 425 (1968).
28. M. Matsuo, S. Sagae and H. Asai. Polymer, 10, 79 (1969).
29. R.L. Scott. J. Chem. Phys. 17, 279 (1949).
30. G. Holden, E.T. Bishop and N.R. Legge. J. Polymer Sci. C 26, 37 (1969)

31. R.J. Ceresa. "Block and Graft Copolymers", Butterworths, London (1962).
32. A. Chapiro. "Radiation Chemistry of Polymeric Systems" (High Polymer Series, Vol. XV), Interscience, New York (1962).
33. "Colloidal and Morphological Behaviour of Block and Graft Copolymers", G.E. Molau ed., Plenum Press, New York (1971).
34. J.A. Reynolds and J.M. Hough. Proc. Phys. Soc. B70, 769 (1957).
35. C.A.R. Pearce. Brit. J. Appl. Phys. 6, 113 (1955).
36. J.H. Petropoulos. IUPAC 4th Discussion Conference on Macromolecules.
37. R.M. Barrer. Op. cit. (1), chapter 6.
38. K. Lichtenecker. Physik. Z. 27, 115 (1926).
39. K. Lichtenecker and K. Rother. Ibid. 32, 255 (1931).
40. S.P. Mitoff. chapter 4 in "Advances in Materials Research" Vol. 3, H. Herman ed., Interscience, New York (1968).
41. M. Salame. Polymer Preprints, 8, 137 (1967).
42. J.C. Maxwell. "Treatise on Electricity and Magnetism" Vol. 1 Oxford University Press, London (1873).
43. H. Fricke. Phys. Rev. 24, 575 (1924).
44. H.C. Burger. Phys. Z. 20, 73 (1951).
45. Lord Rayleigh. Phil. Mag. 34, 481 (1892).
46. I. Runge. Z. Tech. Phys. 6, 61 (1925).
47. D.A. de Vries. Meded LandbHoogesch. Wageningen, 52(1), 1 (1952).
48. R.E. Meredith and C.W. Tobias. J. Appl. Phys. 31, 1270 (1960).
49. D.A.G. Bruggeman. Annln. Phys. V 24, 636 (1935).
50. R.E. Meredith and C.W. Tobias. J. Electrochem. Soc. 108, 286 (1961).
51. C.J.F. Böttcher. Recl. Trav. Chim. Pays-Bas Belg. 64, 47 (1945).
52. D. Polder and J.H. van Santen. Physica, 12, 257 (1946).
53. W.I. Higuchi. J. Phys. Chem. 62, 649 (1958).
54. W.I. Higuchi and T. Higuchi. J. Amer. Pharm. Assoc. Sci. Ed. 49, 598 (1960).
55. R.M. Barrer and J.H. Petropoulos. Brit. J. Appl. Phys. 12, 691 (1961).
56. M. Kubin and P. Spacek. Collect. Czech. Chem. Comm. 38, 3258 (1973).
57. G.E. Bell and J. Crank. J. Chem. Soc. Faraday Trans. II, 70, 1259 (1974).
58. L.E. Nielsen. J. Macromol. Sci. A1, 929 (1967).
59. W.F. Brown. J. Chem. Phys. 23, 1514 (1955).

60. S. Prager. J. Chem. Phys. 33, 122 (1960).
61. G.J. van Amerongen. Rubber Chem. Tech. 28, 821 (1955).
62. R.M. Barrer, J.A. Barrie and M.G. Rogers. J. Polymer Sci. A1, 2565 (1963).
63. T.K. Kwei. J. Polymer Sci. A3, 3229 (1965).
64. T.K. Kwei and W.M. Arnheim. J. Polymer Sci. C10, 103 (1965).
65. P. Meares. J. Amer. Chem. Soc. 76, 3415 (1954).
66. J.A. Barrie and D. Machin. J. Macromol. Sci.-Phys. B3(4), 645 (1969).
67. J.A. Barrie and D. Machin. Ibid. B3(4), 673 (1969).
68. K.F. Finger, A.P. Lemberger, T. Higuchi, L.W. Busse and D.E. Wurster. J. Amer. Pharm. Assoc. Sci. Ed. 49, 569 (1960).
69. E.R. Cooper. J. Colloid and Interface Sci. 48, 516 (1974).
70. C.F. Most. J. Appl. Polymer Sci. 14, 1019 (1970).
71. G.L. Flynn and T.J. Roseman. J. Pharm. Sciences, 60, 2480 (1971).
72. D.R. Paul and D.R. Kemp. J. Polymer Sci. C41, 79 (1973).
73. D.R. Paul. J. Polymer Sci. A-2, 7, 1811 (1969).
74. D.R. Kemp and D.R. Paul. J. Polymer Sci. Polymer Phys. Ed. 12, 485 (1974).
75. C.H. Klute. J. Appl. Polymer Sci. 1, 340 (1959).
76. A.S. Michaels and H.J. Bixler. J. Polymer Sci. 50, 413 (1961).
77. C.E. Rogers, V. Stannett and M. Szwarc. Ibid. 45, 61 (1960).
78. H. Alter. Ibid. 57, 925 (1962).
79. W.R. Brown, R.B. Jenkins and G.S. Park. J. Polymer Sci. C41, 45 (1973).
80. D. Jeshke and H.A. Stuart. Z. Naturf. 16a, 37 (1961).
81. A.C. Sheer. Ph.D. Thesis, University of London (1976).
82. R.Y.M. Huang and P.J.F. Kanitz. J. Appl. Polymer Sci. 13, 669 (1969).
83. P.J.F. Kanitz and R.Y.M. Huang. Ibid. 15, 67 (1971).
84. M. Fels and R.Y.M. Huang. Ibid. 14, 537 (1970).
85. K. Toi, K. Igarashi and T. Tokuda. Ibid. 20, 703 (1976).
86. A.W. Myers, C.E. Rogers, V. Stannett and M. Szwarc. Ibid. 11, 159 (1960).
87. J.D. Wellons, J.L. Williams and V. Stannett. J. Polymer Sci. A-1, 5, 1341 (1967).
88. C.E. Rogers, S. Yamada and M.I. Ostler. Polymer Science and Technology, 6, 155 (1974).
89. J.L. Williams and V. Stannett. J. Appl. Polymer Sci. 14, 1949 (1970).

90. S.P. Chen and J.D. Ferry. Macromolecules, 1, 270 (1968).
91. L.M. Robeson, A. Noshay, M. Matzner and C.N. Merriam. Angew. Makromol. Chem. 29, 47 (1973).
92. E.H. Kerner. Proc. Phys. Soc. B69, 808 (1956).
93. A.E. Barnabeo, W.S. Creasy and L.M. Robeson. J. Polymer Sci. Polymer Chem. Ed. 13, 1979 (1975).
94. K.D. Ziegel. J. Macromol. Sci.-Phys. B5, 11 (1971).
95. K.D. Ziegel, H.K. Frensdorff and D.E. Blair. J. Polymer Sci. A-2, 7, 809 (1969).
96. H. Odani, K. Taira, N. Nemoto and M. Kurata. Bull. Inst. Chem. Res. Kyoto Univ. 53, 216 (1975).
97. H. Odani, K. Taira, T. Yamaguchi, N. Nemoto and M. Kurata. Ibid. 53, 409 (1975).
98. M.J.L. Williams. Ph.D. Thesis, University of London (1978).
99. H.B. Hopfenberg and D.R. Paul. chapter 10 in "Polymer Blends", D.R. Paul and S. Newman eds., Academic Press, New York (1978).
100. J. Barbier. Rubber Chem. Tech. 28, 814 (1955).
101. Y. Ito. Kogyo Kagaku Zasshi 63, 2016 (1960).
102. E.T. Pieski. "Polythene" (2nd Edition), A. Renfrew and P. Morgan eds., Interscience, New York (1960).
103. Y.J. Shur and B. Ranby. J. Appl. Polymer Sci. 19, 1337 (1975).
104. Y.J. Shur and B. Ranby. Ibid. 19, 2143 (1975).
105. Y.J. Shur and B. Ranby. Ibid. 20, 3105 (1976).
106. Y.J. Shur and B. Ranby. Ibid. 20, 3121 (1976).
107. B.G. Ranby. J. Polymer Sci. C51, 89 (1975).
108. R.L. Stallings, H.B. Hopfenberg and V. Stannett. Ibid. C41, 23 (1973).
109. C.M. Peterson. J. Appl. Polymer Sci. 12, 2649 (1968).
110. W.R. Vieth, J.M. Howell and J.H. Hsieh. J. Membrane Sci. 1, 177 (1976).
111. W.J. Koros, D.R. Paul and A.A. Rocha. J. Polymer Sci. Polymer Phys. Ed. 14, 687 (1976).
112. W.J. Koros and D.R. Paul. Ibid. 16, 1947 (1978).
113. A.H. Chan, W.J. Koros and D.R. Paul. J. Membrane Sci. 3, 117 (1978).
114. D.R. Paul and W.J. Koros. J. Polymer Sci. Polymer Phys. Ed. 14, 675 (1976).
115. J.H. Petropoulos. J. Polymer Sci. A-2, 8, 1797 (1970).
116. J.A. Tshudy and C. von Frankenberg. J. Polymer Sci. Polymer Phys. Ed. 11, 2027 (1973).

117. R.A. Assink. Ibid. 13, 1665 (1975).
118. W.R. Vieth, P.M. Tam and A.S. Michaels. J. Colloid and Interface Sci. 22, 360 (1966).
119. R.M. Barrer and H.T. Chio. J. Polymer Sci. C10, 111 (1965).
120. J.B. Alexopoulos, J.A. Barrie, J.C. Tye and M. Frederickson. Polymer, 9, 56 (1968).
121. R.M. Barrer and B.E.F. Fender. J. Phys. Chem. Solids, 21, 12 (1961).
122. R.M. Barrer, J.A. Barrie and M.G. Rogers. Trans. Faraday Soc. 58, 2473 (1962).
123. W.R. Vieth, C.S. Frangoulis and J.A. Rionda. J. Colloid and Interface Sci. 22, 454 (1966).
124. W.R. Vieth and K.J. Sladek. Ibid. 20, 1014 (1965).
125. W.J. Koros, A.H. Chan and D.R. Paul. J. Membrane Sci. 2, 165 (1977).
126. J.A. Barrie, K. Munday and M.J.L. Williams. Polymer Eng. and Sci. (in press).
127. A.S. Michaels and H.J. Bixler. J. Polymer Sci. 50, 413 (1961).
128. T.G. Fox and P.J. Flory. J. Polymer Sci. 14, 315 (1954).
129. J.A. Manson and L.H. Sperling. Op. cit. (23), chapter 12.
130. T.T. Wang and T.K. Kwei. J. Polymer Sci. A-2, 7, 889 (1969).
131. T. Inoue, T. Soen, T. Hashimoto and H. Kawai. Macromolecules 3, 87 (1970).
132. D.C. Kuo. Unpublished data.
133. A.C. Sheer. Unpublished data.

SORPTION AND DIFFUSION OF HYDROCARBON VAPOURS IN GLASSY POLYMERS

JAMES A. BARRIE, KEITH MUNDAY and MICHAEL J.L. WILLIAMS

Chemistry Department,
Imperial College of Science and Technology,
London SW7 2AY.

ABSTRACT

SORPTION AND DIFFUSION OF HYDROCARBON VAPOURS IN GLASSY POLYMERS

J.A. Barrie, M.J.L. Williams and K. Munday, The Chemistry Department, Imperial College of Science and Technology, London SW7 2AY.

Sorption isotherms in the region of low relative pressures have been determined at several temperatures for methane, propane and chlorodifluoromethane in polystyrene and for propane in bisphenol-A polycarbonate and polyvinylacetate. The results are well represented by the isotherm equation of Dual Sorption Theory as applied to glassy polymers. The temperature dependence of the isotherm parameters is examined and discussed; the Langmuir component to sorption decreases as the glass transition temperature is approached and measurements with polyvinylacetate confirm that this component is absent above the transition. Average diffusion coefficients were obtained from sorption (desorption) rate curves at constant pressure for propane in polystyrene and polycarbonate and a procedure developed for their analysis to yield the diffusion coefficients of the two sorbed species of penetrant. For the polycarbonate there is evidence of mobility in that fraction of the penetrant population exhibiting Langmuir-type sorption.

INTRODUCTION

The concept of microcavities frozen into polymer structures below the glass transition temperature and the subsequent formation of a dual mode mechanism for the sorption of gases and vapours in glassy polymers has played an important part in the interpretation of the transport process for penetrants in these systems. It is postulated that in addition to the dissolution of penetrant in the matrix similar to the sorption mode of the rubbery state there is a component associated with localized sorption of penetrant in microvoids; in the region of lower relative pressures dissolution obeys Henry's law while microvoid sorption may be described by the Langmuir isotherm. To develop a model for the transport of penetrant it was assumed in earlier treatments that both species of penetrant were in local equilibrium and further that penetrant sorbed in microvoids was immobilized relative to dissolved species. In later studies the effect of relaxing these constraints was examined and there is now evidence that the microvoid population can contribute to the flux. Much of this work has been reviewed (1,2) or discussed in more recent publications (3,4). It should be noted that the concept of mobile and immobile species had already been used by several investigators to describe the diffusion of water in polymers; also the use of combined isotherm equations for these systems had been considered by several workers (5).

Although a large number of polymer-penetrant systems has been examined only in a few of these (6,7,8) has the temperature dependence of the dual sorption parameters been studied in any detail. In the present investigation sorption equilibria have been studied at several temperatures for propane in polycarbonate, polystyrene and polyvinyl-acetate and for chlorodifluoromethane and, to a lesser extent, methane in polystyrene; also sorption kinetic measurements have been made for propane in polycarbonate and polystyrene. The results are analysed and discussed in terms of the dual-sorption model.

EXPERIMENTAL

The samples studied were polystyrene in both film and powder form, polycarbonate film and a thin sheet of polydimethylsiloxane-g-polyvinylacetate. Films of polystyrene and bisphenol A polycarbonate were cast from methylene chloride solutions on mercury and glass surfaces respectively and were outgassed for several days in the temperature range 50 to 70°C. Average film thicknesses were determined from mass and density measurements and were 107 and 27.2 μm for polystyrene used in the methane and propane studies respectively and 7.8 μm for the polycarbonate; the corresponding film areas were 179, 75 and 200 cm^2. For sorption measurements each film was wound in the form of a spiral with copper wire spacers.

Polydimethylsiloxane-g-polyvinylacetate containing 44.2% vol. polyvinylacetate was prepared by γ-irradiation from a ^{60}Co source of a lightly crosslinked polydimethylsiloxane sheet (~ 100 μm) swollen with vinyl acetate. Irradiation was performed in the absence of air which inhibited grafting, after which the sheet was refluxed with ethyl acetate for several days to constant weight to remove homopolymer and finally outgassed under high vacuum. Electron micrographs indicated that the polyvinylacetate was present as heterodisperse domains of average size 0.08 μm in a continuum of polydimethylsiloxane.

A monodisperse sample of emulsion polymerized microspheres of polystyrene was prepared and characterized by the B.F. Goodrich Company Research Centre, Brecksville, Ohio; the particle diameter was 0.53 μm.

Glass transition temperatures determined by differential scanning calorimetry were as follows; polystyrene film and polystyrene powder 101, polycarbonate film 147 and polyvinylacetate disperse phase 32°C.

The purity of the propane and methane was > 99.9 mol % and of the chlorodifluoromethane > 99.5 mol %; the latter was subjected to several freeze-pump-thaw cycles before use.

Sorption isotherms and kinetics were measured with an electronic vacuum microbalance (Model 4102, Sartorius Instruments Ltd., U.K.) as described earlier (9) and corrections made for buoyancy effects.

RESULTS AND ANALYSIS

SORPTION

Sorption isotherms for the various penetrant-polymer systems at several temperatures are shown in Figures 1 to 6. Those for polystyrene and polycarbonate exhibit clearly the curvature now well established for vapour sorption in glassy polymers at lower relative pressures and characteristic of isotherms of the Langmuir type; an exception is the methane-polystyrene system where the range of relative pressure is not sufficiently large to observe departure from Henry's law. A small but definite amount of curvature is also present in the isotherms for the graft copolymer below the glass transition temperature; at higher temperatures the isotherms are linear as are those for crosslinked polydimethylsiloxane. Isotherms for the polyvinylacetate disperse phase were "extracted" from those of the graft copolymer and of the polydimethylsiloxane and are shown in Figure 6 ; the accuracy here is less than for the other systems studied as the major part of the sorption occurs in the continuous polydimethylsiloxane phase. Dispersion of the polyvinylacetate in this manner gave short equilibration times and avoided possible problems arising from softening of the polymer above the glass transition temperature.

The results were analysed in terms of the dual-sorption theory as applied to glassy polymers for which the isotherm equation is

$$C = C_D + C_H = k_D p + \frac{C'_H b p}{1+bp} \qquad (1)$$

where C, the total concentration of sorbed penetrant comprises a component C_D for dissolved species and a component C_H for molecules localized in microvoids. It is assumed that sorption of the dissolved component obeys

Henry's law and that the microvoid component obeys the Langmuir equation for sorption on a fixed number of equivalent sites with not more than one molecule per site. The temperature dependence of k_D, the Henry's law constant for dissolved species is given by $k_D = (k_D)_o \exp(-\Delta\bar{H}_D/RT)$ where $\Delta\bar{H}_D$ is the heat of sorption for this component. From a statistical thermodynamic consideration of ideal localized monolayers the Langmuir parameter b is given by $b = b_o \exp(q/kT)$ where q is the minimum energy required to evaporate a molecule from its lowest energy state in the monolayer and b_o is a weak function of temperature. The quantity C'_H is the value of C_H in the limit $p \to \infty$ and corresponds to saturation of the adsorption sites; if C'_H is independent of temperature then q is simply related to the isosteric heat of adsorption on sites $-\Delta\bar{H}_H = -R\left(\frac{\partial \ln p}{\partial 1/T}\right)_{C_H}$

A non-linear regression analysis described in the Appendix was used to obtain values for k_D, b and C'_H which are shown in Table 1. The programme also estimated by what amount each parameter could be altered within the limits of a standard deviation; these values are quoted as average percentages in parenthesis in Table 1. Clearly the uncertainties in the sorption parameters are relatively large especially for C'_H and b, however, for the product $C'_H b$ they are much less as has already been pointed out (10). Because of the larger uncertainties attached to the isotherms for polyvinylacetate as a disperse phase the errors in the parameters C'_H and b were too large for a meaningful analysis, accordingly individual values of C'_H and b are not recorded in Table 1; also included in Table 1 are values of the Henry's law constant for the limit $p \to 0$, namely $k = k_D + C'_H b$. The temperature dependence of k is given by $k = k_o \exp\left\{-(\Delta\bar{H})_{c=o}/RT\right\}$ where $-(\Delta\bar{H})_{c=o}$ is the isosteric heat of sorption in the limit $C \to o$.

The temperature dependence of k_D, b and k is illustrated in Figure 7 with some typical examples and values of $\Delta\bar{H}_D$, q and $(\Delta\bar{H})_{c=o}$ are given in Table 2. The temperature dependence of k_D and k for the polyvinylacetate disperse phase both above and below the glass transition temperature is shown in Figure 8; no attempt was made to estimate the

heats of sorption below the glass transition temperature. Finally, in Figure 9 the variation with concentration of $\Delta\overline{H}$, the overall heat of sorption, is shown.

DIFFUSION

Integral sorption (desorption) rate curves were measured with constant pressure maintained at the film interface and diffusion coefficients obtained from the initial slopes by conventional procedures. For the propane-polystyrene system average coefficients were obtained from conjugate sorption-desorption curves and the arithmetic mean approximation used to relate these to the differential coefficient D such that $\overline{D} \equiv (\overline{D}_s+\overline{D}_d)/2 = \frac{1}{C}\int_o^C DdC$ (11). For the propane-polycarbonate system, sorption rate curves only were measured and the average and differential coefficients were related through the weighted-mean approximation $\overline{D}_s = rC^{-r}\int_o^C C^{r-1}DdC$ where r = 1.67 (11). The concentration dependence of $\overline{D}$ and $\overline{D}_s$ is shown in Figures 10 and 11 respectively.

In the development and application of dual-sorption theory several notations have been used for the experimental diffusion coefficient and the diffusion coefficient for dissolved penetrant some examples of which are, $D_{eff}D$ (2,12), D_aD_{eff} (13), DD' (3), D_aD' (14) and DD' (15). In what follows the experimental diffusion coefficient determined from the total flux and gradient of the total concentration is denoted by D.

Extensions of the earlier analyses of gas transport in glassy polymers assign diffusion coefficients to penetrant both in dissolved state and sorbed in microvoids respectively. Denoting these coefficients by D_D and D_H respectively and assuming that the populations of these two states obey Henry's law and the Langmuir isotherm respectively then the flux per unit area is given by (3,4)

$$J = -D_D\frac{\partial C_D}{\partial x} - D_H\frac{\partial C_H}{\partial x} \equiv -D\frac{\partial C}{\partial x} \qquad (2)$$

It follows that,

$$D = (D_D - D_H)\frac{\partial C_D}{\partial C} + D_H \tag{3}$$

From equation (1),

$$\frac{\partial C_D}{\partial C} = 1/\left\{1 + \frac{C'_H b/k_D}{(1+bp)^2}\right\} \tag{4}$$

and hence D is obtained as a function of pressure. Alternatively, from equation (1),

$$p = \frac{\left\{(C'_H b + k_D - bC)^2 + 4k_D bC\right\}^{\frac{1}{2}} - (C'_H b + k_D - bC)}{2k_D b} \tag{5}$$

which with equations (3) and (4) gives D as a function of C or C_D (12). The resulting expressions are quite general in the sense that D_D and D_H may be functions of concentration; however, it is generally assumed that both coefficients are constant and this approach is adopted from here on. In the limit $bp \ll 1$,

$$D_{c=o} = \frac{D_D k_D + D_H C'_H b}{k_D + C'_H b} \tag{6}$$

and for $p \to \infty$, $D = D_D$. In principle, the concentration dependence of D can be obtained from the plots of $\bar{D}$ against C by conventional methods involving differentiation, graphical or otherwise, of the data and a best fit made with equation (3) using D_D and D_H as adjustable parameters. However, as the expression for D(C) is cumbersome and differentiation introduces additional errors it is better to make the comparison with the average diffusion coefficient data. The corresponding theoretical expressions are easily obtained as follows,

$$\bar{D}_s \equiv rC^{-r}\int_o^C C^{r-1} D\,dC$$

$$= rC^{-r}\left\{\int_o^C C^{r-1}(D_D - D_H)\frac{\partial C_D}{\partial C} + \int_o^C C^{r-1} D_H\,dC\right\} \tag{7}$$

$$= (D_D - D_H)X + D_H \tag{8}$$

The integral X which may be computed by numerical integration was expressed as follows using integration by parts,

$$X = rC^{-r}\left\{C^{r-1} k_D p - k_D(r-1)\int_o^C C^{r-2} p\,dC\right\} \tag{9}$$

A plot of $\overline{D}_s$ versus X is then linear with slope $(D_D - D_H)$ and intercept D_H; If the arithmetic mean of the average coefficients from conjugate sorption and desorption rate curves is used to obtain $\overline{D} = \frac{1}{C}\int_o^C DdC$ then the corresponding expressions for $\overline{D}$ are obtained with r = 1 in equations (7) to (9) and reduce to the relatively simple expression

$$\overline{D} = \frac{pD_D}{C}\left\{k_D + \frac{D_H}{D_D}\frac{C'_H b}{(1+bp)}\right\} \qquad (10)$$

In this instance the average coefficient $\overline{D}$ is identical with that obtained from steady-state permeation so that using Fick's equation for the permeability $\overline{P}$,

$$\overline{P} = \overline{D}\frac{C}{p} = k_D D_D\left\{1 + \frac{D_H}{D_D}\frac{(C'_H b/k_D)}{(1+pb)}\right\} \qquad (11)$$

which is the expression obtained earlier (3,4) for the steady-state permeability as a function of the pressure. The corresponding expressions for the concentration dependence of $\overline{D}$ and $\overline{P}$ are obtained using equation (5). In the limit $p \to o$ equation (10) reduces to equation (6) and for $p \to \infty$, $\overline{D} = D_D$.

The results for the C_3H_8- polycarbonate system plotted according to equation (8) are shown in Figure (12) and indicate a finite but small D_H for microvoid population. Attempts to analyse or curve fit the results with $D_H = 0$ were not successful in that the values of D_D displayed a small but definite trend with concentration. The solid curves in figure (11) were computed using equation (8). For the C_3H_8- polystyrene (film) system the accuracy of the data was such that it was not possible to establish whether or not $D_H = 0$; within the limits of experimental error the results were represented satisfactorily by equation (10) with $D_H = 0$. Values of D_D and D_H are given in Table (3); also included are values of the limiting coefficients $D_{c=o}$ calculated from equation (6) and of the activation energy in the limit $C \to o$.

DISCUSSION

SORPTION

The solid curves of Figures 1 to 6, computed using equation (1) and the parameters of Table 1, are in good agreement with the experimental points but the errors in the sorption parameters are comparatively large and tend to increase with temperature. This may be partly a reflection of the difficulty in ensuring that relaxation and hysteresis effects are negligible in glassy polymer systems. This aspect was studied in more detail with the microsphere samples; it was observed that the bulk of the sorption was rapid followed by a small uptake which slowly approached an equilibrium value while in all cases desorption was rapid (16). Thus even at low levels of sorption, less than 1% by volume, some degree of relaxation would appear to be present; also some thermal hysteresis was observed on cycling the sample over the temperature range. Although the uncertainties introduced by these effects were in general small, at worst not more than a few per cent, nevertheless they limit the accuracy with which one may determine the sorption parameters in these systems. The value of .0069 for the overall solubility k determined directly for methane in polystyrene at 30°C may be compared with the value of 0.00126 obtained earlier from a dual-sorption analysis of high pressure isotherm data for the same system at 25°C. The discrepancy between the two figures is not serious in view of the difference in temperature and sample preparation and the use of a graphical rather than a least-squares regession analysis to fit the high pressure data (18)

According to equation (1) the ratio C_H/C_D varies from $C'_H b/k_D$ to zero as the pressure changes from 0 to ∞ and so from the results in Table 1 it is inferred that for sorption in glassy polymers the Langmuir component is the major one in the region of lower pressures. A comparison of the propane data for the polystyrene film and powder indicates that although the overall solubility k for both samples is similar, the Langmuir component for the powder is higher and has

increased at the expense of the Henry's law component; this behaviour may reflect differences in the thermal histories of the samples with the microspheres having a larger microvoid volume. It has already been demonstrated that annealing of the microspheres has quite a significant effect on their sorption behaviour (16). Although chlorodifluoromethane is sorbed more strongly than propane the ratio $C'_H b/k_D$ is not significantly different for these two vapours. In polycarbonate, propane is sorbed more strongly than in polystyrene in both the Langmuir and Henry's law modes; also the ratio $C'_H b/k_D$ is relatively large but this may simply reflect the higher glass transition of the polycarbonate and the fact that this ratio increases steadily as the temperature is lowered below the transition temperature for all of the polymers studied.

The decline in the relative magnitude of the Langmuir component as the glass transition temperature is approached is in accord with earlier observations and the view that this component of the sorption should tend to zero in the region of the transition (7). The results for the polyvinylacetate disperse phase demonstrate directly that this is the case with no Langmuir component to the sorption in evidence above the glass transition temperature. Somewhat similar behaviour has been reported for the vinylchloride-polyvinylchloride system (16) and reference has also been made to the system CO_2-poly(ethyleneterephthalate) (17).

The parameter C'_H has been used as a measure of the surface area bounding the microvoids by assuming that the molecules sorbed in these have the same hexagonal packing as the plane of closest packing in the liquid state (18) or as a measure of the microvoid volume using an appropriate density for the sorbed phase, generally that of the liquid for vapours above their critical temperature (7,10). The density of liquid propane decreases from ~ 0.5 at 20°C to ~ 0.425 at 60°C; the corresponding variation of C'_H particularly for the propane-polystyrene system is much larger and in terms of these earlier analyses (18,7,10) one may conclude that the microvoid surface area or microvoid volume decreases as the temperature is increased.

It is pertinent at this stage to re-emphasize some observations which have been made with regard to testing theoretical isotherm equations. It has long been recognized that agreement between the theoretical and experimental isotherm does not constitute proof of the model on which the theoretical equation is based and furthermore even if sensible values of the parameters emerge these may result from a mutual cancellation of different effects (19,20,21,22,23). It is unlikely that sorption of penetrant in microvoids conforms exactly to the ideal localized model of sorption according to which molecules are sorbed on a set of sites with no interaction between sorbed molecules and no more than one molecule allowed per site; on this basis C'_H is constant and independent of temperature and is a measure of the number of sorption sites in the system. Invariably C'_H is observed to vary with temperature and it has been argued that for several reasons this effect may be more apparent than real (19, 20, 21) Nevertheless this parameter has been used to estimate saturation capacities of real systems such as the zeolites where Langmuir-type sorption is often observed (24). In experiments with glassy polymers the degree of saturation C_H/C'_H attained is usually large and in the present investigation was rarely less than 80% and usually greater than 90% so that good agreement with the Langmuir equation is obtained over a large part of the isotherm. In the light of these earlier observations it would appear that the parameter C'_H is related to the saturation capacity but that some care should be exercised in the use of absolute values.

Similar strictures apply to the interpretation of the parameter b and its temperature coefficient q; in terms of the Langmuir model q is constant and a measure of the isosteric heat of sorption in the microvoids. A comparison of the data of Table 2 indicates that in general q is numerically larger than ΔH_D which might have been anticipated; however, in some instances the difference is small and in others $|q| < |\Delta H_D|$. Similar

behaviour was observed for hydrocarbon vapours in ethylcellulose (7) and for methane in oriented polystyrene (6). The isosteric heat of sorption in microvoids in the limit C→0 is given by $-(\Delta\bar{H}_H)_{c=0} = \frac{d\ln C'_H b}{dI/T}$ and values are included in Table 2; if C'_H is temperature independent then $(\Delta\bar{H}_H)_{c=0} = -q$. Also since $k = k_D + C'_H b$ it follows that

$$\Delta\bar{H}_{c=0} = \frac{k_D}{k}\Delta\bar{H}_D + \frac{C'_H b}{k}(\Delta\bar{H}_H)_{c=0} \qquad (12)$$

The difference in the values of q and $-(\Delta\bar{H}_H)_{c=0}$ of Table 2 is substantial and the question arises as to which of these two quantities is more representative of the true heat of sorption in microvoids. Using the parameters C'_H and b of Table 1 adsorption isosteres were constructed for the Langmuir component of the sorption for constant values of C_H. Smoothed values of $\Delta\bar{H}_H$ were obtained from linear isosteres only and the variation with concentration is shown in Figure (14); at higher concentrations approaching saturation the isosteres became non-linear. $\Delta\bar{H}_H$ tends to become more exothermic as C_H increases; it is conceivable that this behaviour is more apparent than real and associated with a perturbation of the polymer matrix as for example, a change in the microvoid content with temperature. If this were so, then $\Delta\bar{H}_H$ would not reflect accurately the heat of sorption in microvoids. The small minimum observed in Figure (9) is also probably associated with the increase in $|\Delta\bar{H}_H|$ with concentration; at higher concentrations the relative contribution to $\Delta\bar{H}$ from the dissolved species increases and $\Delta\bar{H}$ tends towards $\Delta\bar{H}_D$.

The results for the polyvinylacetate disperse phase in Figure (8) are of interest in that they indicate that $\Delta\bar{H}_D$ may be more exothermic above the glass transition temperature than below it, suggesting perhaps that hole formation in the dissolved state is more endothermic below the transition. In view of the reduced accuracy of the isotherms for this system a more detailed study over a wider range of temperature is required to substantiate these observations.

DIFFUSION

The earlier work on the application of dual-sorption theory in this area made use of pressure decay in a system of finite volume; the analysis was then based on an empirical correlation relating parameters obtained from a numerical solution of the diffusion equation and has been described in detail elsewhere (2). In later developments the restriction $D_H=0$ was removed and the pressure dependence of the steady-state permeability and the time-lag analysed to obtain D_D and D_H (3,4). The procedure developed here and incorporated in equations (8) and (9) enables one to determine both D_D and D_H from the initial slopes of either sorption or desorption rate ($\propto/t$) curves determined at constant pressure; the accuracy of the method will depend among other things on that of the weighted-mean approximation.

The data for polycarbonate in Table 2 support the view that immobilization of the Langmuir component is only partial (7,10). Although D_H is relatively small the contribution to the flux from this component can be large at low pressures; for example, in the limit $p \to o$, the ratio of the flux of dissolved species to that of penetrant in microvoids is $\frac{C'_H b}{k_D} \frac{D_H}{D_D}$ and at 30°C is estimated as 1.95. Substituting 1.95 for the ratio of the fluxes in equation (11) it is estimated that the permeability for propane in polycarbonate varies from $\sim 3.2.\ 10^{-12}$ to $1.6.\ 10^{-12}$ cc stp. cm/cm^2 s. cm Hg as the pressure changes from 0 to 10 cm g and thereafter approaches asymptotically the limiting value of $k_D D_D = 1.07.\ 10^{-12}$. The results for polystyrene in Fig.13 are inconclusive and/or more data points are required to establish whether $D_H=0$. As indicated earlier (3) the average coefficient $\overline{D}$ may be converted to the corresponding $\overline{P}$ ($=\overline{D}\,\overline{C}_p$) and the latter examined for pressure dependence. In this instance no advantage is gained as the scatter in the $\overline{P}$ values obscures any trend with pressure; The average values of $\overline{P}$ at 30 and 50°C are $3.72.10^{-12}$ and $5.12.10^{-12}$ respectively.

The temperature dependence of the diffusion coefficients is shown in Figure (15) and the corresponding energies of activation in Table 2. From equation (6) it follows that

$$(E_D)_{c=o} = -(\Delta\bar{H})_{c=o} + (E_{D_D} + \Delta\bar{H}_D)\frac{D_D k_D}{D_{c=o} k} + \left\{E_{D_H} + (\Delta\bar{H}_H)_{c=o}\right\}\left(1 - \frac{D_D k_D}{D_{c=o} k}\right) \quad (13)$$

and the $\Delta\bar{H}$ terms are related through equation (12). In view of the relatively large errors attached to the values of D_H it is not possible to attach too much significance to the relative values of E_{D_D} and E_{D_H}. One might have anticipated E_{D_H} to be larger than E_{D_D}; this tends to be so for hydrocarbon diffusion in ethylcellulose although in general the differences are not large (7). It is conceivable that the transition state for penetrant diffusing out of microvoids into the dissolved state differs from that for penetrant diffusing in the dissolved state.

In conclusion the analysis is consistent with the view that the localized microvoid space may be a function of temperature and, in particular, decreases as the temperature of the glass approaches Tg but it is difficult to draw firm conclusions. Essentially the dual- sorption theory postulates two modes of sorption the isotherms for which are described by the Henry's law and Langmuir equations; in this respect the theory gives good agreement with experiment in a large number of systems. If one proceeds further and identifies the parameters of the Langmuir equation with those of the Langmuir model for ideal localized sorption then it should be borne in mind that isotherm equations of this form are not specific to this mode of sorption and too literal an interpretation of the isotherm parameters and their temperature dependence in this fashion could be misleading. Finally a method for analysing average diffusion coefficient data from constant pressure sorption analysis is suggested; the results for polycarbonate indicate a component to the flux from the Langmuir component but for polystyrene are inconclusive.

Acknowledgements

We thank the SRC for maintenance awards (to K.M. and M.J.L.W.) and both the SRC and the University of London Research Fund for grants to purchase equipment. We are grateful to Professor H.B. Hopfenberg for the sample of polystyrene microspheres.

APPENDIX

The least-squares values of the dual-mode sorption coefficients cannot be determined by any simple closed expression. If α, β and γ are approximations to the desired coefficients k_D, C_H and b, we define

$$C' = \alpha p + \beta \left(\frac{\gamma p}{1+\gamma p}\right) \tag{1}$$

and

$$S = \sum_{i=1}^{n} (C'-C)^2$$

$$= \alpha^2 \Sigma p^2 + \beta^2 \Sigma f(p)^2 + 2\alpha\beta \Sigma p f(p)$$

$$-2\alpha \Sigma C p - 2\beta \Sigma C f(p) + \Sigma C^2 \tag{2}$$

where $f(p) = \frac{\gamma p}{1+\gamma p}$ and C,p are the experimental values.

Then for any given value of γ the corresponding approximations α and β are uniquely defined by the simultaneous equations

$$\frac{\partial S}{\partial \alpha} = 2\alpha \Sigma p^2 + 2\beta \Sigma p.f(p) - 2\Sigma C p = 0 \tag{3}$$

$$\frac{\partial S}{\partial \beta} = 2\beta \Sigma f(p)^2 + 2\alpha \Sigma p.f(p) - 2\Sigma C.f(p) = 0 \tag{4}$$

It is then required only to find the value of γ giving the minimum value of the sum of the squares of the deviations, S, which is easily achieved by a computer program employing a systematic variation in γ. We then define the mean deviation of the experimental points as $S/(n-3)$, where n is the number of points and $n-3$ the remaining degrees of freedom, and estimate the uncertainties in the best fit parameters k, C'_H, and b, from the maximum variations of these parameters giving isotherms which lie within one mean deviation of the best fit isotherm over the range of the experimental data.

REFERENCES

1. H.B. Hopfenberg and V. Stannett, "The Physics of Glassy Polymers", (Ed. R.N. Haward), Chapter 9. Applied Science Publishers, London (1973).
2. W.R. Vieth, J.M. Howell and J.H. Hsieh, J. Membrane Sci., 1, 177 (1976).
3. J.H. Petropoulos, J. Polym. Sci., Pt.A-2, 8, 1797 (1970).
4. D.R. Paul and W.J. Koros, J. Polym. Sci.; Polym. Phys. Ed., 14, 675 (1976).
5. J.A. Barrie "Diffusion in Polymers" (Eds. J. Crank and G.S. Park), Chapter 8, Academic Press. London and New York (1968).
6. W.R. Vieth, C.S. Fragoulis and J.A. Rionda, Jr., J. Colloid Interface Sci., 22, 454 (1966).
7. A.H. Chan, W.J. Koros and D.R. Paul, J. Membrane Sci., 3, 117 (1978).
8. S.A. Stern and A.H. De Meringo, J. Polym. Sci.; Polym. Phys Ed., 16, 735, (1978).
9. J.A. Barrie and D. Machin, J. Macromol Sci. Phys. B3(4) 645 (1969).
10. W.J. Koros, A.H. Chan and D.R. Paul, J. Membrane Sci., 2, 165 (1977).
11. J. Crank, "The Mathematics of Diffusion" p 244, 250 Clarendon Press, Oxford (1975).
12. W.J. Koros, D.R. Paul and A.A. Rocha, J.Polym. Sci.; Polym. Phys. Ed., 14, 687 (1976).
13. K. Toi, J. Polym. Sci.; Polym.Phys. Ed., 11, 1829 (1973).
14. A.S. Michaels, W.R. Vieth and J.A. Barrie, J. App. Phys., 34, 13 (1963).
15. J.A. Barrie, A.S. Michaels and W.R. Vieth, J. Polym. Sci.; Polym. Phys. Ed., 13, 859 (1975)

16. A.R. Berens, J. Membrane Sci., 3, 247 (1978).

17. W.J. Koros, D.R. Paul, M. Fujii, H.B. Hopfenberg and V. Stannett, J. App. Polym. Sci., 21, 2899 (1977).

18. W.R. Vieth, Phi M. Tam and A.S. Michaels, J. Colloid Interface Sci., 22, 360 (1966).

19. D.H. Everett, Trans. Faraday Soc., 46, 453 (1950).

20. D.H. Everett, Trans. Faraday Soc., 46, 942, (1950).

21. D.H. Everett, Trans. Faraday Soc., 46, 957, (1950).

22. D.H. Everett, Proc. Chem. Soc. (London) 37 (1957).

23. D.M. Young and A.D. Crowell "Physical Adsorption of Gases" Chapter 3,4. Butterworth, London (1962).

24. L.V.C. Rees and C.J. Williams, Trans. Faraday Soc., 60, 1973 (1964).

Table 1. Dual Sorption Parameters

T/°C	$10^2 k_D$ $cm^3(stp)/cm^3 cmHg$	C'_H $cm^3(stp)/cm^3$	b $(cmHg)^{-1}$	10k $cm^3(stp)/cm^3 cmHg$	$C'_H b/k_D$
		CH_4/Polystyrene			
30	-	-	-	0.069	5.0*
50	-	-	-	0.044	
		C_3H_8/Polystyrene (film)			
30	4.69	1.01	0.18	2.29	3.88
50	2.82	0.735	0.071	0.804	1.85
		C_3H_8/Polystyrene (powder)			
20	4.39(±5%)	1.32(±9%)	0.209(±18%)	3.2(±9%)	6.28
30	3.30(±11%)	1.36(±17%)	0.136(±28%)	2.18(±11%)	5.60
40	2.93(±6%)	0.90(±12%)	0.127(±20%)	1.43(±8%)	3.80
50	2.46(±6%)	0.70(±16%)	0.106(±23%)	0.984(±7%)	3.02
60	2.29(±14%)	0.51(±45%)	0.108(±62%)	0.776(±17%)	2.41
		$CHClF_2$/Polystyrene (powder)			
20	7.34(±8%)	2.16(±15%)	0.18(±28%)	4.71(±13%)	5.3
30	5.42(±9%)	1.95(±14%)	0.150(±25%)	3.47(±11%)	5.4
40	4.49(±7%)	1.50(±13%)	0.110(±20%)	2.10(±7%)	3.67
50	3.81(±7%)	1.20(±15%)	0.089(±20%)	1.45(±6%)	2.80
60	3.18(±18%)	0.80(±59%)	0.071(±63%)	0.89(±9%)	1.79
		C_3H_8/Polycarbonate			
30	6.03(±7%)	1.67(±11%)	0.311(±30%)	5.79(±18%)	8.6
40	5.01(±2%)	1.25(±4%)	0.254(±9%)	3.68(±5%)	6.3
50	4.01(±8%)	1.02(±21%)	0.167(±43%)	2.10(±19%)	4.3
60	2.55(±17%)	1.22(±31%)	0.094(±50%)	1.40(±19%)	4.5
		C_3H_8/Polyvinylacetate (disperse)			
2.7	2.29(±5%)	-	-	0.999(±8%)	3.4
12.1	2.24(±5%)	-	-	0.786(±14%)	2.5
22.4	1.89(±5%)	-	-	0.52	1.76
40.15	1.83(±1%)	-	-	-	
50.0	1.66(±5%)	-	-	-	
60.2	1.45(±3%)	-	-	-	

* data from (18)

Table 2. Heats of Sorption.

System	$-\Delta\overline{H}_D$ kJmol^{-1}	q kJmol^{-1}	$-(\Delta\overline{H})_{c=o}$ kJmol^{-1}	$-(\Delta\overline{H}_H)_{c=o}$ kJmol^{-1}
CH_4-polystyrene (film)	-	-	-	18†
C_3H_8-polystyrene (film)	21†	38†	51†	43†
C_3H_8-polystyrene (powder)	13	13	34	30
$CHClF_2$-polystyrene (powder)	17	20	39	34
C_3H_8-polycarbonate	24	34	43	41
C_3H_8-polyvinylacetate (T > Tg)	10	-	-	-
C_3H_8-polydimethylsiloxane	17	-	-	-

† From two temperatures only.

TABLE 3. Diffusion Coefficients and Activation Energies for Diffusion

T/°C	$10^{11}D_D$	$10^{12}D_H$	$10^{11}D_{c=o}$	E_{D_D}	E_{D_H}	$E_{D_{c=o}}$
	cm^2/s	cm^2/s	cm^2/s	kJ/mol	kJ/mol	kJ/mol
			CH_4/Polystyrene			
30	-	-	1270	-	-	39
50	-	-	3330	-	-	
			C_3H_8/Polystyrene (film)			
30	8	-	1.64	33	-	55
50	18	-	6.3			
			C_3H_8/Polycarbonate			
30	1.77(±4%)	4.0(∓9%)	0.54			
40	3.43(±1.5%)	5.4(∓1.4%)	0.93			
50	8.3(±12%)	6.6(∓17%)	2.12	69	49	67
60	20.3(±19%)	27.1(∓88%)	5.9			

CAPTIONS FOR FIGURES

Figure 1. Sorption isotherms for polystyrene (film).

C_3H_8: O 30°, ● 50°C. Solid lines computed from equation (1); dotted line is the asymptote at 30°C.

CH_4: ordinate is CX4; □ 30° ■ 50°C.

Figure 2. Sorption isotherms for propane in polystyrene (powder).

■ 20, ▲ 30, ● 40, ◆ 50, ▼ 60°C. Solid lines computed for equation (1); dotted line is the asymptote to the curve at 20°C.

Figure 3. Sorption isotherms for propane in polycarbonate

■ 30, ▲ 40, ● 50, ▼ 60°C. Solid lines computed from equation (1); dotted line is the asymptote to the curve at 30°C.

Figure 4. Sorption isotherms for chlorodifluoromethane in polystyrene (powder).

■ 20, ▲ 30, ● 40, ◆ 50, ▼ 60°C. Solid lines computed from equation (1); dotted line is the asymptote to the curve at 20°C.

Figure 5. Sorption isotherms for propane in polydimethylsiloxane-g-polyvinylacetate and polydimethylsiloxane.

PDMS-g-PVAc: ■ 2.7, ▲ 12.1, ● 22.4°C; ▼ 50°C, typical linear isotherm obtained above Tg. Solid lines computed from equation (1).

PDMS : O 11.7°C, typical linear isotherm.

Figure 6. Sorption isotherms for propane in polyvinylacetate disperse phase.

■ 2.7, ▲ 12.1, ● 22.4; ▼ 50°C, typical linear isotherm obtained above Tg. Solid lines computed from equation (1); dotted line is the asymptote to the curve at 2.7°C.

Figure 7. Temperature dependence of dual-sorption parameters; typical behaviour illustrated by results for the propane-polycarbonate system.

● $Z - k$, ▲ $Z - b$, ■ $Z - k_D$, ▼ = $C'_H b$.

Figure 8. Temperature dependence of k_D and k for the propane–polyvinylacetate (disperse phase) system.

● $Z = k_D$, ■ $Z = k$.

Figure 9. Concentration dependence of the heat of sorption $\Delta\bar{H}$; smoothed values obtained from the curves computed from equation (1).

—— C_3H_8-polystyrene, --- $CHClF_2$-polystyrene, ····· C_3H_8-polycarbonate.

Figure 10. Concentration dependence of the average diffusion coefficient $\bar{D}$ for the propane–polystyrene (film) system.

○ 30, ● 50 °C; Solid curves computed from equation (10) with $D_H=0$.

Figure 11. Concentration dependence of the average diffusion coefficient $\bar{D}_s$ for propane–polycarbonate system.

■ 30, ▲ 40, ● 50, ▼ 60 °C; solid curves computed from equation (8).

Figure 12. Plots of $\bar{D}_s$ versus X, where X is given by equation (9), r=1.67 for propane in polycarbonate.

■ 30, ▲ 40, ● 50, ▼ 60 °C.

Figure 13. Plots of $\bar{D}$ versus X, where X is given by equation (9), r=1, for propane in polystyrene.

○ 30, ● 50 °C.

Figure 14. Concentration dependence of the heat of sorption $\Delta\bar{H}_H$.

-·-·-· C_3H_8-polystyrene (sheet), ····· C_3H_8-polystyrene (powder), ----- C_3H_8-polycarbonate, ———— $CHClF_2$-polystyrene (powder).

Figure 15. Temperature dependence of diffusion coefficients; typical behaviour as illustrated by results for the propane–polycarbonate system.

● D_D, ▲ $D_{C=O}$, ■ D_H.

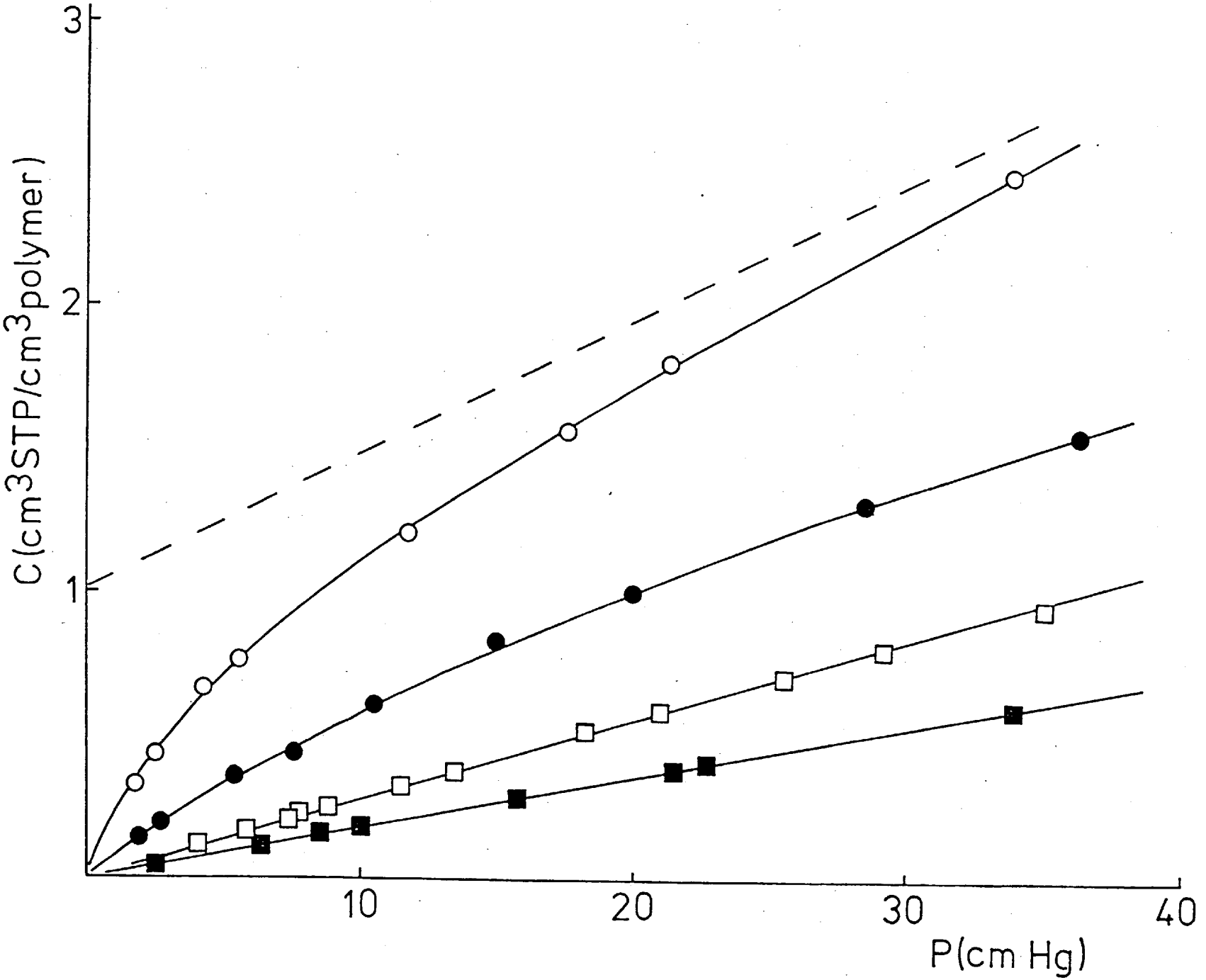
3
2
1
C(cm3STP/cm3polymer)
10
20
30
40
P(cm Hg)

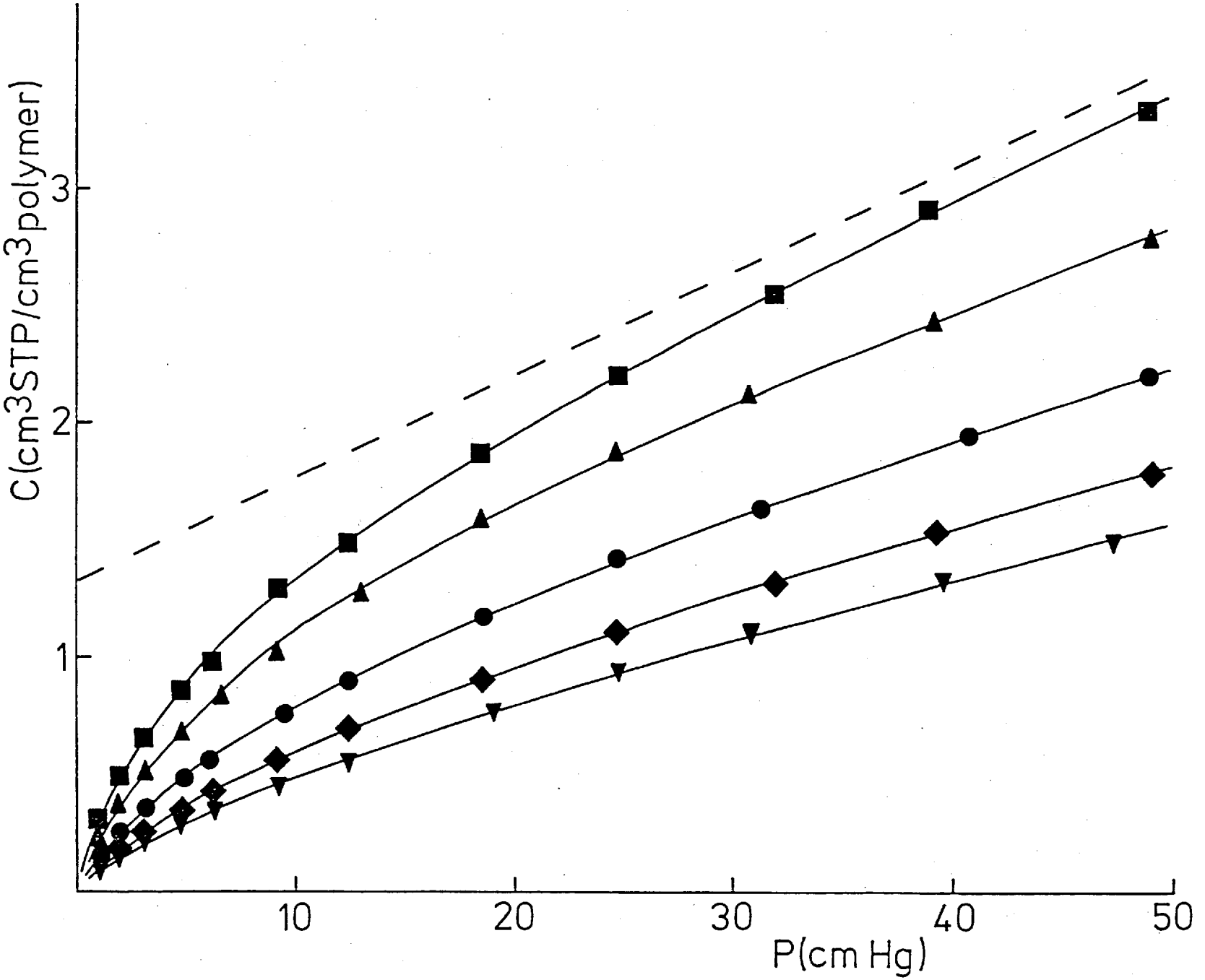
C(cm3STP/cm3polymer)
1
2
3
10
20
30
40
50
P(cm Hg)

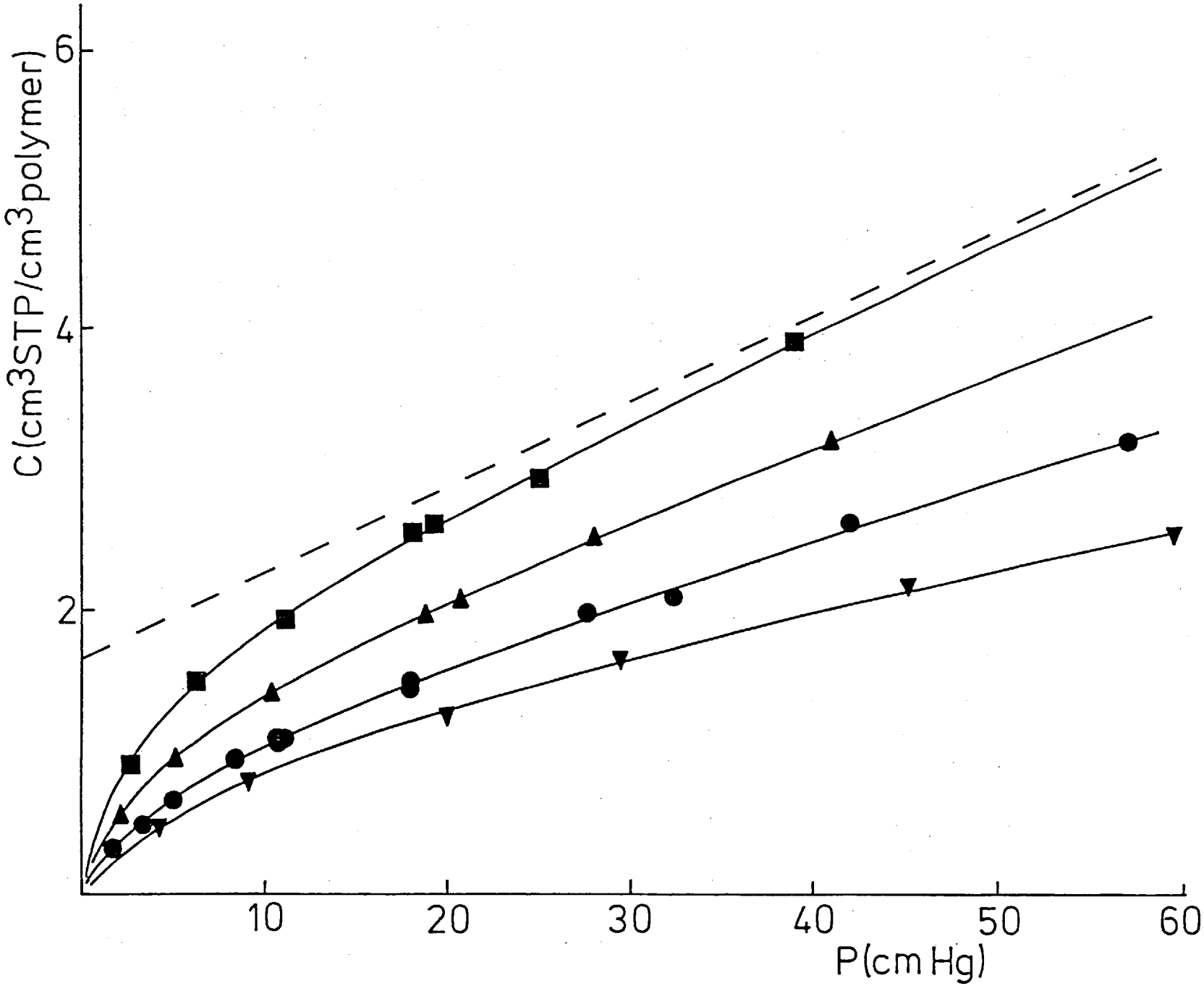
C(cm3STP/cm3polymer)
6
4
2
10
20
30
40
50
60
P(cm Hg)

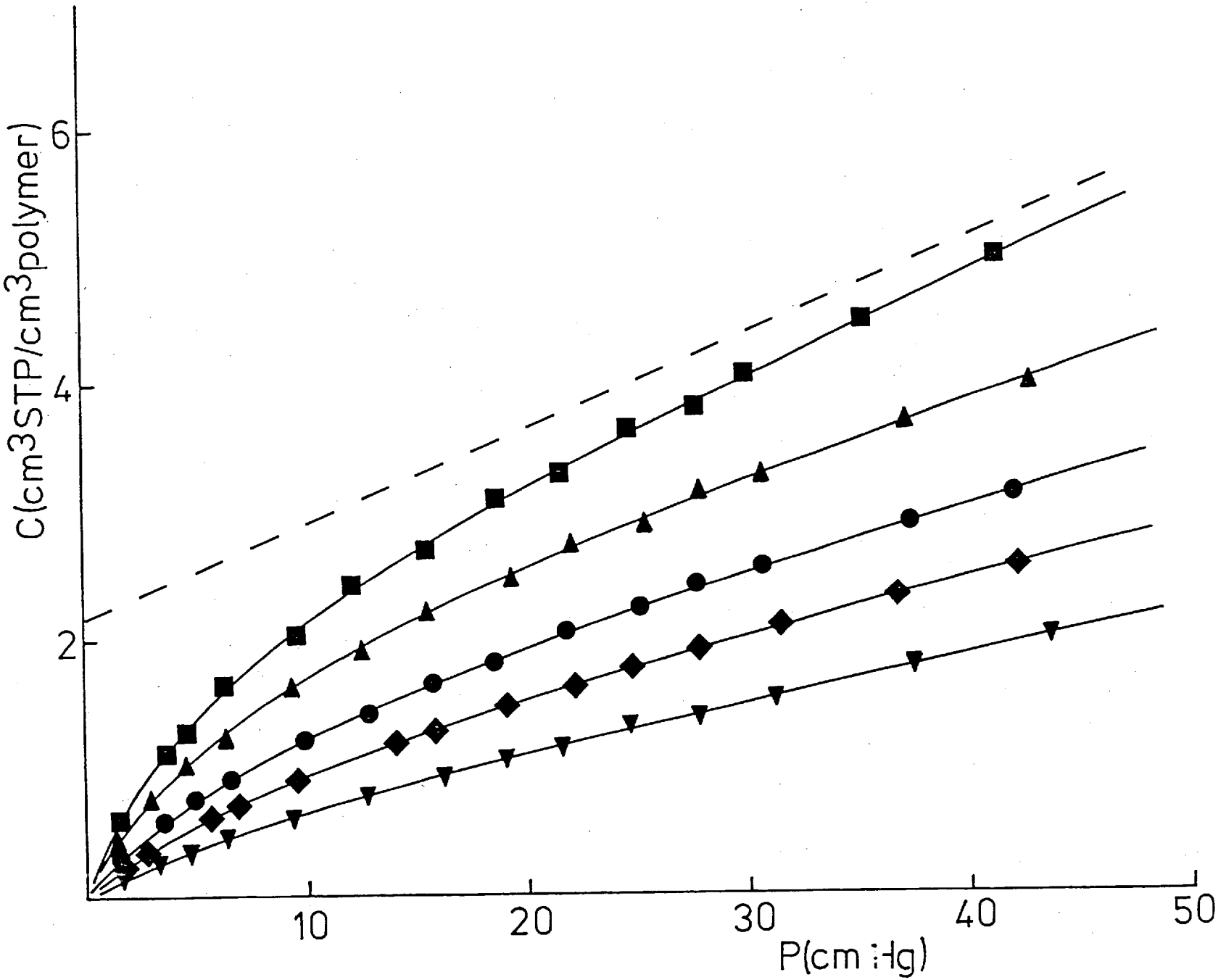
C(cm3STP/cm3polymer)
6
4
2
10
20
30
40
50
P(cm Hg)

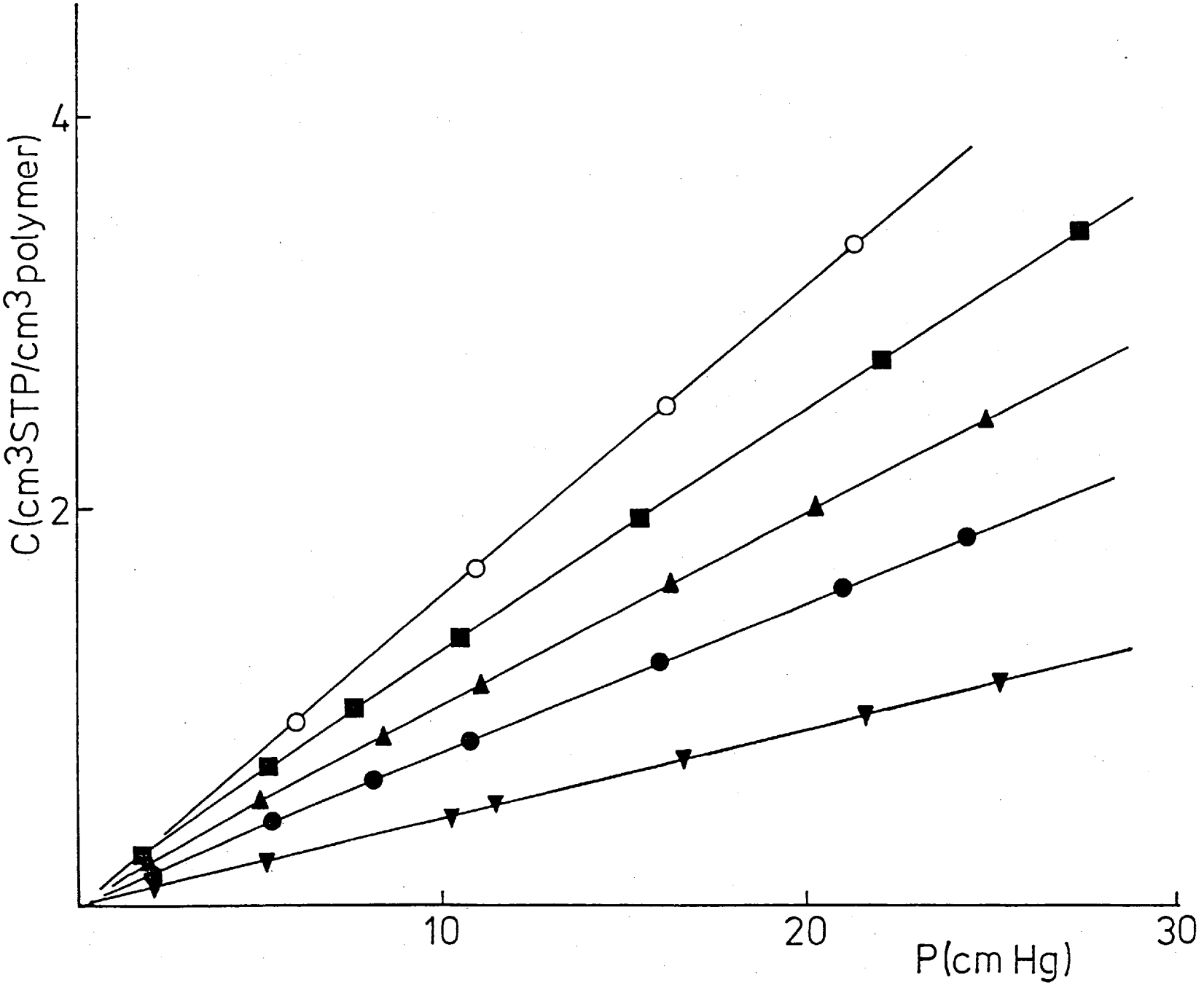
C(cm3STP/cm3polymer)
4
2
10
20
30
P(cm Hg)

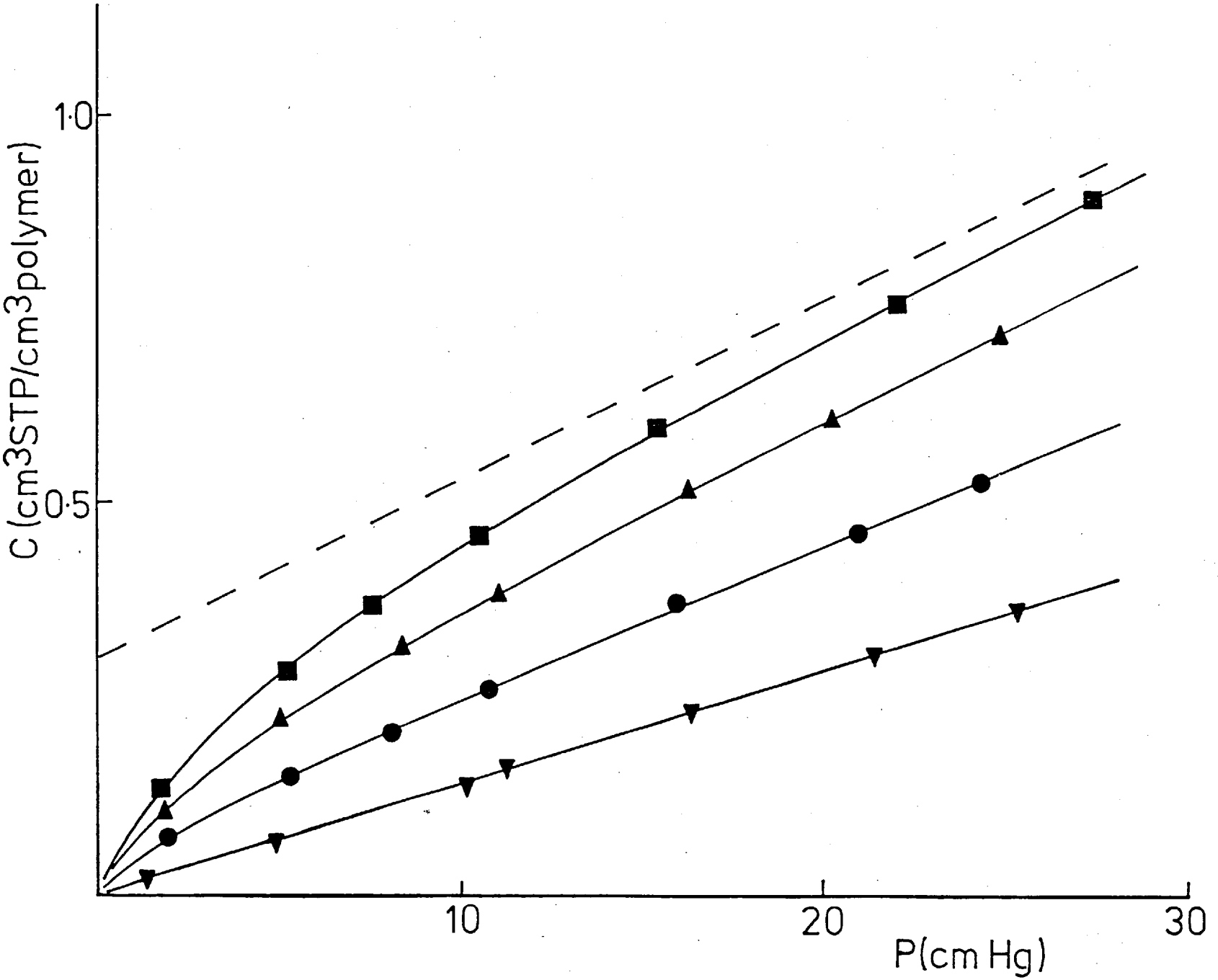
1·0
0·5
C (cm3STP/cm3polymer)
10
20
30
P(cm Hg)

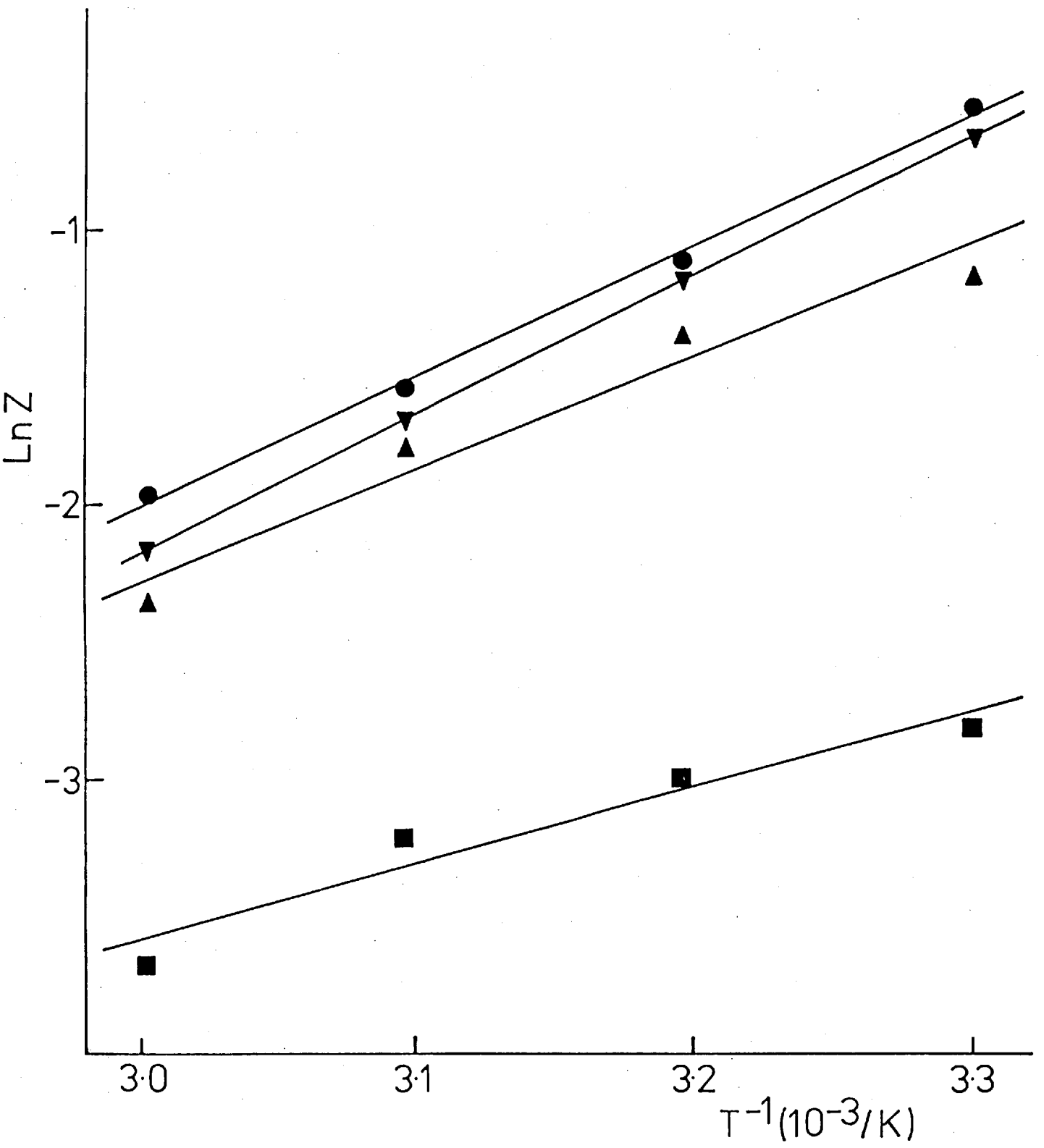
-1
-2
-3
Ln Z
3·0
3·1
3·2
3·3
T⁻¹(10⁻³/K)

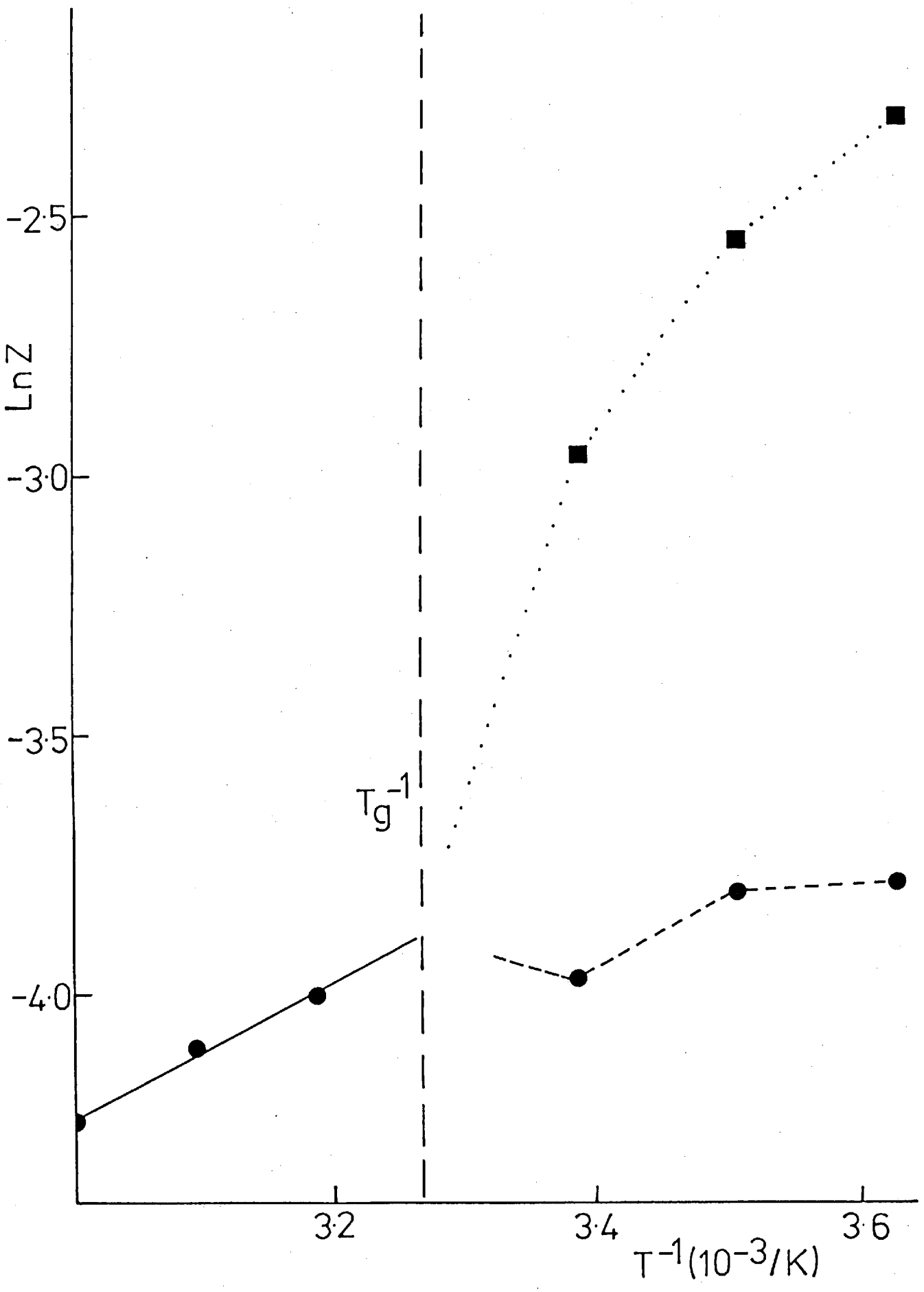
-2·5
-3·0
-3·5
-4·0
Ln Z
T_g^{-1}
3·2
3·4
3·6
$T^{-1}(10^{-3}/K)$

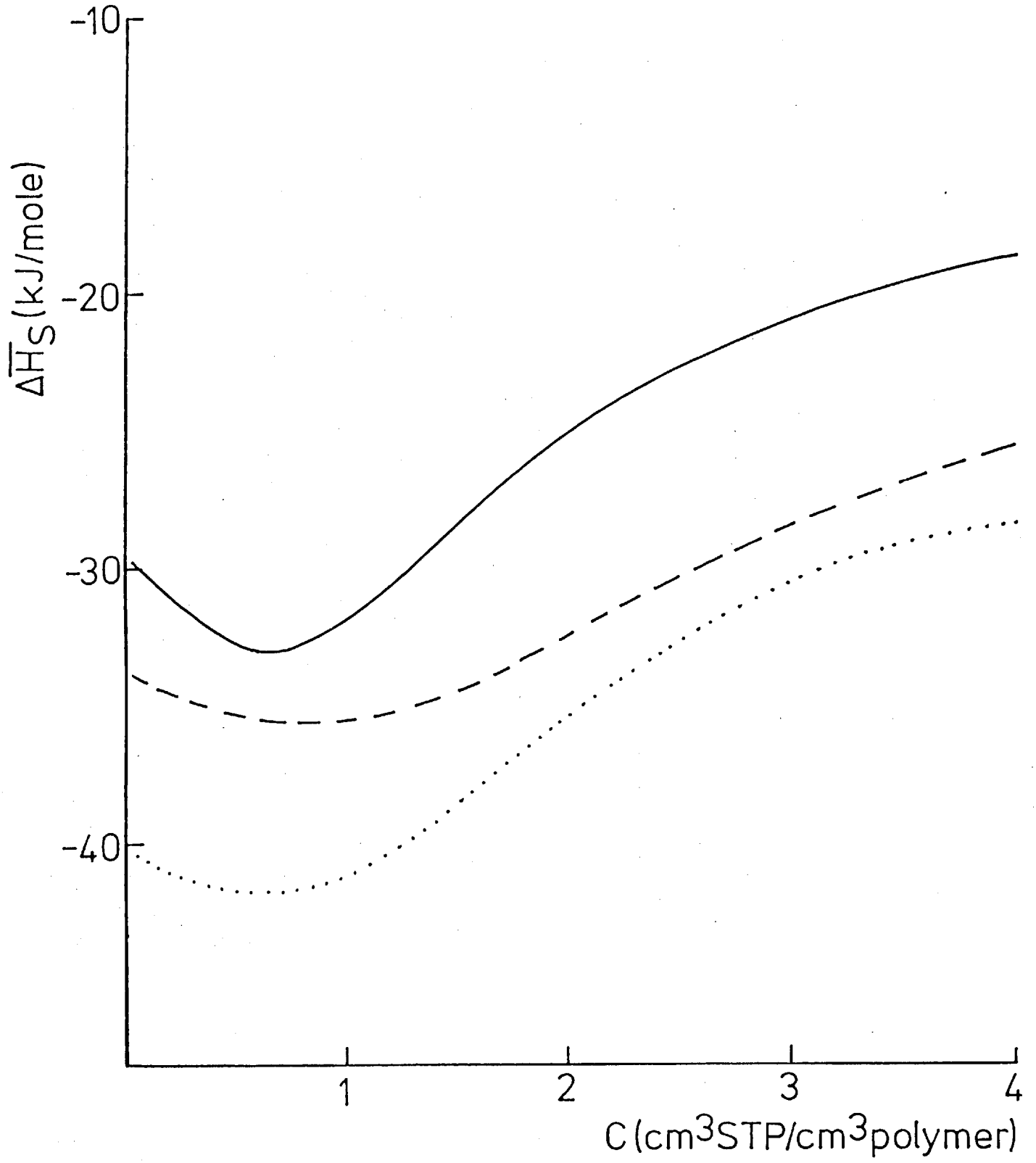
-10
-20
-30
-40
$\Delta\overline{H}_S$ (kJ/mole)
1
2
3
4
C (cm^{3}STP/cm^{3}polymer)

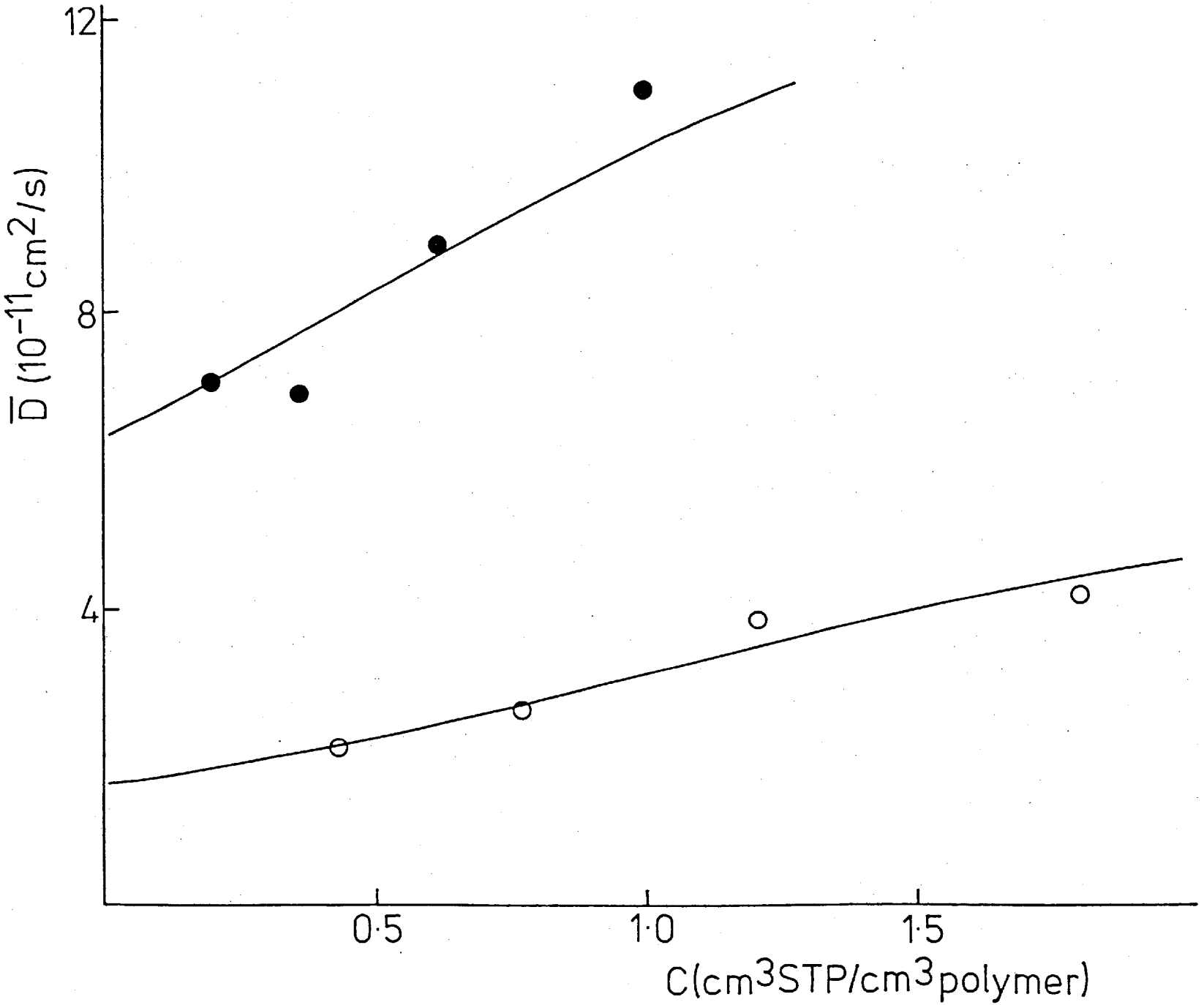
12
8
4
$\overline{D}$ (10^{-11} cm^2/s)
0·5
1·0
1·5
C(cm^3STP/cm^3polymer)

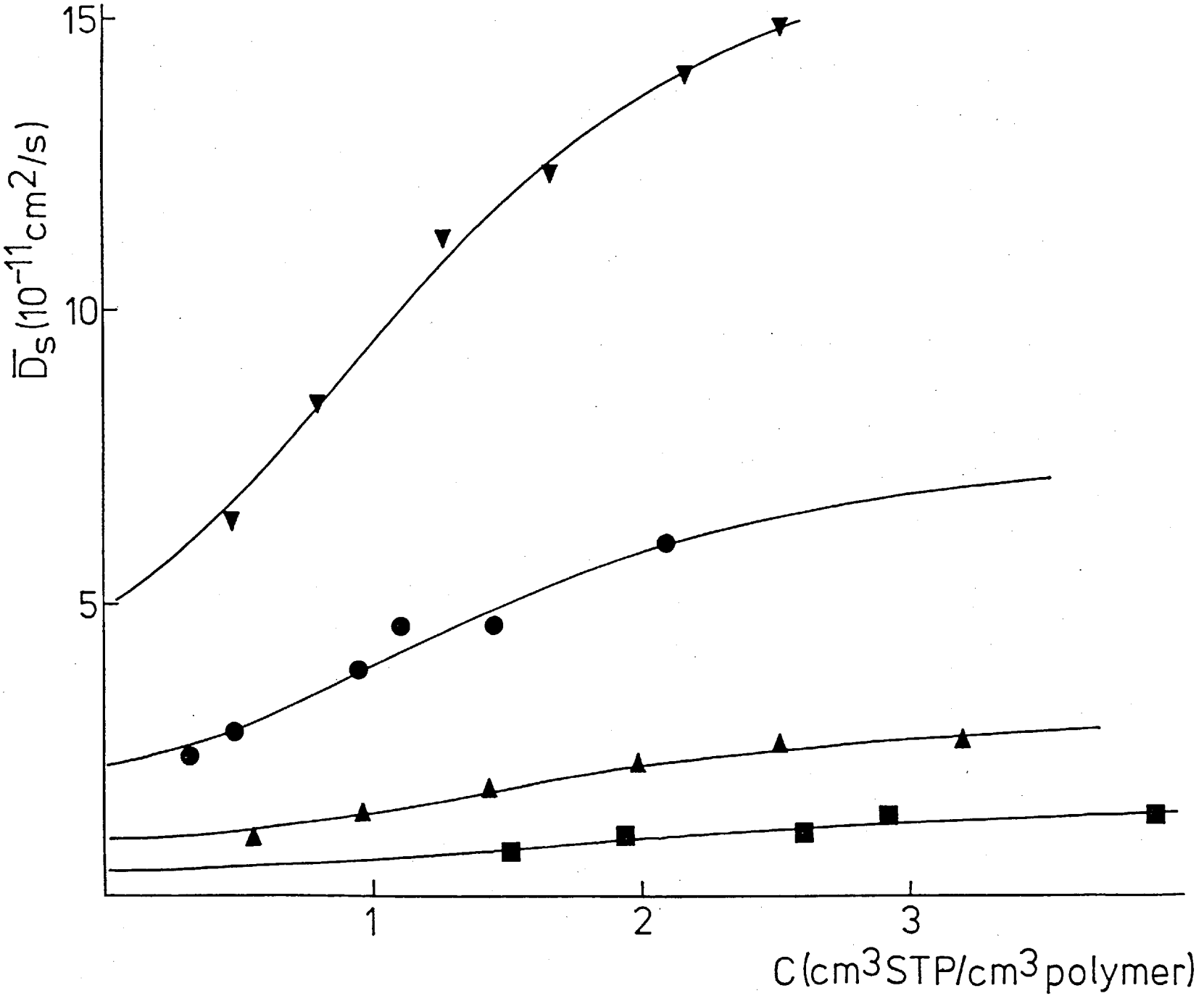
15
10
5
$\bar{D}_S$ (10^{-11} cm^2/s)
1
2
3
C (cm^3 STP/cm^3 polymer)

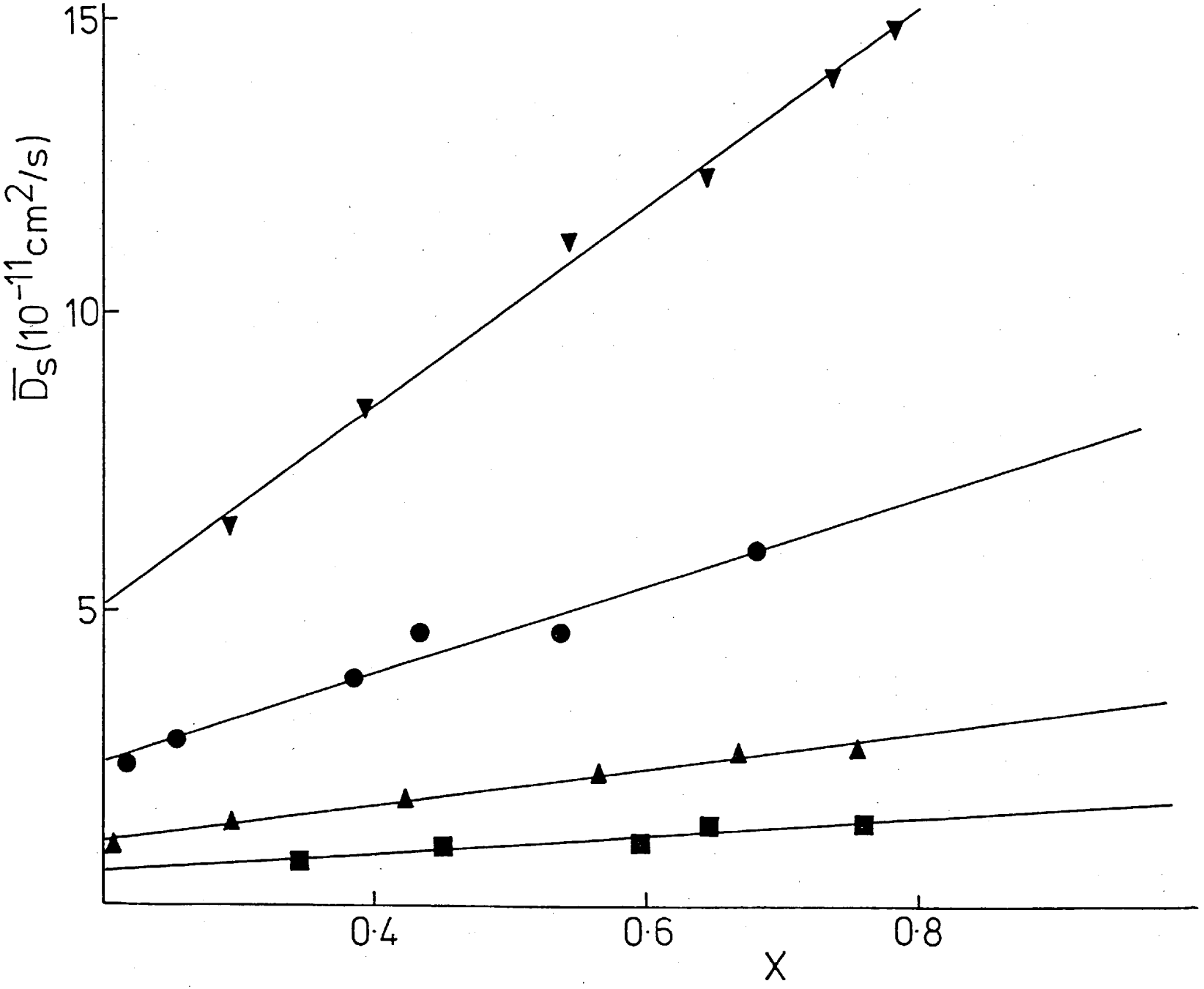
15
10
5
$\overline{D}_S(10^{-11}cm^2/s)$
0·4
0·6
0·8
X

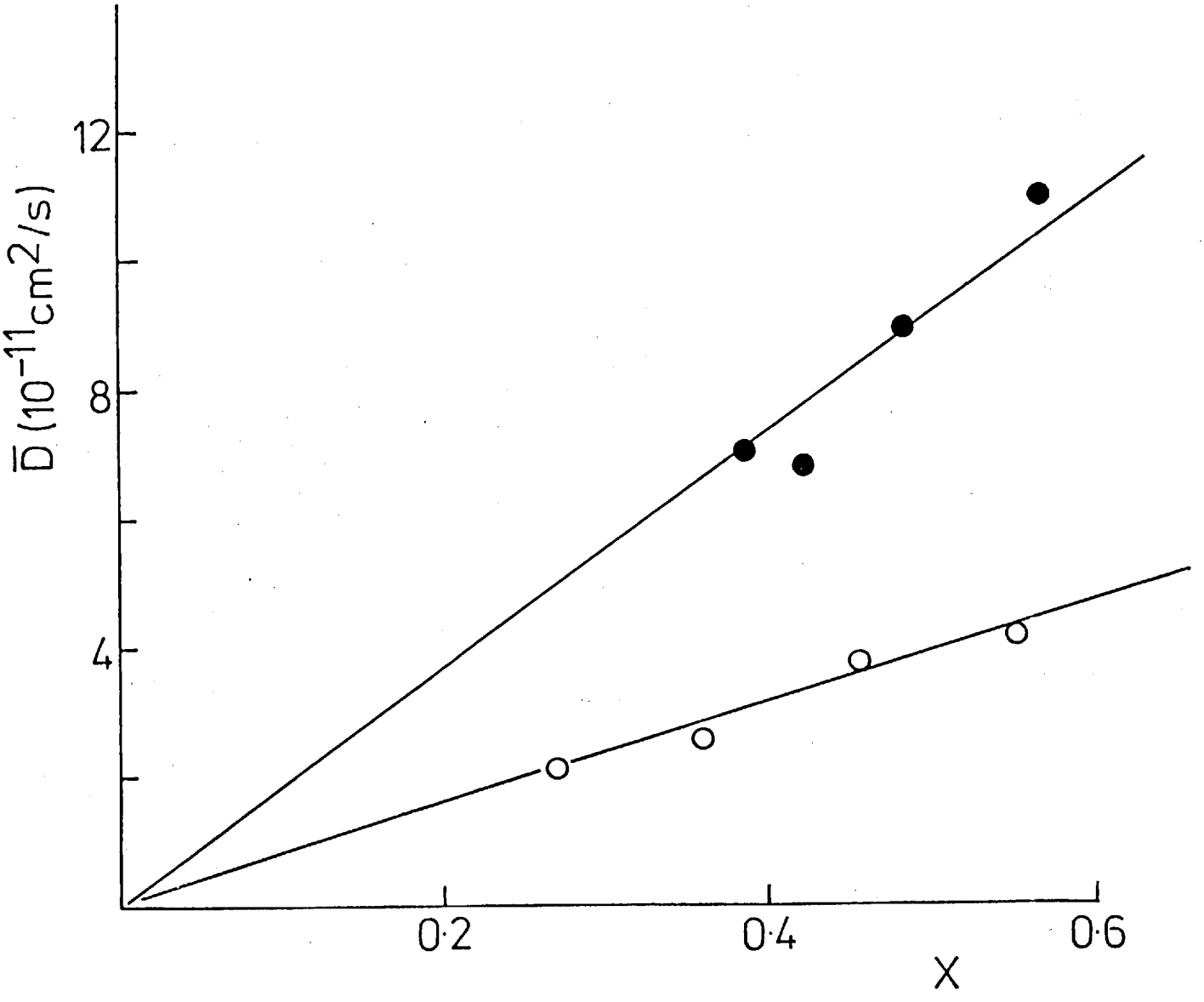
$\bar{D}$ (10^{-11} cm^2/s)
12
8
4
0·2
0·4
0·6
X

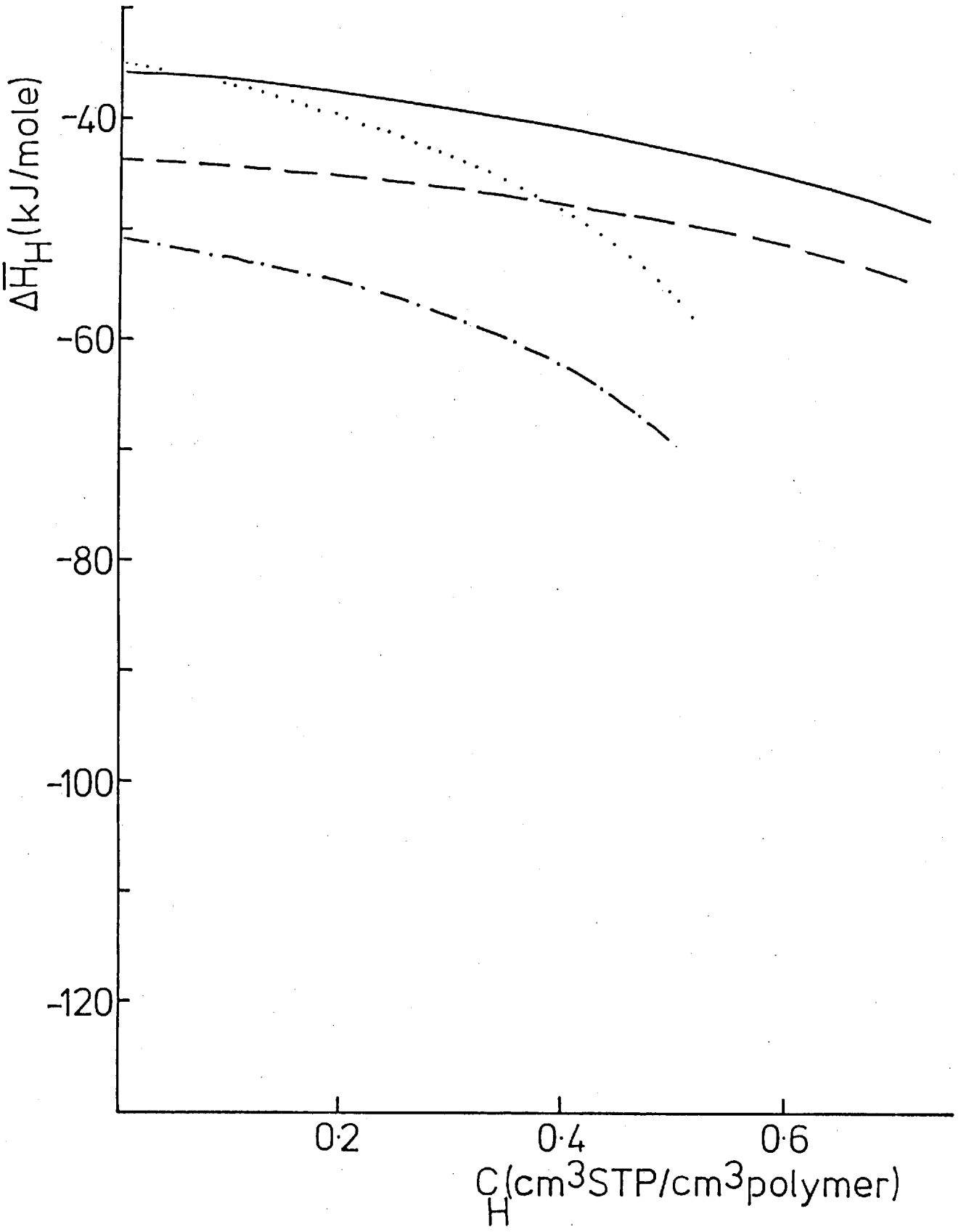
$\Delta\bar{H}_H$(kJ/mole)
-40
-60
-80
-100
-120
0·2
0·4
0·6
C_H(cm³STP/cm³polymer)

Bonnet Fig 15